CT CORONARY ANGIOGRAPHY TO DETECT CORONARY ARTERY DISEASE: LOW DOSE RADIATION IN HIGH RISK INDIVIDUALS

LISAN NEEFJES

CT CORONARY ANGIOGRAPHY TO DETECT CORONARY ARTERY DISEASE: LOW DOSE RADIATION IN HIGH RISK INDIVIDUALS

Lisan Anna Elisabeth Neefjes

CT CORONARY ANGIOGRAPHY TO DETECT CORONARY ARTERY DISEASE: LOW DOSE RADIATION IN HIGH RISK INDIVIDUALS

CT CORONAIR ANGIOGRAFIE OM CORONAIR VAATLIJDEN OP TE SPOREN: LAGE STRALINGSDOSIS IN INDIVIDUEN MET EEN HOOG RISICO

Proefschrift

ter verkrijging van de graad van doctor aan de
Erasmus Universiteit Rotterdam
op gezag van de rector magnificus

Prof.dr. H.G. Schmidt

en volgens besluit van het College voor Promoties.

De openbare verdediging zal plaatsvinden op
dinsdag 4 juni 2013 om 11.30 uur door

Lisan Anna Elisabeth Neefjes
geboren te Roosendaal en Nispen

Erasmus ERASMUS UNIVERSITEIT ROTTERDAM

PROMOTIECOMMISSIE

Promotor: Prof.dr. G.P. Krestin
               Prof.dr. P.J. de Feyter

Overige leden: Prof.dr. P.P.T. de Jaegere
               Prof.dr. W.J. Niessen
               Prof.dr. A. de Roos

CONTENTS

Chapter 11
Detection and quantification of coronary atherosclerotic plaque by
64-slice multidetector CT: a systematic head-to-head comparison with
intravascular ultrasound.
Atherosclerosis. 2011 Nov;219(1):163-70.
Papadopoulou SL, Neefjes LA, Schaap M, Li HL, Capuano E, van der Giessen
AG, Schuurbiers JC, Gijsen FJ, Dharampal AS, Nieman K, van Geuns RJ, Mollet
NR, de Feyter PJ.

Part 4: Summary and conclusions

Chapter 12

Chapter 13

Part 1

Introduction

Chapter *1*

General introduction and
outline of the thesis

GENERAL INTRODUCTION

Coronary atherosclerosis is a frequently encountered chronic disease of the arteries of the heart with very high mortality rates worldwide. It occurs predominantly in individuals with acquired risk factors and a genetic predisposition [1]. Progression of atherosclerosis develops from early asymptomatic stages to advanced stages that may cause cardiac symptoms already starting in the 2nd or 3rd decades in life [2].

In the last one and a half decades Computed Tomography Coronary Angiography (CTCA) has emerged as modality for imaging of the coronary arteries of the heart. A non-enhanced scan shows the total amount of coronary calcium; while a contrast-enhanced CT coronary angiography permits evaluation of narrowing of the vessel lumen as well as detection of both calcified and non-calcified atherosclerotic plaques.

Radiation exposure for the patient is inherent to CT technique and the related risk of cancer is of major concern [3-4]. The average radiation dose of a CTCA has decreased over the years from 20-30 mSv to <3 mSv [5] which is below the dose of nuclear cardiac imaging techniques or conventional invasive coronary angiography.[6]

Several studies acknowledge the high diagnostic accuracy of CTCA compared to the gold standard invasive coronary angiography. CTCA reliably detects, and especially rules out significant stenosis in stable patients with a low or intermediate pre-test probability of having coronary artery disease (CAD) [7]. Besides these direct diagnostic purposes, CTCA has incremental prognostic value over traditional risk factors (i.e. hypertension, diabetes mellitus, smoking, cholesterol blood values etc.) to predict adverse cardiac events in symptomatic patients [8]. Nevertheless clinical guidelines only recommend CTCA as first choice diagnostic modality in a limited number of specified symptomatic patients [9]. Further lowering of radiation dose and improvement of the diagnostic performance of CTCA will probably expand the number of appropriate indications for CTCA. This might even include screening of high risk individuals when supported by extended research in the future.

OUTLINE OF THE THESIS

In part 2 the image quality, diagnostic accuracy and radiation dose of CT coronary angiography is discussed. The influence of heart rate and heart rate variability on these outcomes is evaluated in chapter 4. A recommendation for appropriate scan protocol selection is investigated in 1) a randomized study of the image quality and radiation dose differences between three low-dose data-acquisition protocols (chapter 5) and 2) a randomized study on the comparison of diagnostic performance of those three protocols (chapter 6) using a second generation Dual Source CT scanner. In chapter 7 the optimization of a prospective triggered sequential scan protocol is described taking into account image quality and radiation dose.

Part 3 emphasizes the applicability of CTCA in detecting atherosclerotic coronary plaque. The first three chapters describe a specific population of cardiac asymptomatic patients with familial hypercholesterolemia (FH) treated with statins. In chapter 8 the plaque burden in these asymptomatic high risk patients is examined and compared to a population of patients with nonspecific cardiac symptoms. In an extended population of asymptomatic patients with FH we evaluated the extent, severity, distribution and type of atherosclerotic coronary plaques in relation to patient specific characteristics (chapter 9). Chapter 10 describes the effect of LDLR-negative genotype on coronary atherosclerosis in the population of asymptomatic statin treated patients with FH. In chapter 11 detection and quantification of coronary plaque by CT coronary angiography is compared with plaque evaluation by Intravascular Ultrasound.

REFERENCES

1   Libby P, Theroux P (2005) Pathophysiology of coronary artery disease. Circulation, 111(25):3481-3488.
2   Falk E (2006) Pathogenesis of atherosclerosis. J Am Coll Cardiol, 47(8 Suppl):C7-12.
3   Einstein AJ, Henzlova MJ, Rajagopalan S (2007) Estimating risk of cancer associated with radiation exposure from 64-slice computed tomography coronary angiography. JAMA, 298(3):317-323.
4   Fazel R, Krumholz HM, Wang Y, et al. (2009) Exposure to low-dose ionizing radiation from medical imaging procedures. N Engl J Med, 361(9):849-857.
5   Alkadhi H, Stolzmann P, Desbiolles L, et al. (2010) Low-dose, 128-slice, dual-source CT coronary angiography: accuracy and radiation dose of the high-pitch and the step-and-shoot mode. Heart, 96(12):933-938.
6   Mettler FA, Jr., Huda W, Yoshizumi TT, Mahesh M (2008) Effective doses in radiology and diagnostic nuclear medicine: a catalog. Radiology, 248(1):254-263.
7   von Ballmoos MW, Haring B, Juillerat P, Alkadhi H (2011) Meta-analysis: diagnostic performance of low-radiation-dose coronary computed tomography angiography. Ann Intern Med, 154(6):413-420.
8   Hulten EA, Carbonaro S, Petrillo SP, Mitchell JD, Villines TC (2011) Prognostic value of cardiac computed tomography angiography: a systematic review and meta-analysis. J Am Coll Cardiol, 57(10):1237-1247.
9   Abidov A, Gallagher MJ, Chinnaiyan KM, Mehta LS, Wegner JH, Raff GL (2009) Clinical effectiveness of coronary computed tomographic angiography in the triage of patients to cardiac catheterization and revascularization after inconclusive stress testing: results of a 2-year prospective trial. J Nucl Cardiol, 16(5):701-713.

Chapter 2

CT coronary plaque imaging

Lisan A. Neefjes
Koen Nieman
Pim J. de Feyter

Chapter 3

CT coronary angiography:
a new unique prognosticator?

Lisan A Neefjes
Pim J de Feyter

Computed tomography coronary angiography (CTCA) has evolved as a non-invasive imaging technology that can be used as an alternative first-line diagnostic test in symptomatic patients with low to intermediate likelihood of coronary artery disease (CAD) [1]. Nevertheless, it has not (yet) fulfilled initial expectations that it would be able to replace conventional invasive coronary angiography because CTCA tends to overestimate the severity of the coronary stenosis resulting in a too high number of patients with false-positive outcomes. This is mainly caused by the blooming effect of calcified lesions in combination with the still too limited spatial resolution of CTCA as compared to invasive coronary angiography. CTCA provides, additional to luminography, comprehensive assessment of the anatomic manifestations of coronary atherosclerosis, including the distribution (proximal, mid and distal) and extent (1, 2, 3 vessel disease, LM disease) of CAD, the presence of "positive remodeling" of the vessel and a, rather crude, assessment of the coronary plaque components (calcified, non-calcified and mixed) and [2].

CTCA is considered a reliable technique providing high quality images at low radiation exposure. It is now timely to explore the full potential of CTCA ranging from the diagnostic accuracy to rule-in or rule-out CAD, to its prognostic potential in symptomatic patients and asymptomatic individuals, and finally to assess the cost effectiveness with clinical outcomes as primary endpoints.

PROGNOSTIC VALUE OF CTCA IN SYMPTOMATIC PATIENTS

In symptomatic patients CTCA is able to non-invasively identify patients at high risk for major adverse cardiac events (MACE) and a negative CTCA is significantly related to an extremely low risk for MACE [3]. In these prognostic CTCA studies, using a retrospective data acquisition scan protocol, the relatively high radiation exposure (10-25 mSv) was worrisome.

CTCA RELATED RADIATION EXPOSURE

CT, and cardiac CT in particular, is a major contributor to ionizing radiation exposure which is known to increase the lifetime attributable risk of cancer[4]. Therefore efforts should be taken to keep the radiation dose of CT as low as reasonably achievable (ALARA). New, recently introduced CT radiation reduction techniques have dramatically reduced the radiation dose. CT investigations using prospectively ECG triggered data acquisition protocols have reported radiation doses of approximately 2 mSv [5] with preserved high diagnostic performance compared to conventional coronary angiography. Studies of a new scan protocol using the conventional spiral mode but with very fast table speed, the

high pitch spiral mode, covering the whole heart in 1 heart beat, reported an effective radiation dose even below 1 mSv[6] while maintaining diagnostic image quality. Iterative reconstruction has been introduced most recently in cardiac CT and preliminary data suggest that these sophisticated reconstruction algorithms may allow a further reduction in radiation dose of approximately 40% irrespective of the used scan protocol [7].

LOW DOSE CTCA: PROGNOSTIC VALUE

The ability of low dose CTCA, as distinct to relatively high dose retrospective gated CTCA, to predict future adverse cardio vascular events is not well established. In this issue of Heart, Buechel et al.[8] assessed, in retrospective analysis, the prognostic value of low dose (mean effective dose 1.8±0.6 mSv) 64-slice CTCA using prospective ECG triggering in patients with known or suspected CAD. Major adverse cardiac events were defined as cardiac death, non-fatal myocardial infarction or the need for revascularization. To minimize that the outcome of CTCA would trigger the need for revascularization, 38 patients that underwent early revascularization (i.e. within 6 weeks after CTCA) were excluded from analysis. They studied 367 patients. Normal coronary arteries were seen in 47% (171) of the patients, non-obstructive lesions were found in 18% (66), and obstructive lesions (>50% luminal diameter stenosis) were identified in 35% (130) patients. The patients were followed for a mean follow-up time of 47±16 weeks. MACE occurred in 30 patients (8.2%). Cardiac death occurred in 1 patient, non-fatal MI in 3 patients and 26 patients underwent revascularization. Patients with non-obstructive or obstructive CAD had a first year event rate of 3% (5 events) and 26% (25 events), respectively.

The prognostic value of CTCA in this study was comparable to the value reported in a recent meta-analysis of Hulten et al. evaluating 9592 patients with a median follow up of 20 months[3]. In this meta-analysis the majority of the analyzed patients had known or suspected CAD. The annualized all cause death rate, non-fatal MI rate and revascularization rate were respectively 0.74%, 0.30% and 1.25% for patients with non-obstructive CAD and 2.22%, 2.12% and 24.82% for patients with obstructive CAD. Buechel et al. report that patients with normal coronary arteries had an annualized event rate of zero which was comparable to the event rate of 0.17% reported in the meta-analysis of Hulten et al. and within the range of the event rate of 0.45% and 0.54%, respectively, seen in patients with normal findings in stress echocardiography or myocardial perfusion [9]. The adverse event rate reported by Buechel et al. was mainly driven by the need for revascularization which may be overrepresented because CTCA already revealed coronary anatomy, although precautions were taken to exclude patients with revascularizations within 6 weeks. However, this was similar in the majority of studies evaluated in the recent meta-analysis [3].

Buechel et al. confirmed the high prognostic value of CTCA in symptomatic patients but the real importance of this study is that this prognostic value was achieved at a very low effective radiation dose of below 2 mSv which drastically lowered the radiation associated lifetime attributable risk of cancer morbidity and mortality of CTCA. This will trigger new avenues of studies evaluating the prognostic power of CTCA.

FUTURE DIRECTIONS

Approximately 50% of the sudden cardiac deaths or non-fatal myocardial infarctions occur in patients without prior diagnosis of CAD. To prevent those unexpected severe adverse events, the first step is to identify the individuals at risk. Nowadays only traditional risk factors are being used for a risk prediction in asymptomatic patients and traditional risk prediction models are based on patient populations and they do not provide direct evidence of the presence of coronary artery disease in an individual patient. However, the unique property of CTCA is its ability to assess the presence and extent of subclinical coronary atherosclerosis in an individual which is not possible with other non-invasive techniques that are better suited to assess more advanced coronary atherosclerosis causing myocardial ischemia. Hence, CTCA has the potential to non-invasively improve traditional risk prediction in asymptomatic patients.

Although CTCA has been used to assess coronary atherosclerosis in asymptomatic individuals [10-11] this was achieved at rather high radiation dose, (>10 mSv) which was met with great concern and raised questions about the risk-benefit ratio in these asymptomatic individuals. This restrained investigators to explore the prognostic potential of CTCA. The prognostic value of CTCA in asymptomatic individuals has only been evaluated in 1 study at an intermediate level of effective radiation dose of 7-8 mSv [12].

Buechel et al.[8] present reliable prognostic CTCA at such low radiation exposure that it may open the door for extensive prognostic studies in asymptomatic populations. These studies are highly needed and may alter the recommendations of the ACCH/AHA Task Force on Practice Guidelines[13] or the Working Group on Nuclear Cardiology and Cardiac CT of the European Society of Cardiology[14], which currently do not recommend CTCA for risk stratification in asymptomatic patients in particular because of the lack of prognostic studies in asymptomatic individuals. Additionally, this study may even trigger studies evaluating repeating CTCA examinations to gain further insights into the natural progression of coronary atherosclerosis or monitoring of CAD treatment.

Low-radiation-dose CT coronary imaging allows further exploration of its prognostic potential in various study populations.

REFERENCES

1   Weustink AC, Mollet NR, Neefjes LA, et al. (2010) Diagnostic accuracy and clinical utility of noninvasive testing for coronary artery disease. Ann Intern Med, 152(10):630-639.

2   Schuijf JD, Achenbach S, de Feyter PJ, Bax JJ (2011) Current applications and limitations of coronary computed tomography angiography in stable coronary artery disease. Heart (British Cardiac Society), 97(4):330-337.

3   Hulten EA, Carbonaro S, Petrillo SP, Mitchell JD, Villines TC (2011) Prognostic value of cardiac computed tomography angiography: a systematic review and meta-analysis. Journal of the American College of Cardiology, 57(10):1237-1247.

4   Einstein AJ, Henzlova MJ, Rajagopalan S (2007) Estimating risk of cancer associated with radiation exposure from 64-slice computed tomography coronary angiography. JAMA, 298(3):317-323.

5   Husmann L, Valenta I, Gaemperli O, et al. (2008) Feasibility of low-dose coronary CT angiography: first experience with prospective ECG-gating. European heart journal, 29(2):191-197.

6   Achenbach S, Marwan M, Ropers D, et al. (2010) Coronary computed tomography angiography with a consistent dose below 1 mSv using prospectively electrocardiogram-triggered high-pitch spiral acquisition. European heart journal, 31(3):340-346.

7   Leipsic J, Labounty TM, Heilbron B, et al. (2010) Estimated radiation dose reduction using adaptive statistical iterative reconstruction in coronary CT angiography: the ERASIR study. Ajr, 195(3):655-660.

8   Buechel RR, Pahzenkottil AP, Herzog BA, et al. (2011) Prognostic performance of low-dose coronary CT angiography with prospective ECG triggering. Heart (British Cardiac Society).

9   Metz LD, Beattie M, Hom R, Redberg RF, Grady D, Fleischmann KE (2007) The prognostic value of normal exercise myocardial perfusion imaging and exercise echocardiography: a meta-analysis. Journal of the American College of Cardiology, 49(2):227-237.

10 Choi EK, Choi SI, Rivera JJ, et al. (2008) Coronary computed tomography angiography as a screening tool for the detection of occult coronary artery disease in asymptomatic individuals. Journal of the American College of Cardiology, 52(5):357-365.

11 Iwasaki K, Matsumoto T, Aono H, Furukawa H, Samukawa M (2008) Prevalence of subclinical atherosclerosis in asymptomatic diabetic patients by 64-slice computed tomography. Coronary artery disease, 19(3):195-201.

12 Hadamitzky M, Meyer T, Hein F, et al. (2010) Prognostic value of coronary computed tomographic angiography in asymptomatic patients. The American journal of cardiology, 105(12):1746-1751.

13 Greenland P, Alpert JS, Beller GA, et al. (2010) 2010 ACCF/AHA guideline for assessment of cardiovascular risk in asymptomatic adults: a report of the American College of Cardiology Foundation/American Heart Association Task Force on Practice Guidelines. Circulation, 122(25):e584-636.

14 Perrone-Filardi P, Achenbach S, Mohlenkamp S, et al. (2010) Cardiac computed tomography and myocardial perfusion scintigraphy for risk stratification in asymptomatic individuals without known cardiovascular disease: a position statement of the Working Group on Nuclear Cardiology and Cardiac CT of the European Society of Cardiology. European heart journal, Published Online First: 14 July, 2010.

Part 2

CT coronary angiography: image quality, diagnostic accuracy and radiation dose

Chapter 4

Impact of heart rate frequency and variability on radiation exposure, image quality, and diagnostic performance in dual-source spiral CT coronary angiography

Annick C. Weustink
Lisan A. Neefjes
Stamatis Kyrzopoulos
Marcel van Straten
Rick Neoh Eu
Willem Bob Meijboom
Marcel L. Dijkshoorn
Ermanno Capuano
Filippo Cademartiri
Eric Boersma
Pim J. de Feyter
Gabriel P. Krestin
Nico R. Mollet

Chapter 4

Impact of heart rate frequency and variability on radiation exposure, image quality, and
diagnostic performance in dual-sourcespiral CT coronary angiography

ABSTRACT

Purpose To investigate the impact of heart rate frequency (HRF) and heart rate variability (HRV) on radiation exposure, image quality, and diagnostic performance to detect significant stenosis (≥50% lumen diameter reduction) using adaptive ECG pulsing at dual-source spiral CT coronary angiography (CTCA).

Materials and methods Institutional review committee approval and informed consent was obtained in all patients. No pre-scan beta-blockers were applied prior to scanning. Non-contrast CT and CTCA using adaptive ECG pulsing was performed in 927 consecutive patients (600 men; 327 women, mean age 60.3±11.0 years). Patients were divided into 3 HRF groups: low (≤65 bpm), intermediate, (66-79 bpm), and high (≥80 bpm), and 4 HRV groups on the basis of the mean inter-beat difference (IBD) during CTCA acquisition: normal (0-1 IBD), minor (2-3 IBD), moderate (4-10 IBD) and severe (>10 IBD). Radiation exposure and image quality regarding the presence of motion artifacts were evaluated in all patients. Diagnostic performance was presented as sensitivity, specificity, positive and negative predictive values, and positive and negative likelihood ratios with corresponding 95% confidence intervals (CIs) in a subpopulation of 444 patients using quantitative coronary angiography as reference standard.

Results CT coronary angiography yielded good image quality in 98% of patients and no significant differences in image quality were found among HRF and HRV groups. Radiation exposure was significantly higher in patients with low versus high HRF and in patients with severe versus normal HRV. No significant differences among HRF and HRV groups in image quality and diagnostic performance were found. A nonsignificant trend was found toward a lower specificity and PPV in patients with a high HRF or severe HRV when compared with low HRF or normal HRV in patients with a low calcium score (Agatston score <100).

Conclusions Dual-source spiral CT coronary angiography using adaptive ECG pulsing results in preserved diagnostic image quality and performance independent of heart rate frequency or heart rate variability at the cost of limited dose reduction in arrhythmic patients.

INTRODUCTION

Spiral CT coronary angiography (CTCA) has emerged as a non-invasive diagnostic modality that reliably excludes the presence of significant coronary artery disease [1, 2[.

Dual-source CT scanners are equipped with 2 X-ray sources and provide a heart rate independent temporal resolution of 83 ms. Such improved temporal resolution may allow more reliable detection or exclusion of significant coronary artery stenosis in patients with fast or irregular heart rates. However, the radiation exposure associated with spiral CT is relatively high [3-5].

ECG-controlled X-ray tube current modulation or 'ECG-pulsing' has been introduced as an effective tool to reduce radiation exposure up to 50% in spiral CTCA [6, 7]. The first generation ECG-pulsing algorithms were not standard used because the occurrence of a single premature beat could result in non-diagnostic image quality due to incorrect timing of the high X-ray tube output. Currently available ECG-pulsing algorithms are able to detect ectopic heart beats and the X-ray tube current modulation is automatically switched off until the heart rate is stable again. Such adaptive ECG-pulsing algorithms in spiral CT are designed to maintain diagnostic image quality in arrhythmic patients since the continuous high X-ray tube output allows flexible selection of the desired reconstruction phase throughout the R-R interval. However, image quality is only maintained at the cost of higher radiation exposure [8].

The purpose of this study was to determine the impact of heart rate frequency (HRF) and heart rate variability (HRV) on radiation exposure and image quality in a large cohort of patients undergoing Dual-source CTCA with adaptive ECG-pulsing. In addition, we evaluated the impact of HRF and HRV on the diagnostic performance of Dual-source CTCA to detect or rule out significant stenoses in a subgroup of patients who underwent additionally conventional coronary angiography (CCA).

MATERIALS AND METHODS

Study Population

During a period from April 2006 to October 2008, 1143 consecutive symptomatic patients with suspected or known coronary artery disease were eligible for inclusion in the study (Figure 1). Excluded were patients with previous surgical revascularization (n=103) and with atrial fibrillation with a fast ventricular response (n=6). CTCA-specific exclusion criteria were known allergy to Iodinated contrast material (n=12) and impaired renal function (serum creatinine >120 μmol/l) (n=35). Thus, the study population comprised 927

Chapter 4

Impact of heart rate frequency and variability on radiation exposure, image quality, and
diagnostic performance in dual-sourcespiral CT coronary angiography

Figure 1 Flow Diagram
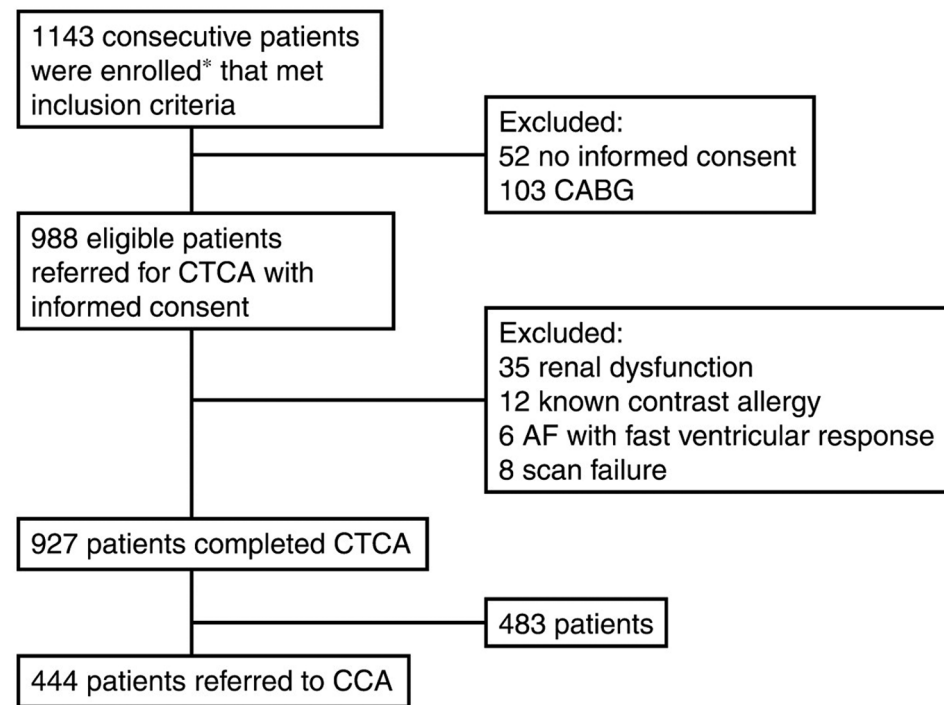
Flowchart of study patients. AF = atrial fibrillation, CABG = coronary artery bypass graft, CCA = conventional
coronary angiography, CTCA = CT coronary angiography. * = Period of enrollment: April 2006 to October 2008.

patients (600 men; 327 women, mean age 60.3±11.0 years). The institutional review board
approved the study and all patients gave informed consent.

Scan Protocol

Patients were scanned using a Dual-source CT scanner (Somatom Definition, Siemens
Healthcare, Forchheim, Germany). No beta-blockers were administered prior to the scan.
Patients received Nitroglycerin (0.4 mg) sublingually just before scanning. A non-en-
hanced calcium scoring scan was performed prior to CTCA. CTCA scan parameters were:
number of X-ray tubes 2, detector collimation 32 x 0.6 mm per tube with double sampling
by rapid alteration of the focal spot in the longitudinal direction (z flying focal spot) [9],
rotation time 330 ms, tube voltage 120 kV, full tube current 625 mA per tube, indepen-
dent of patient size. Prior to scanning, the pitch was set automatically by the scanner's
software. Pitch varied between 0.20 for low HRF (<40 bpm) and 0.53 for high HRF (>100
bpm), with individually adapted pitch values for HRF >40 and <100 bpm.

A bolus of iodinated contrast material (Ultravist® 370 mgI/ml, Schering AG, Germany),
which varied between 60-100 ml depending on the expected scan time, was injected

Figure 2 Schematic illustrations of adaptive ECG pulsing in spiral dual-source CTCA (A, B) and Step-and-Shoot
(SAS) scan mode (C)
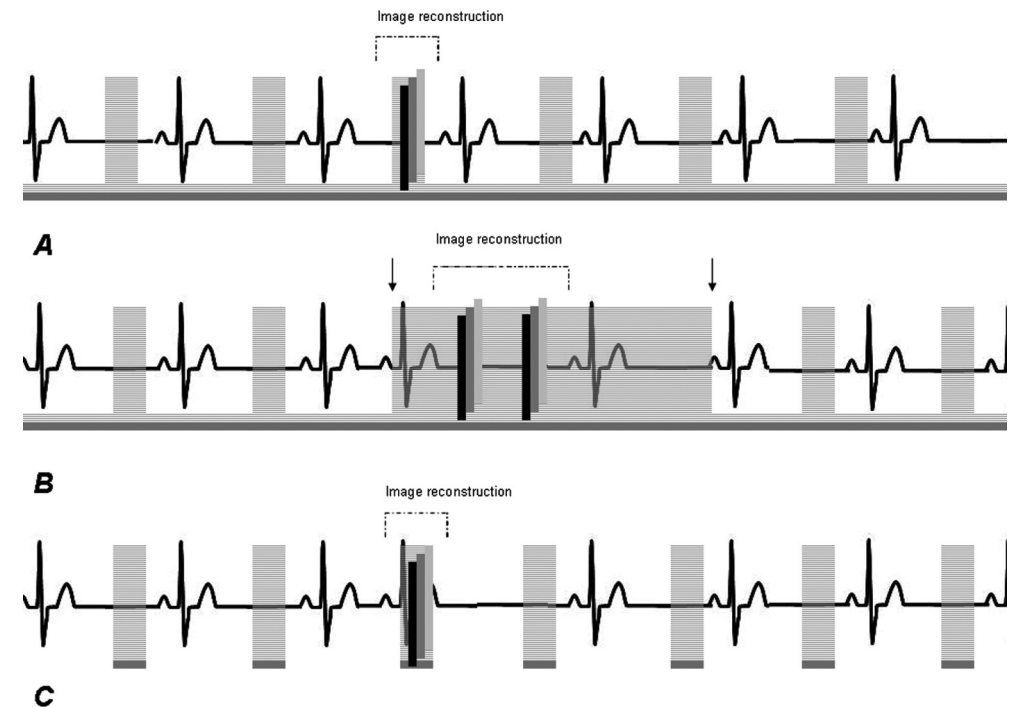
A: Spiral CTCA in a low and regular heart rate. The ECG pulsing window is set during mid-to-end diastole and
    radiation exposure is reduced outside the ECG pulsing window. The red line correlated with X-ray tube
    output, the pink bar indicates full or reduced X-ray tube output.

B: Spiral CTCA in a low and irregular heart rate. The adaptive ECG pulsing algorithm adapts to the occurrence
    of a premature beat by switching off the ECG pulsing algorithm and full X-ray is given during two subse-
    quent heart beats (between arrows). Image reconstruction is performed by manual repositioning of the
    reconstruction windows as previously described (12).

C: Step-and-shoot (SAS) CTCA in a low and irregular heart rate. Full X-ray during predefined time intervals in
    the cardiac cycle is given and image reconstruction can only be performed during the premature ectopic
    beat resulting in severe motion artifacts.

(flow rate: 5.5 ml/s) in an antecubital vein followed by a saline chaser (40 ml; flow rate: 5.5
ml/s). A bolus tracking technique was applied to synchronize the data acquisition with
the arrival of contrast in the coronary arteries.

All patients were scanned using an adaptive ECG pulsing algorithm (Figure 2).

The first enrolled 640 patients were scanned from April 2006 to November 2007 and stan-
dard ECG pulsing was applied using a fixed pulsing window (full tube current was given
from 25 to 70% of the R-R-interval). Outside the ECG pulsing window, the tube current
was reduced to 20% of the full current. The subsequent 287 patients were scanned from

Chapter 4

Impact of heart rate frequency and variability on radiation exposure, image quality, and
diagnostic performance in dual-sourcespiral CT coronary angiography

December 2007 to September 2008 and optimal ECG pulsing was applied using validated ECG pulsing windows during mid-to-end-diastole (60-76% of R-R-interval) in low HRF (≤65 bpm), during end-systole (31-47%) for high HRF (≥80 bpm), and during both mid-to-end-diastole and end-systole (30-77%) for intermediate HRF (66-79 bpm), respectively [6]. Outside the ECG pulsing window the tube current was reduced to 4% of the full current (Mindose®, Siemens Healthcare, Forchheim, Germany).

CT Image Reconstruction
All CTCA datasets were reconstructed using a single-segment reconstruction algorithm resulting in 83 ms temporal resolution; slice thickness 0.75 mm; increment 0.4 mm; medium-to-smooth (B26f) and sharp (B46f) convolution kernel. Standard reconstruction algorithms were applied using an absolute reverse or percentage technique to obtain datasets during end-systole and/or mid-to-end diastole according to heart rate frequency [6]. In case the standard reconstruction algorithm provided datasets with insufficient image quality of one or more coronary segments, additional datasets were manually reconstructed. If necessary, multiple datasets of a single patient were used separately in order to obtain optimal image quality for all coronary segments. Image reconstruction windows were manually repositioned to achieve high image quality in patients with arrhythmia, as previously described [12]. For CTCA analysis, the best selected datasets were transferred to an offline work-station (MMWP®, Siemens Healthcare, Forchheim, Germany).

Quantitative Coronary Angiography (QCA)
A subpopulation of patients (48%, 444/927) underwent CCA. All conventional angiograms were carried out within four weeks before or after CCA. Three experienced cardiologists (R.N.E., S.K, and C.A.M., 5 or more years of interventional cardiology experience) unaware of the results of CTCA, identified all available coronary segments at invasive CA using a 17-segment modified American Heart Association (AHA) classification [10]. All segments, irrespective of size, were included for comparison with CTCA. Segments were visually classified as normal or luminal irregularities (<20% lumen diameter reduction), or diseased (≥20% lumen diameter reduction). The stenoses in segments visually scored as having more than 20% narrowing, were quantified by a validated quantitative coronary angiography (QCA) algorithm [11]. Stenoses were evaluated in the worst angiographic view and classified as significant if the lumen diameter reduction was 50% or more.

CT image evaluation
The total calcium scores (Agatston score) per patient were calculated using dedicated software (Syngo Calcium Scoring ®, Siemens, Forchheim, Germany). One experienced observer (A.C.W, 5 or more years of CT coronary angiography training) graded the overall image quality of the best selected CTCA datasets.

A dataset, or the combination of datasets, was classified as good, if no or mild coronary motion was present and the observer was confident in the diagnostic evaluation, or im-

paired if extensive coronary motion was present and the observer experienced impairment in performing the diagnostic evaluation.

Two experienced observers (A.C.W., N.R.M., 5 or more years of CT coronary angiography training) unaware of the results of CCA, independently scored all CTCA datasets for the presence of significant stenoses using axial source images, as well as multiplanar or curved reformatted reconstructions and maximum intensity projections. Stenoses were visually classified into significant (≥50% lumen diameter reduction) or non-significant (<50% reduction). Segments distal to a chronic total occlusion were excluded. An intention to diagnose design was used: all scanned patients including all segments were analyzed even if the image quality was impaired. Interobserver disagreements were resolved by consensus in a joint session.

Classification according to heart rate frequency and variability
Patients were categorized into 3 HRF groups: low (≤65 bpm), intermediate (66-79 bpm) and high (≥80 bpm). The absolute difference between two consecutive heart beats was recorded during CTCA. HRV was defined as the sum of these absolute differences divided by the number of heart beats and expressed as mean interbeat difference (IBD, Figure 3). Patients were categorized into 4 HRV groups: normal (0-1 IBD), minor (2-3 IBD), moderate (4-10 IBD) and severe (>10 IBD).

Figure 3 Schematic Illustration of Heart rate Variability (HRV) Assessment

The absolute difference (Δ) between two consecutive heart beats was recorded. HRV was expressed as mean interbeat difference (IBD) defined as the sum of these absolute differences (3+0+60+80+20+3) divided by the number of heart beats during CTCA (7) = 448 / 7 = 23

Subanalysis according to Agatston score
A subanalysis on diagnostic performance in patients with low (≤100 Agatston score) and high (>100 Agatston score) was performed and sensitivity, specificity, and positive and negative predictive values among HRF groups and HRV groups were calculated.

Radiation Exposure
The radiation exposure for Dual-source CTCA was quantified by the CTDIvol values obtained from the CT scanner console. The CTDIvol estimates the average dose within the scanned volume based on a standardized phantom [12] and takes the influence of both the ECG-pulsing and the pitch on the dose into account. In order to study solely the effect

Chapter 4

Impact of heart rate frequency and variability on radiation exposure, image quality, and
diagnostic performance in dual-sourcespiral CT coronary angiography

of ECG-pulsing on the dose, the CTDIw values were calculated [CTDIw = CTDIvol x pitch], which are a measure for radiation dose independent of pitch.

Statistical Analysis

The statistical analyses were performed using SPSS (version 12.1 SPSS Inc., Chicago, Ill, USA.) and STATA (SE 8.2, College Station, Texas, USA).

Categorical patient and scan characteristics were expressed as numbers and percentages and continuous variables were expressed as mean (standard deviation) values. Diagnostic performance of CTCA for the diagnosis of significant CAD compared to the standard of reference QCA on CCA was determined with sensitivity, specificity, positive predictive value, and negative predictive value and their corresponding 95% confidence intervals. The difference in age between males and females was calculated using the student-T test.

The image quality and diagnostic performance according to Agatston scores among HRF groups and among HRV groups were compared using the Fisher exact test and a p-value <0.05 was considered statistically significant. For the dose estimates, the two-way Anova test was performed to evaluate the effect of HRF and HRV on the radiation exposure (CT-DIvol and CTDIw) for both fixed ECG pulsing and optimal ECG pulsing windows. A p-value <0.05 was considered statistically significant. Inter-observer variability for the detection of significant stenoses was determined by kappa-statistics. Intra-observer agreement of one observer was determined in a set of 100 patients and presented by kappa-statistics. The data was clustered implying that potential correlation existed between the multiple (seventeen) segments analyzed per patient. To adjust for the clustered nature of the data, sensitivity, specificity, negative and positive predictive values were studied by a bootstrap analysis [13, 14]. A total of 1000 replications of the dataset were obtained by sampling segments (with replacement), with the patient as cluster.

RESULTS

Patient and scan characteristics are listed in Table 1. There was no significant difference (p = 0.33) in age between males (60.6±11.0 years) and females (59.9±11.1). Mean scan length for the CTCA-protocol was 11.0±3.1 cm. A total of 428 (46%, 428/927) of patients received long-term β-blockers. In patients with moderate HRV (13%, 124/927), 6% (7/124) presented with ventricular extra-systolic beats, 1% (1/124) with atrial fibrillation and 94% (116/124) with mild sinus node arrhythmia. In patients with severe HRV (6%, 52/927), 37% (19/52) presented with ventricular extra-systolic beats, 19% (10/52) with atrial fibrillation, 2% (1/52) with ventricular bigeminy, and 2% (1/52) with ventricular trigemini, and 40% (21/52) with sinus node arrhythmias.

Table 1. Patient and Scan Characteristics.

| | OVERALL | HRF GROUPS | | | HRV GROUPS | | | |
		Low ≤65 bpm	Intermediate 66-79 bpm	High ≥80 bpm	Normal 0-1 IBD	Minor 2-3 IBD	Moderate 4-10 IBD	Severe >10 IBD
N	927	423 (46)	333 (36)	171 (18)	372 (40)	379 (41)	124 (13)	52 (6)
Male	600 (65)	319 (75)	193 (58)	88 (51)	251 (67)	239 (63)	76 (61)	34 (65)
Age (yrs)	60.3±11.0	61.5±10.6	61.0±11.4	56.2.0±10.3	61.8±10.6	58.5.±11.0	60.1±11.2	63.7±11.7
Long-term β-blockers	428 (46)	241 (57)	134 (40)	53 (31)	204 (55)	160 (42)	39 (31)	9 (17)
Mean HRF (bpm)	69.1±11.3	57.6±5.5	71.9±3.7	88.8±8.4	66.4±12.7	69.4±11.9	73.0±14.6	67.7±13.9
Mean HRV (IBD)	3.9±8.4	3.2±8.2	3.4±5.7	3.1±3.8	0.9±0.4	2.2±0.5	5.1±1.6	23.3±18.5
SCAN PARAMETERS								
Pitch‡	0.30±0.07	0.25±0.04	0.31±0.05	0.38±0.07	0.29±0.07	0.30±0.07	0.30±0.07	0.26±0.06
Pitch╤	0.29±0.06	0.25±0.03	0.30±0.04	0.38±0.05	0.27±0.05	0.29±0.06	0.31±0.06	0.25±0.06
Fixed ECG pulsing ‡	640 (69)	303 (72)	218 (66)	119 (70)	304 (82)	236 (62)	65 (52)	35 (67)
Optimal ECG pulsing ╤	287 (31)	120 (28)	115 (34)	52 (30)	68 (18)	143 (38)	59 (48)	17 (33)
CTDI_{VOL} (mGy) ‡	65.6±15.1	73.1±13.5	62.0±11.5	53.6±14.4	63.6±13.4	64.7±12.3	69.6±16.6	83.9±19.0
CTDI_{VOL} (mGy) ╤	50.6±16.5	48.3±11.7	56.1±14.0	42.7±16.9	47.1±10.8	47.3±12.1	52.2±19.4	82.3±19.2
CTDI_{w} (mGy) ‡	18.5±1.7	18.1±1.8	18.7±1.5	19.5±1.4	18.0±1.5	18.7±1.3	19.8±1.9	20.4±1.9
CTDI_{w} (mGy) ╤	14.3±4.3	11.7±3.5	16.6±3.5	14.9±4.1	12.8±3.8	13.7±3.9	15.4±3.9	20.4±2.8

N indicates number; HRF, heart rate frequency; HRV, heart rate variability, ; bpm; IBD, interbeat difference; CCA, conventional coronary angiography; CTDI; computed tomography dose index; ‡ indicates a fixed adaptive ECG pulsing algorithm (ECG pulsing window: 25-70% of R-R interval (all HRF), and reduced exposure to 20% of maximum outside the ECG pulsing window) ╤ indicates optimal adaptive ECG pulsing algorithms (ECG pulsing windows: 60-76% of R-R-interval in HRF ≤ 65 , 30-77% of R-R-interval in HRF 66-79 , 31-47% of R-R-interval in HRF ≥80 , and reduced exposure to 4% of maximum outside the ECG pulsing window)

Chapter 4

Impact of heart rate frequency and variability on radiation exposure, image quality, and
diagnostic performance in dual-sourcespiral CT coronary angiography

Radiation exposure

Adaptive ECG pulsing was successfully applied in all patients and no cases were excluded due to incorrect timing of the high X-ray tube output. In patients scanned with a fixed ECG pulsing window and 20% tube current reduction outside the ECG pulsing window, mean CTDIvol was significantly (p <0.05) lower in high HRF (53.6 mGy) compared to low HRF (73.1 mGy). This dose reduction can be contributed to the increase of pitch values for higher heart rates. The efficacy of ECG-pulsing in this group of patients is significantly (p <0.001) influenced by HRF and HRV. However, the impact of HRV and HRF in this group is moderate: the mean CTDIw was only 7% higher in the high HRF group (19.5 mGy) compared to the low HRF group (18.1 mGy), and 12% in the severe HRV group (20.4 mGy) compared to the normal HRV group (18.0 mGy). The impact on radiation exposure due to HRV within the different groups of HRF was not significantly different (p = 0.1). In patients scanned with optimal ECG pulsing windows and 4% tube current reduction outside the ECG pulsing window, differences in CTDIvol between low HRF and high HRF were smaller compared to the corresponding differences in patients scanned with fixed ECG pulsing windows. Both the HRF and HRV have a significant (p < 0.001) impact on the efficacy of ECG-pulsing in the group of patients with optimized ECG-pulsing. The mean CTDIw was 30% higher in the intermediate HRF group (16.6 mGy) compared to the low HRF group (11.7 mGy), and 21% higher in the high HRF group (14.9 mGy) compared to the low HRF group. The mean CTDIw was even 37% higher in patients with severe HRV (20.4 mGy) as compared to the normal HRV group (12.8 mGy). We observed a significant difference (p = 0.01) on the impact of radiation exposure due to HRV within the different groups of HRF, which can be explained by the relatively low number of patients with both a high HRF and HRV in this group of patients.

Image quality

The best selected datasets yielded good image quality in 98% (910/927) and impaired image quality in 2% (18/927) of patients. Impaired image quality was more frequently found in patients with high HRF (5%, 8/171) compared to intermediate (2%, 8/333) or low (1%, 2/423) HRF, and in patients with severe HRV (10%, 5/52) compared to moderate (7%, 9/124), minor (1%, 3/379), or normal (1%, 1/201) HRV. However, these differences in image quality found among HRF or HRV groups were not statistically different.

Diagnostic performance

The diagnostic performance of CTCA to detect significant coronary artery stenosis according to HRF and HRV are detailed in Table 2 (segment-by-segment and patient-by-patient analysis).

The analysis per segment was confirmed by bootstrap analysis. Kappa-values for the inter- and intra-observer variability on a per segment level were 0.70 and 0.73, respectively. In patients with low (≤65 bpm), intermediate (66-79 bpm) and high (≥80 bpm) HRF, sensitivity was 100%, 99%, and 100% on an overall patient-by-patient analysis.

Table 2. Impact of Heart Rate Frequency (HRF) and Heart Rate Variability (HRV) on Diagnostic Performance of Dual-source CTCA to Detect Significant (≥50% lumen diameter reduction) Coronary Artery Stenosis.

	OVERALL	HRF GROUPS			HRV GROUPS			
		Low ≤65 bpm	Intermediate 66-79 bpm	High ≥80 bpm	Normal 0-1 IBD	Minor 2-3 IBD	Moderate 4-10 IBD	Severe >10 IBD
PATIENT LEVEL								
N	444	189	170	85	201	163	52	28
Prevalence of significant stenosis, %	71	81	69	55	75	71	65	61
Sensitivity, %	100 (98-100)	100 (97-100)	99 (95-100)	100 (91-100)	100 (97-100)	99 (96-100)	100 (87-100)	100 (77-100)
Specificity, %	85 (77-91)	81 (63-91)	87 (74-94)	87 (71-95)	80 (66-90)	90 (77-96)	83 (58-96)	91 (57-100)
PPV, %	94 (91-97)	96 (91-98)	94 (88-97)	90 (87-100)	94 (89-97)	96 (90-98)	92 (77-98)	94 (71-100)
NPV, %	99 (94-100)	100 (85-100)	98 (87-100)	100 (87-100)	100 (89-100)	98 (87-100)	100 (75-100)	100 (66-100)
SEGMENT LEVEL								
N	6788	2848	2613	1327	3066	2497	801	424
Prevalence of significant stenosis, %	11	14	10	8	12	11	10	8
Sensitivity, %	95 (93-96)	96 (93-96)	92 (88-95)	96 (90-99)	93 (90-96)	97 (94-98)	96 (89-99)	88 (72-96)
Specificity, %	96 (96-97)	96 (95-96)	97 (96-98)	96 (95-97)	96 (95-97)	96 (96-97)	97 (96-98)	96 (93-97)
PPV, %	76 (73-78)	77 (73-81)	77 (72-81)	69 (61-76)	75 (71-79)	77 (72-81)	80 (71-87)	64 (49-77)
NPV, %	99 (99-100)	99 (99-100)	99 (99-100)	100 (99-100)	99 (99-99)	100 (99-100)	100 (99-100)	99 (97-100)

N indicates number; HRF, heart rate frequency; HRV, heart rate variability; bpm; IBD, interbeat difference; PPV, positive predictive value; NPV, negative predictive value; number between parentheses indicates 95% confidence intervals. Values in parentheses represent upper and lower bound for 95% confidence interval.

Chapter 4

Impact of heart rate frequency and variability on radiation exposure, image quality, and
diagnostic performance in dual-sourcespiral CT coronary angiography

Figure 4 Subanalysis of Diagnostic Performance in Patients with Low (<100) and High (<100) Agatston.
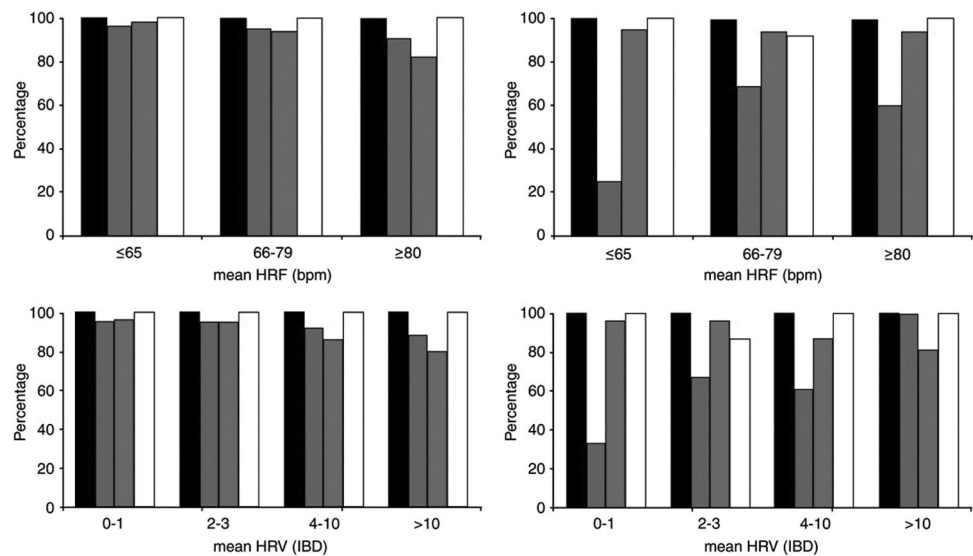
Graphs show subanalysis of diagnostic performance (black = sensitivity, blue = specificity, red = PPV, white = NPV) in patients with low (≤100, upper and lower left) and high (>100, upper and lower right) Agatston scores. bpm = beats per minute.

Specificity was 81%, 87%, and 87%; positive predictive value 96%, 94%, and 90%; and negative predictive value 100%, 98% and 100%. In patients with normal (0-1 IBD), minor (2-3 IBD), moderate (4-10 IBD) and severe (>10 IBD) HRV, sensitivity was 100%, 99%, 100%, and 100% on an overall, patient-by-patient analysis. Specificity was 80%, 90%, 83% and 91%; positive predictive value 94%, 96%, 92%, 94%; and negative predictive value 100%, 98%, 100%, and 100%. A subanalysis according to Agatston calcium scores showed no significant differences in sensitivity, specificity, positive and negative predictive value among HRF or HRV groups in patients with low Agatston scores (≤100). However, there was a nonsignificant trend towards a lower specificity (96% vs. 91%) and lower positive predictive value (98% vs. 82%) in patients with low vs. high HRF. A similar trend was observed in patients with normal vs. severe HRV (specificity: 95% vs. 88%; positive predictive value: 95% vs. 88%) (Figure 4). In patients with high Agatston scores (>100), we did not observe such a trend and diagnostic performance did not correlate to HRV or HRF.

Figure 5
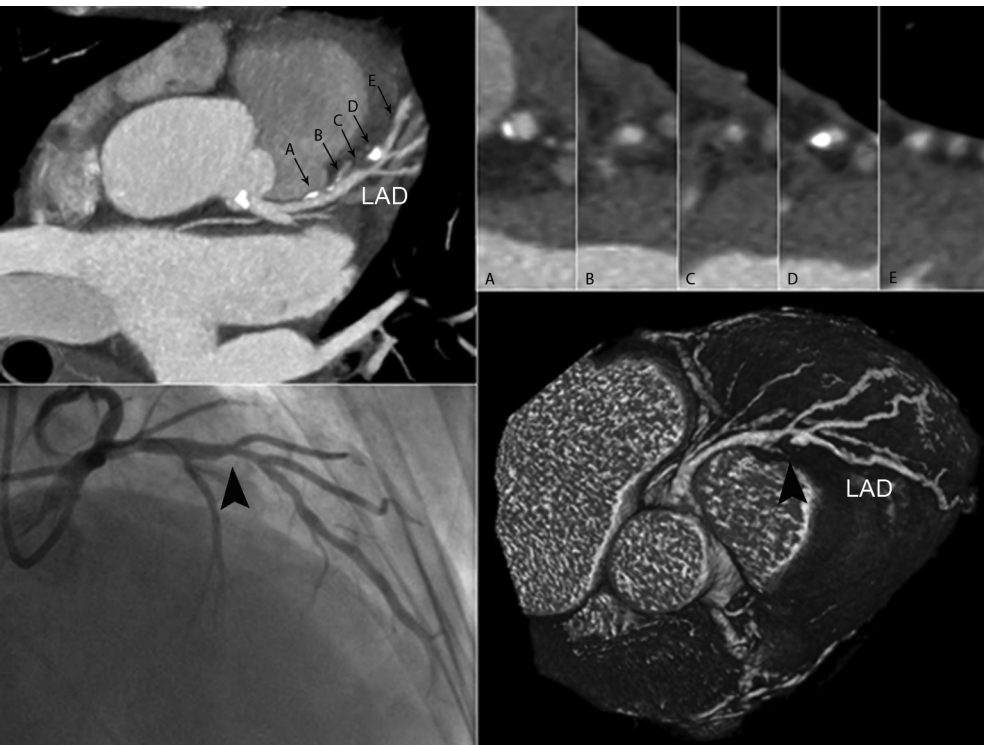
Coronary angiography in patient with atrial fibrillation with slow ventricle response. CT coronary angiogram (upper left) shows cross-sections of proximal left anterior descending artery (LAD) A–E (upper right). Conventional coronary angiogram (lower left) and volume-rendered reconstruction (lower right) show stenosis (arrowhead).

DISCUSSION

CT coronary angiography has emerged as a reliable tool to detect or rule out significant stenoses in selected patients with regular and preferably low (<65 bpm) heart rates. Beta-blockers are commonly administered prior to CTCA to lower the heart rate, thereby reducing the number of image-degrading motion artifacts. Dual-source CT scanners provide an improved temporal resolution compared to conventional (single-source) CT equipment and may obviate the need for pre-scan beta-blockers [15, 16]. Previous small-sized studies demonstrated an increased diagnostic performance of spiral CTCA using dual-source equipment in patients with various HRF. However, the number of included patients with high HRF (>80 bpm) was consistently low, and the vast majority of studies excluded patients with arrhythmias [15-21]. Few studies have investigated the impact of heart rate variability on image quality and diagnostic performance. In these studies, HRV was defined as the standard deviation of the mean heart rate during CTCA. However, this definition of HRV may not give accurate insight of the impact of HRV during spiral CTCA;

Chapter 4

Impact of heart rate frequency and variability on radiation exposure, image quality, and
diagnostic performance in dual-sourcespiral CT coronary angiography

Figure 6
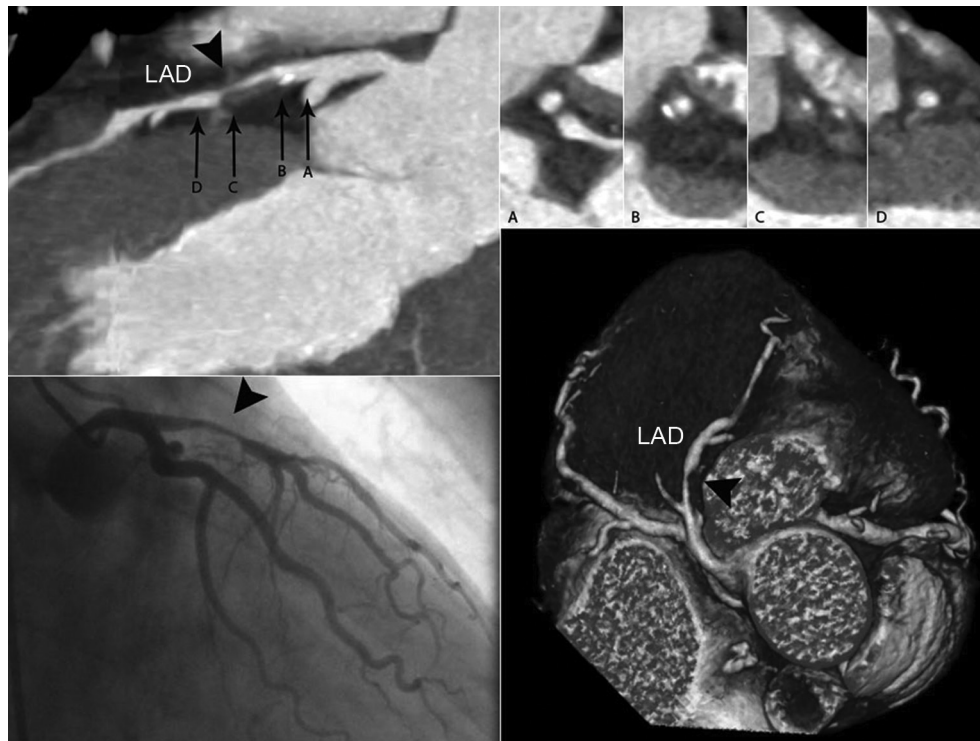
Coronary angiography in patient with high HRF (84 beats/min). CT coronary angiogram (upper left) shows cross-sections of proximal left anterior descending artery (LAD) A–D (upper right). Conventional coronary angiogram (lower left) and volume-rendered reconstruction (lower right) show stenosis (arrowhead).

a gradual increase in heart rate frequency does not generally impact on image quality, while the SD of the mean HR may be high. Instead, a sudden change in heart rate may cause several problems in the acquisition of spiral CTCA, such as: 1) mis-triggering of the ECG pulsing algorithm resulting in low-dose images at the desired phase of image reconstruction, and 2) artifacts due to differences in image reconstruction phases between consecutive heart beats. Previously, ECG pulsing could not be applied in patients with arrhythmias. The adaptive ECG pulsing algorithm reacts to such a sudden change in R-R interval by switching off the ECG pulsing during subsequent R-R-intervals. We therefore defined HRV as the mean inter-beat difference between 2 consecutive heart beats, and studied the impact of adaptive ECG pulsing on radiation exposure, image quality and diagnostic performance of dual-source CTCA in a large patient population with a wide variety of heart rates. We tested the use of a newly developed, adaptive ECG pulsing algorithm in a large cohort of patients with various HRF and HRV. We observed no patients with impaired image quality on the basis of mis-triggering of the ECG pulsing algorithm, even in patients with severe HRV. This finding indicates that adaptive ECG pulsing is now robust and should be used in all patients undergoing spiral CTCA. However, it should be

noted that the dose reduction feature of ECG pulsing is almost completely eliminated in patients with severe HRV, because the ECG pulsing is partly or totally or switched off throughout the scan in patients with arrhythmia to maintain diagnostic image quality. Therefore, the potential benefit of spiral CTCA should be carefully weighed against the risk of developing radiation induced cancer, in particular, in young patients presenting with arrhythmias [22]. We found a high overall diagnostic performance of Dual-source CTCA in the detection or exclusion of significant coronary artery stenosis with a sensitivity of 100% and a negative predictive value of 99% on a per patient basis. These results were obtained without exclusion of any segments or patients on the basis of impaired image quality. We found no significant differences in image quality or diagnostic performance among HRF and HRV groups. We only observed a trend towards more 'false positive' results reflected by a lower specificity and positive predictive value in patients with low calcium scores (<100 Agatston score) and HRF ≥80 bpm or HRV >10 IBD. We did not find this trend in patients with higher calcium scores, which indicates that the well known impact of severe coronary calcifications outweighs the limited impact of HRF or HRV on diagnostic performance of CTCA. An important disadvantage of spiral CTCA is its relatively high radiation exposure [3]. Recently, sequential or step-and-shoot (SAS) CTCA has gained renewed interest as a scan technique to reduce radiation exposure while preserving diagnostic image quality. However, SAS CTCA is currently limited to selected patients with low and regular heart rates only [23-26]. Although this scan mode was not yet available during the inclusion period of our study, we estimated on the basis of heart rate characteristics (low HRF and normal to minor HRV) in our study population (n=927) that SAS CTCA could have been successfully carried out in approximately 38% (355/927) of patients. The majority of these patients (57%, 204/355) were already on long term beta-blockers, and it may be expected that the number of patients suitable for SAS CTCA would significantly increase by the use of pre-scan beta-blockers. However, spiral CTCA still remains the preferred scan mode in patients with arrhythmias and or fast HRF. Particularly, spiral CTCA can be used as an alternative to the SAS CTCA in patients with contraindications to administration of beta-blockers (e.g. overt heart failure) or in patients with insufficient decrease of HRF (<65 bpm) despite the use of pre-scan beta-blockers.

Limitations
In our study, arrhythmic patients were not excluded from CTCA with the exception of a small number (n=6) of patients with atrial fibrillation with fast ventricle response and inclusion of these patients would most likely result in a lower diagnostic performance of dual-source CTCA. We believe that dual-source CTCA is not yet ready for clinical use in these specific patients, because of the occurrence of severe motion artifacts despite the improved temporal resolution of dual-source CT scanners. Future developments such as complete data acquisition during a single heart beat combined with a further increase in temporal resolution of e.g. 25 ms may result in a true heart rate independent image acquisition, even in patients with severe arrhythmia.

Chapter 4

Impact of heart rate frequency and variability on radiation exposure, image quality, and
diagnostic performance in dual-sourcespiral CT coronary angiography

CONCLUSION

The use of adaptive ECG pulsing at Dual-source spiral CT coronary angiography provides
diagnostic image quality and reliable detection and rule out of obstructive coronary ar-
tery disease independent of heart rate frequency or heart rate variability at the cost of a
limited dose reduction in arrhythmic patients.

REFERENCES

1. Garcia MJ, Lessick J, Hoffmann MH. Accuracy of 16-row multidetector computed tomography
    for the assessment of coronary artery stenosis. Jama 2006; 296:403-411.
2. Stein PD, Yaekoub AY, Matta F, Sostman HD. 64-slice CT for diagnosis of coronary artery disease:
    a systematic review. Am J Med 2008; 121:715-725.
3. Einstein AJ, Moser KW, Thompson RC, Cerqueira MD, Henzlova MJ. Radiation dose to patients
    from cardiac diagnostic imaging. Circulation 2007; 116:1290-1305.
4. Brenner DJ, Hall EJ. Computed tomography--an increasing source of radiation exposure. N Engl
    J Med 2007; 357:2277-2284.
5. Zanzonico P, Rothenberg LN, Strauss HW. Radiation exposure of computed tomography and
    direct intracoronary angiography: risk has its reward. J Am Coll Cardiol 2006; 47:1846-1849.
6. Weustink AC, Mollet NR, Pugliese F, et al. Optimal electrocardiographic pulsing windows
    and heart rate: effect on image quality and radiation exposure at dual-source coronary CT
    angiography. Radiology 2008; 248:792-798.
7. Stolzmann P, Scheffel H, Schertler T, et al. Radiation dose estimates in dual-source computed
    tomography coronary angiography. Eur Radiol 2008; 18:592-599.
8. Cademartiri F, Mollet NR, Runza G, et al. Improving diagnostic accuracy of MDCT coronary
    angiography in patients with mild heart rhythm irregularities using ECG editing. AJR Am J
    Roentgenol 2006; 186:634-638.
9. Flohr TG, Stierstorfer K, Ulzheimer S, Bruder H, Primak AN, McCollough CH. Image reconstruction
    and image quality evaluation for a 64-slice CT scanner with z-flying focal spot. Med Phys 2005;
    32:2536-2547.
10. Austen WG, Edwards JE, Frye RL, et al. A reporting system on patients evaluated for coronary
    artery disease. Report of the Ad Hoc Committee for Grading of Coronary Artery Disease, Council
    on Cardiovascular Surgery, American Heart Association. Circulation 1975; 51:5-40.
11. Reiber JH, Serruys PW, Kooijman CJ, et al. Assessment of short-, medium-, and long-
    term variations in arterial dimensions from computer-assisted quantitation of coronary
    cineangiograms. Circulation 1985; 71:280-288.
12. McCollough CH. Patient dose in cardiac computed tomography. Herz 2003; 28:1-6.
13. Efron B TR. An Introduction to the Bootstrap. 1993.
14. Zhou XH ON, McClish DK. . Statistical Methods in Diagnostic Medicine, 2002.
15. Weustink AC, Meijboom WB, Mollet NR, et al. Reliable high-speed coronary computed
    tomography in symptomatic patients. J Am Coll Cardiol 2007; 50:786-794.
16. Ropers U, Ropers D, Pflederer T, et al. Influence of heart rate on the diagnostic accuracy of dual-
    source computed tomography coronary angiography. J Am Coll Cardiol 2007; 50:2393-2398.
17. Leber AW, Johnson T, Becker A, et al. Diagnostic accuracy of dual-source multi-slice CT-coronary
    angiography in patients with an intermediate pretest likelihood for coronary artery disease. Eur
    Heart J 2007; 28:2354-2360.
18. Johnson TR, Nikolaou K, Busch S, et al. Diagnostic accuracy of dual-source computed
    tomography in the diagnosis of coronary artery disease. Invest Radiol 2007; 42:684-691.

Chapter 4

Impact of heart rate frequency and variability on radiation exposure, image quality, and diagnostic performance in dual-sourcespiral CT coronary angiography

19. Scheffel H, Alkadhi H, Plass A, et al. Accuracy of dual-source CT coronary angiography: First experience in a high pretest probability population without heart rate control. Eur Radiol 2006; 16:2739-2747.

20. Matt D, Scheffel H, Leschka S, et al. Dual-source CT coronary angiography: image quality, mean heart rate, and heart rate variability. AJR Am J Roentgenol 2007; 189:567-573.

21. Brodoefel H, Burgstahler C, Tsiflikas I, et al. Dual-source CT: effect of heart rate, heart rate variability, and calcification on image quality and diagnostic accuracy. Radiology 2008; 247:346-355.

22. Einstein AJ, Henzlova MJ, Rajagopalan S. Estimating risk of cancer associated with radiation exposure from 64-slice computed tomography coronary angiography. Jama 2007; 298:317-323.

23. Husmann L, Valenta I, Gaemperli O, et al. Feasibility of low-dose coronary CT angiography: first experience with prospective ECG-gating. Eur Heart J 2008; 29:191-197.

24. Stolzmann P, Leschka S, Scheffel H, et al. Dual-Source CT in Step-and-Shoot Mode: Noninvasive Coronary Angiography with Low Radiation Dose. Radiology 2008; 249:71-80.

25. Scheffel H, Alkadhi H, Leschka S, et al. Low-Dose CT Coronary Angiography in the Step-and-Shoot Mode: Diagnostic Performance. Heart 2008.

26. Hsieh J, Londt J, Vass M, Li J, Tang X, Okerlund D. Step-and-shoot data acquisition and reconstruction for cardiac x-ray computed tomography. Med Phys 2006; 33:4236-4248.

Chapter 5

Image quality and radiation
exposure using different low-dose
scan protocols in dual-source CT
coronary angiography:
a randomized study

Lisan A. Neefjes
Anoeshka S. Dharampal
Alexia Rossi
Koen Nieman
Annick C. Weustink
Marcel L. Dijkshoorn
Gert-Jan R ten Kate
Admir Dedic
Stella L. Papadopoulou
Marcel van Straten
Filippo Cademartiri
Gabriël P. Krestin
Pim J. de Feyter
Nico R. Mollet

Chapter 5

Image quality and radiation exposure using different low-dose scan protocols
in dual-source CT coronary angiography: a randomized study

ABSTRACT

Objective To compare image quality, radiation dose, and their relation with heart rate of different CT coronary angiography (CTCA) scan protocols using a 128-slice Dual-Source CT scanner.

Materials and Methods The institutional review board approved the study and all patients gave informed consent. We included 272 patients (175 men; mean age, 58 years) referred to CTCA. Patients were categorized according to heart rate: less than 65 beats per minute (group A) and 65 beats per minute or greater (group B). Patients were randomized to undergo prospective high-pitch spiral scanning and narrow-window prospective sequential scanning in group A (n=160) or wide-window prospective sequential scanning and retrospective spiral scanning in group B (n=112). Image quality was graded (1 = non-diagnostic, 2 = artifacts present but diagnostic, 3 = no artifacts) and compared (Mann-Whitney and Student's t tests).

Results In group A, image quality grade was significantly lower with high pitch spiral versus sequential scanning (2.67 ± 0.38 [standard deviation] vs 2.86 ± 0.21; P < .001). In a subpopulation (heart rate, <55 beats per minute), mean image quality grade was similar (2.81 ± 0.30 vs 2.94 ±0.08; P = .35).

In group B, image quality grade was comparable between sequential and retrospective spiral scanning (2.81 ± 0.28 vs 2.80 ± 0.38; P = .54).

Mean estimated radiation dose was significantly lower (high pitch spiral vs sequential scanning) in group A (for 100 kV, 0.81 mSv ± 0.30 vs 2.74 mSv ± 1.14; P < .001; for 120 kV, 1.65 mSv ± 0.69 vs 4.21 mSv ± 1.20; P < .001) and in group B (sequential vs retrospective spiral scanning) (for 100 kV, 4.07 mSv ± 1.07 vs 5.54 ± 1.76; P < .02; for 120 kV, 7.50 mSv ± 1.79 vs 9.83 ± 3.49; P < .1).

Conclusion A high pitch spiral CT coronary angiographic protocol should be applied in patients with regular and low (<55 beats per minute) heart rates; a sequential protocol is preferred in all others.

INTRODUCTION

CT coronary angiography (CTCA) has evolved into a reliable, non-invasive technique to detect or rule out significant coronary stenosis [1-4]. However, the expanding application of CT in general [5-6], and especially of CTCA with its relatively high dose, has led to concerns about radiation exposure [7-9].

The second generation dual source CT scanner is equipped with radiation reducing technology. Firstly, prospective ECG-triggered sequential scanning may be used in patients with high (>65 bpm) heart rates due to a high temporal resolution of 75 ms [10]. Secondly, a prospective ECG-triggered high pitch spiral (HPS) scan protocol has been developed, which allows scanning of the heart with a total scan time of approximately 270 ms [11-14]. Especially the latter scan mode shows promise for substantial reduction of radiation exposure in CTCA with reported dose values even below 1 mSv [11-14]. However, the feasibility and effect on both image quality and radiation exposure in a large patient population with various heart rates using these low-dose scan modes is currently unknown.

The purpose of this randomized study is to compare image quality, radiation dose, and their relation with heart rate of different CTCA scan protocols using a second generation Dual-Source CT scanner.

MATERIALS AND METHODS

The institutional review board approved the study and all patients gave informed consent. No conflict of interest is reported for all authors. Authors had full control of all the data and information presented in this manuscript.

Patient Population
During a 9-month period, 386 patients were referred to CTCA in our institution. Only patients without a previous history of percutaneous intervention (n=47) or bypass surgery (n=13) were eligible for our study. Patients with known allergy to iodinated contrast material (n=7), impaired renal function (serum creatinine>120 μmol/l) (n=10), persistent arrhythmias (n=14), and patients who refused to give informed consent (n=22) were excluded. Hence, we prospectively included 273 consecutive patients and they all underwent CTCA. One scan was excluded during the inclusion period because of lack of contrast material in the coronary arteries due to subcutaneous extravasation of contrast material (Fig 1).

All patients received nitroglycerin (0.4 mg/dose) sublingually just prior to the CT scan. Patients with a heart rate above 65 bpm, in the absence of contra-indications, received
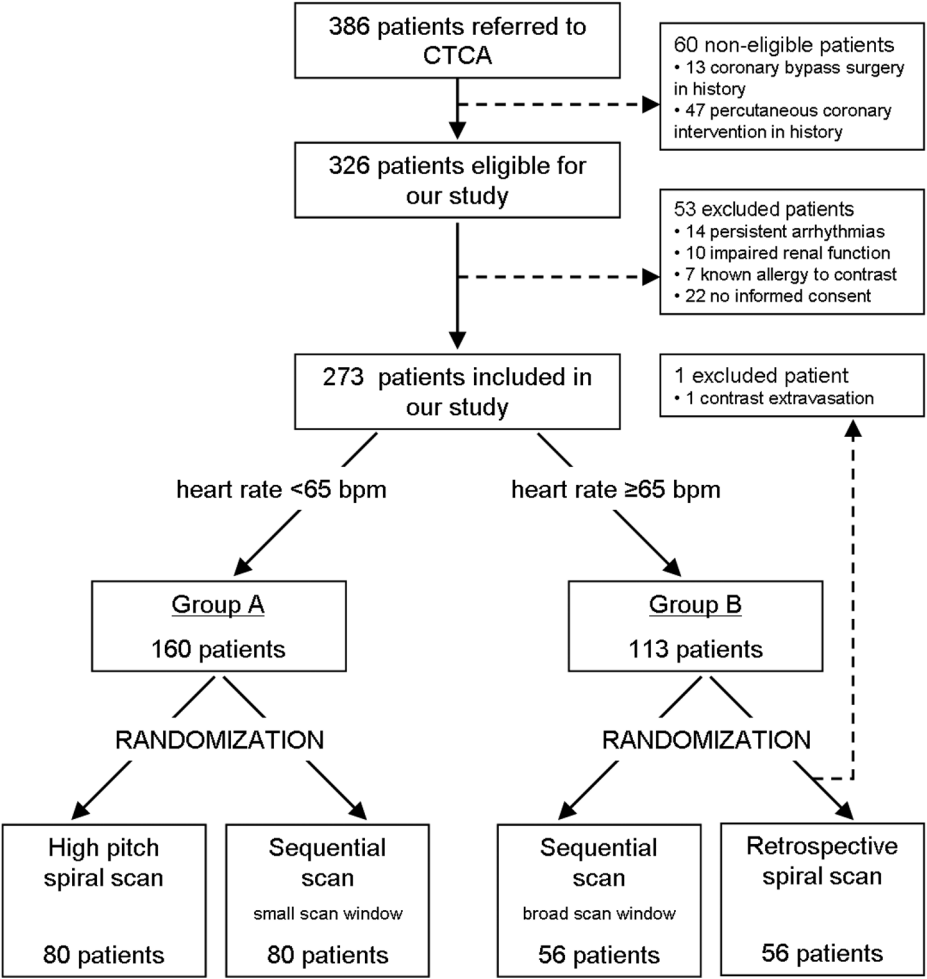
Chapter 5

Image quality and radiation exposure using different low-dose scan protocols
in dual-source CT coronary angiography: a randomized study

Figure 1 Flow chart showing patient inclusion and study design.
CTCA, CT coronary angiography.

a single dose of 100 mg metoprolol (Metoprololtartraat; Pharmachemie B.V., Haarlem, the Netherlands) 1 hour prior to the scan. A heart rate above 65 bpm was accepted in patients with contra-indications to β-blockade or patients not properly responding to the administered β-blocker. Finally 272 patients (175 men, mean age 58 years ± 11, range 34-82, and 97 women, mean age 59 years ± 12, range 25-83) were eligible for analysis.

Scan Protocol and Scan Parameters
Patients were divided into 2 groups on the basis of the heart rate just prior to the scan after administration of oral β-blockers in patients with initial heart rates >65 bpm: patients with low heart rates (≤65 bpm) were categorized into group A, patients with high

heart rates (>65 bpm) into group B. Patients in group A were randomized using a block randomization (block size 10), to have a prospective ECG-triggered high pitch spiral or a prospective ECG-triggered sequential scan with a narrow scan window (62-75% of the R-R interval [15]). Patients in group B were randomized to have a prospective ECG-triggered sequential scan with a wide scan window (31-75% of the R-R interval) or a retrospective ECG-gated spiral scan (RS) with ECG-pulsing (maximum tube current at 31-75% of the R-R interval [15]) (Fig 1).

All CT scans were performed using a Dual-Source CT scanner (Somatom Definition Flash, Siemens Healthcare, Forchheim, Germany). This CT scanner is equipped with 2 X-ray tubes and 2 detectors rotating in the same plane around the patient, with an angular offset of 95°. Gantry rotation time is 0.28 s which provides a temporal resolution of 75 ms using a heart rate independent single-segment reconstruction. Detector collimation is 2 x 64 x 0.6 mm. A z-axis flying focal spot is applied which results in an acquisition of 2 x 128 slice per rotation.

CTCA scan parameters: Cranio-caudal scan direction. Tube voltage and reference tube current were adapted to the BMI of the patient: ≤30 kg/m^2 BMI 100 kV and 370 mAs, >30 kg/m^2 BMI 120 kV and 320 mAs. In addition automated tube current modulation was applied.

The scan parameters per scan protocol are summarized in Table 1.

High pitch spiral scan protocol (Fig 2a): Prospective ECG-triggering. Data obtained in a single heart beat, no phase selection possible. Scan time depending on the size of the heart, range: 269 (±28) ms. An automated check for feasibility of a high pitch spiral scan depending on the heart rate just prior to the scan was manually overruled if negative, so the study randomization for the scan protocol was not influenced.

Sequential scan protocol (Figs 2b and 2c): Prospective ECG-triggering. Scan window 62-75% of the R-R interval (group A) or 31-75% (group B). Dependent on the size of the heart 3 or 4 scan blocks (102 scans of 4 blocks (75%); mean scan length 129 mm).

Retrospective spiral scan protocol (Fig 2d): Retrospective ECG-gating with prospective ECG-pulsing. Maximum tube current output during 31-75% of the R-R interval. Outside this high output window a tube current of 4% of the reference mAs (320 or 370 mAs). Scan time depending on the size of the heart and heart rate (automatic pitch selection), range: 461 (±118) ms.

Contrast Protocol
A single bolus of Iodinated contrast media (Ultravist 370 mgI/ml, Bayer-Schering AG, Berlin, Germany) was used. Contrast volume was adapted to the scan protocol: high pitch spiral 75ml, sequential 100 ml, and retrospective spiral 75-100 ml (dependent of the scan

Chapter 5

Image quality and radiation exposure using different low-dose scan protocols
in dual-source CT coronary angiography: a randomized study

Table 1 Scan parameters of the different scan protocols.

Scan protocol	GROUP A		GROUP B	
	High pitch spiral	Sequential narrow scan window	Sequential wide scan window	Retropsective spiral
Detector configuration	2x64x0.6	2x64x0.6	2x64x0.6	2x64x0.6
Z-coverage detector (mm)	38.4	38.4	38.4	38.4
Scan FOV (mm)	332	500	500	500
Tube power (kW)	2x100	2x100	2x100	2x100
ATCM	Yes	Yes	Yes	Yes
Rotation time (s)	0.28	0.28	0.28	0.28
Temporal resolution (ms)	75	75	75	75
Spatial resolution (mm)	0.33	0.33	0.33	0.33
Pitch	3.4	-	-	0.17-0.35[1]
Scan window (% of the RR-interval)	Variable [2]	62% – 75%	31% – 75%	31% – 75%
Scan time (s)	0.22 - 0.35[2]	Variable[3]	Variable[3]	2.80 - 7.40[3]
Contrast agent	Ultravist 370	Ultravist 370	Ultravist 370	Ultravist 370
Volume (ml)	75	100	100	75-100[3]
Concentration (mgI/ml)	370	370	370	370
Injection flow rate (ml/s)	6.0	5.5	5.5	5.5

ATCM, automated tube current modulation; FOV, field of view. [1]heart rate dependent; [2]scan length dependent; [3]heart rate and scan length dependent.
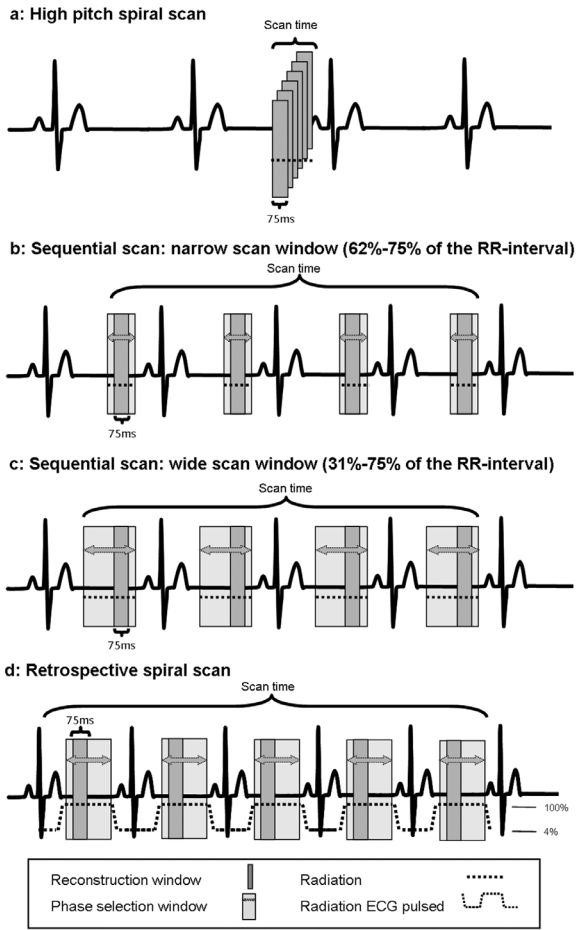
Figure 2 Schematic overview of the different CT coronary angiography scan protocols.

time). Contrast media was injected with a flow rate of 6.0 ml/s (high pitch spiral) or 5.5 ml/s (sequential and retrospective spiral) through an antecubital vein, followed by a saline chaser of 45 ml with the same flow rate. A bolus tracking technique was used to synchronize the arrival of the contrast media in the coronary arteries and the start of the CT scan.

Image Reconstruction

CTCA datasets were reconstructed with a slice thickness of 0.75 mm, an increment of 0.4 mm, a field of view of 180 mm, and a medium-soft convolution kernel (B26). An additional dataset with a sharp convolution kernel (B46) was reconstructed in patients with coronary calcifications. Datasets were manually (sequential scan protocol) or automatically and additionally manually (retrospective scan protocol) reconstructed in the optimal diastolic and, if possible, systolic phase to obtain maximum image quality. The high pitch spiral data acquisition does not allow for phase selection after the scan has been completed.

Image Evaluation

All datasets were sent to a dedicated workstation (MMWP, Siemens Healthcare, Forchheim, Germany). Image quality was evaluated on a per segment basis, using the 16-segment AHA classification model, by 2 independent observers (L.A.N. and A.S.D., each with more than 3 years of CTCA experience). If necessary multiple datasets were used for the quality assessment in sequential and retrospective spiral scans. Small segments with a diameter <1.5 mm were excluded from analysis. If necessary multiple datasets were used for the quality assessment in sequential and retrospective spiral scans.

Chapter 5

Image quality and radiation exposure using different low-dose scan protocols
in dual-source CT coronary angiography: a randomized study

Image quality was classified into three groups (Fig 3): 1: Poor image quality due to major motion artifacts; no diagnostic evaluation possible, 2: motion artifacts present, but adequate image quality for diagnostic evaluation, and 3: no motion artifacts present, good image quality. Discrepancies in image quality assessment were resolved in consensus during a joint evaluation. Inter-observer variability was assessed in all patients. One observer rescored a subpopulation of 50 randomly selected patients with a minimum time interval of 1 month between the initial and the second evaluation to assess intra-observer variability.

Figure 3 Curved Multiplanar reformatted images (cMPR) of the RCA of three different patients using a high pitch spiral scan protocol showing (A) poor image quality due to major motion artifacts; no diagnostic evaluation possible, (B) motion artifacts present, but adequate image quality for diagnostic evaluation, and (C) no motion artifacts present, optimal image quality.
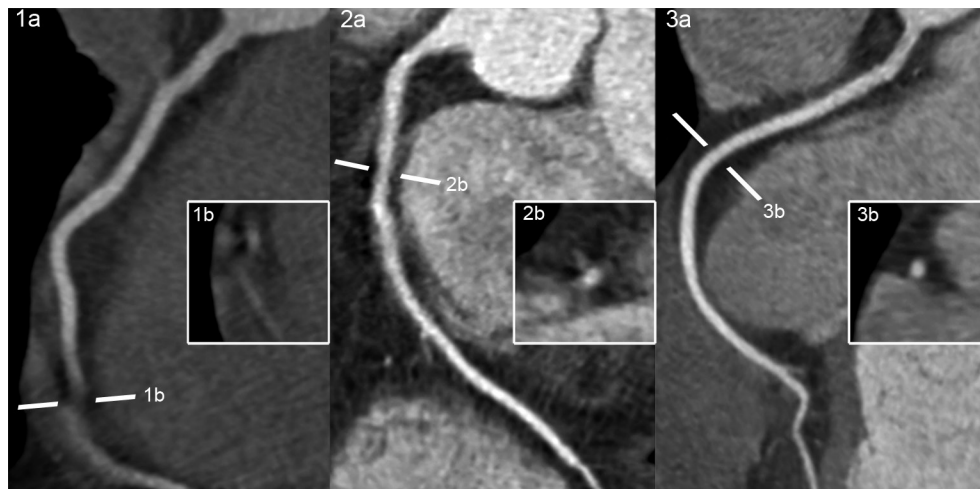
Image quality per patient was defined as the mean image quality of all coronary segments per patient. A CT scan was considered to have high quality if none of the segments was of poor quality graded as 1. A sub-analysis based on the heart rate during CTCA was performed to determine the influence of heart rate on image quality within a certain scan protocol.

Effective Dose Estimation

The mean estimated radiation dose per CTCA was calculated by multiplying the dose length product (DLP) by the conversion coefficient of 0.014 mSv·mGy^{-1}·cm^{-1} for the chest [16].

The expected overall mean estimated radiation dose in patients in group A and in patients in group B was calculated presuming we would have used the optimal scan protocols indicated by the results of our study, taking into account the BMI and heart rates of the patients.

Statistical Analysis

Continuous variables are shown as mean [±SD] or median [inter quartile range] if not normally distributed and categorical variables are expressed as number [frequency]. Differences in patient characteristics, heart rate and number of high quality scans were compared between the scan protocols in group A and in group B using a Student's T-test or the Mann-Whitney test for continuous variables and the chi square or the Fischer exact test for categorical data. Mean image quality was compared between the protocols in the A or B group with the Mann-Whitney test. Additionally a sub-analysis was performed to compare the mean image quality in different heart rate-categories. Pearson's correlation analysis was performed to assess the relation between mean image quality and heart rate variability, expressed as the standard deviation of the heart rate during CTCA.

Radiation dose was compared between the two scan protocols in group A and in group B, separately for the scans obtained with a tube voltage of 100 kV and of 120 kV, using a Student's T-test. In this latter case of multiple comparisons the p-value was corrected according to the Bonferroni method.

Inter- and intra-observer variability is described with κ-statistics. A p-value of <0.05 was considered statistically significant. All analyses were performed using SPSS for windows (version 15.0, SPSS, Chicago, USA).

RESULTS

Baseline characteristics

Baseline characteristics and primary results are shown in Table 2.
In group A, 80 patients (54 men (68%); mean age, 60 years [±11]) underwent a high pitch spiral scan (Fig 4), and 80 patients (59 men (74%); mean age, 59 years [±10]) a narrow-
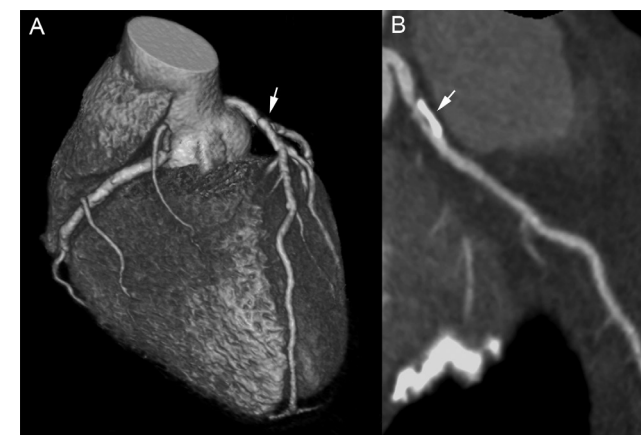
Figure 4 CT coronary angiography performed with the high pitch spiral scan protocol. Male, 58 years old, presenting with stable angina pectoris. Mean heart rate during the scan 54 beats per minute. Optimal image quality in all segments. Estimated radiation dose 0.67 mSv (tube voltage 100 kV). Volume Rendered Technique (VRT) image (A) revealing the anatomy of the coronary tree. Curved Multiplanar reformatted image (cMPR) of the LAD (B) showing a calcified obstructive lesion in the proximal part of the vessel.

Chapter 5

Image quality and radiation exposure using different low-dose scan protocols
in dual-source CT coronary angiography: a randomized study

Figure 5 CT coronary angiography performed with the prospective sequential scan protocol with a wide scan window. Female, 77 years old, presenting with stable angina pectoris. Mean heart rate during the scan was 78 bpm. Optimal image quality in all segments. Estimated radiation dose 3.05 mSv (tube voltage 100kV). Volume Rendered Technique (VRT) image (A) revealing the anatomy of the coronary tree. Curved Multiplanar reformatted image (MPR) of the LAD (B) showing a non-diseased coronary artery.
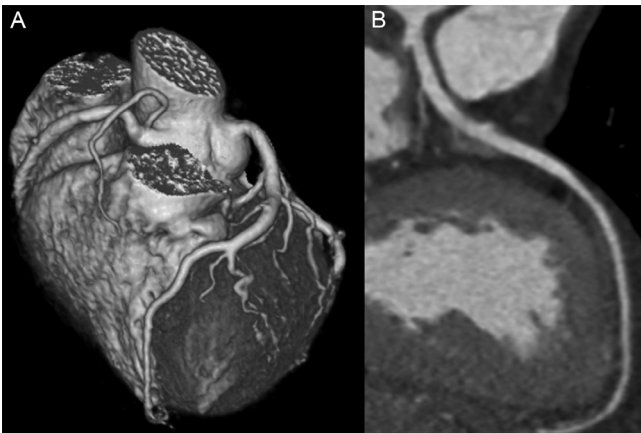
window sequential scan. In group B, 56 patients (30 men (54%); mean age, 57 years [±11]) underwent a wide-window sequential scan (Fig 5), and 56 patients (32 men (57%); mean age, 57 years [±12]) a retrospective spiral scan. The heart rate was not significantly different between the patients randomized in group A (high pitch spiral 58 [±7], sequential 59 [±6] bpm, p=0.30) and in group B (sequential 74 [±10], retrospective spiral 77 [±13] bpm, *P*=0.33).

Image quality

In group A, 1092 coronary segments were scanned by using a high pitch spiral scan protocol: 843 (77%) segments were classified as having good image quality (grade 3), 143 (13%) segments showed impaired image quality (grade 2), and 106 (10%) were non-diagnostic (grade 1). A total number of 1120 segments were scanned with a narrow-window sequential scan protocol: 996 (89%) segments were classified as grade 3, 98 (9%) as 2 and 26 (2%) as 1. In group B, 633 (85%) segments of 746 segments scanned with the sequential scan protocol were classified as grade 3, 87 (12%) as 2 and 26 (3%) as 1. A total number of 721 segments were scanned with the retrospective spiral scan protocol: 605 (84%) were classified as grade 3, 82 (11%) as 2 and 34 (5%) as 1.

In group A, the average mean image quality per patient was statistically significantly lower with the high pitch spiral scan protocol (2.67 [±0.38]) than with the sequential scan protocol (2.86 [±0.21], *P*<0.001). In a selected patient population of patients with a heart rate below 55 bpm (*n*=40) our study was unable to show a significant difference in image quality between the high pitch spiral scan protocol (2.81 [±0.30]) and the sequential scan protocol (2.94 [±0.08], *P*=0.35) (Fig 6a). The overall number of high-quality scans was significantly lower using the high pitch spiral scan protocol (56/80) than using the sequential protocol (69/80, *P*<0.01).

In group B the average image quality per patient is not significantly different with the sequential scan (2.81 [±0.28]) and the retrospective spiral scan (2.80 [±0.38], *P*=0.54) (Fig 6b).

Table 2 Patient characteristics

Scan protocol	GROUP A			GROUP B		
	High pitch spiral	Sequential narrow scan window	p-value	Sequential wide scan window	Retrospective spiral	p-value
	n=80	n=80		n=56	n=56	
Age (years)	60 (11)	59 (10)	0.36	57 (11)	57 (12)	0.76
Sex (male)	54 (68%)	59 (74%)	0.39	30 (54%)	32 (57%)	0.70
Heart rate (bpm)	58 (7)	59 (6)	0.30	74 (10)	77 (13)	0.33
HR range	44-78	40-70		56-109	51-110	
Risk factors						
Hypertension†	38 (48%)	38 (48%)	0.88	24 (43%)	28 (50%)	0.45
Diabetes Mellitus‡	13 (16%)	11 (14%)	0.63	6 (11%)	15 (27%)	0.03
Smoking‖	24 (30%)	16 (20%)	0.15	21 (38%)	19 (34%)	0.42
Hypercholesterolemia§	39 (49%)	49 (61%)	0.13	24 (43%)	24 (43%)	1.00
Family history of CAD	40 (50%)	43 (54%)	0.69	24 (43%)	23 (41%)	0.85
Body Mass Index (kg/m2)	28 (4)	27 (4)	0.39	27 (5)	29 (6)	0.35
Mean image quality CTCA						
Per patient	2.67 (0.38)	2.86 (0.21)	<0.001	2.81 (0.28)	2.80 (0.38)	0.54
Proximal segments	2.67 (0.56)	2.94 (0.15)	<0.001	2.93 (0.15)	2.86 (0.32)	0.32
Mid segments	2.59 (0.50)	2.81 (0.30)	0.02	2.76 (0.35)	2.75 (0.41	0.65
Distal segments	2.69 (0.47)	2.81 (0.31)	0.28	2.74 (0.47)	2.80 (0.42)	0.63

Continuous data is expressed as mean (SD) and dichotomous data as n (%). CAD, Coronary Artery Disease; CTCA Computed Tomography Coronary Angiography. †Blood pressure >140/90 mm Hg or treatment for hypertension. ‡Treatment with oral anti-diabetic medicine or insulin. ‖Currently and/or in the past. §Total cholesterol >180ml/dl or treatment for hypercholesterolemia.

Chapter 5

Image quality and radiation exposure using different low-dose scan protocols
in dual-source CT coronary angiography: a randomized study

The number of high-quality scans was comparable between the sequential scan protocol (47/56) and the retrospective spiral scan protocol (50/56, P=0.54).

No significant correlation was found between the mean image quality and the heart rate variability using the high pitch spiral scan (R=0.122, P=0.32), sequential scan with narrow scan window (R=0.071, P=0.53), sequential scan with broad scan window (R=0.143, p=0.30) and with the retrospective spiral scan (R=0.248, P=0.07).

The κ-statistics of the inter-observer agreement for the evaluation image quality per coronary segment of all scans was 0.78. The intra-observer agreement was 0.83.

Radiation exposure
The estimated radiation dose in group A was significantly lower with the high pitch spiral scan protocol than with the narrow-window sequential protocol for both tube voltage of 100 kV (0.81 [±0.30] mSv, n=32 vs. 2.74 [±1.14] mSv, n=40, P<0.001) and 120 kV (1.65 [±0.69] mSv, n=48 vs. 4.21 [±1.20] mSv, n=40, P<0.001).

Figure 6 Mean image quality in relation to heart rate per scan protocol (a: group A; b: group B).
Error bars represent the standard deviation.
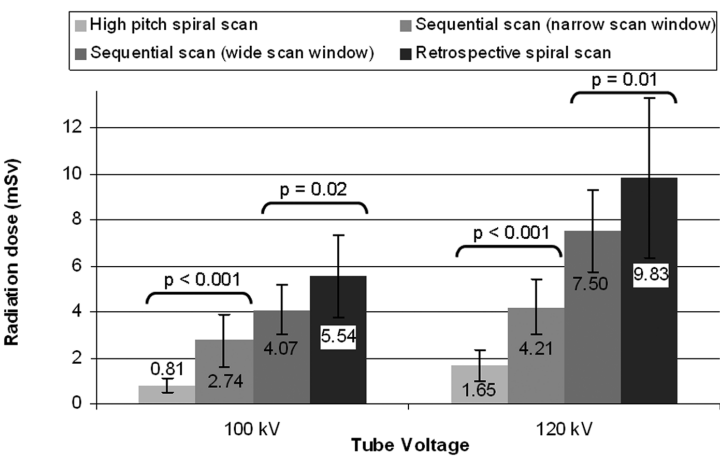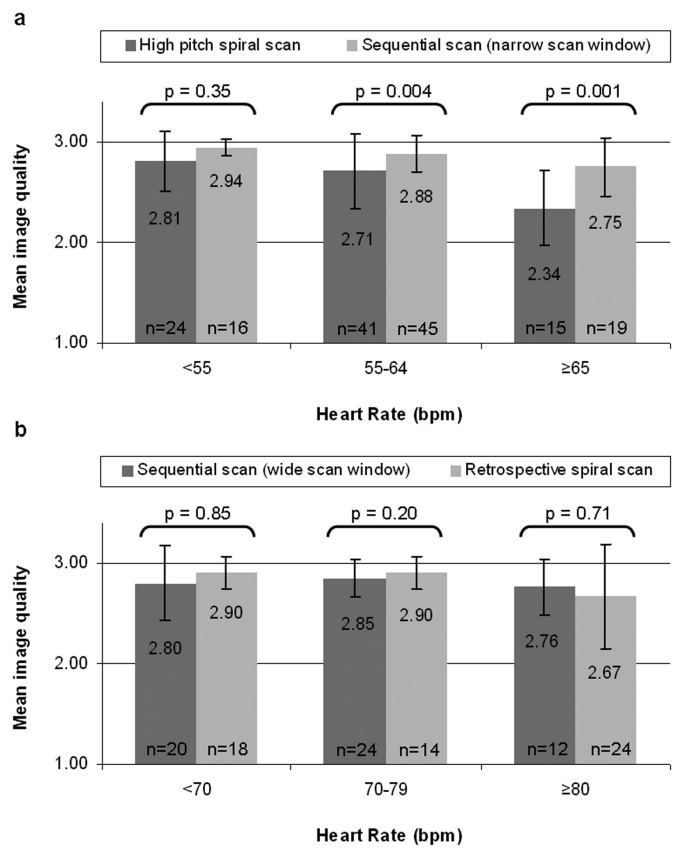
Figure 7 Estimated radiation dose in relation to tube voltage per scan protocol

Error bars represent the standard deviation.

In group B the dose was significantly lower using the wide-window sequential scan protocol compared to the retrospective scan protocol for both 100 kV (4.07 [±1.07] mSv, n=21 vs. 5.54 [±1.76] mSv, n=28, P=0.02) and 120 kV (7.50 [±1.79] mSv, n=35 vs. 9.83 [±3.49] mSv, n=28, P=0.01) (Fig 7).

On the basis of our results, we suggest the following scan protocol selection according to the ALARA principle: a high pitch spiral scan in patients with a heart rate <55bpm, a sequential scan protocol with a narrow scan window in patients with a heart rate between 55 and 65 bpm and a sequential scan with a wide scan window in patients with a heart rate > 65bpm. In our study population, the expected mean estimated radiation dose would have been 2.9 mSv in group A and 6.0 mSv in group B (Fig 8) if we would have followed these recommendations.
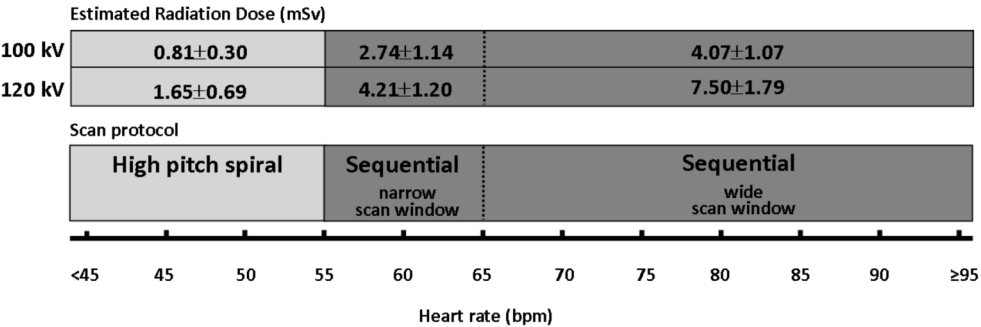
Figure 8 Proposed heart rate dependent selection of the appropriate CT coronary angiography scan protocol using a 128-slice Dual Source CT scanner and the concomitant estimated radiation exposure
Estimated radiation dose expressed as value±SD.

Chapter 5

Image quality and radiation exposure using different low-dose scan protocols
in dual-source CT coronary angiography: a randomized study

DISCUSSION

This randomized study shows that a high pitch spiral CTCA scan protocol offers a significant reduction in radiation dose compared to a narrow-window sequential scan protocol. However, in our study image quality is only maintained in a selected patient population with a very low (<55 bpm) heart rate. A wide-window sequential scan protocol offers a significant reduction in radiation dose compared to a retrospective spiral scan protocol and provides similar image quality.

The major challenge when selecting the appropriate CTCA scan protocol is to obtain optimal image quality and an as-low-as-reasonable-achievable radiation exposure. Especially the presence of coronary motion artifacts is related to the selected scan protocol, taking into account heart rate, systolic or diastolic phase acquisition and scan time. Other image degrading artifacts are thought to be patient-specific and not related to the selected scan protocol (e.g. 'blooming' artifacts related to coronary calcifications or 'beam hardening' artifacts). We therefore focused in this study on the presence of coronary motion artifacts using 4 different clinically used scan protocols.

We randomized between a high pitch spiral and a sequential (with a narrow, diastolic scan window) scan protocol in patients with a heart rate ≤65 bpm, because the feasibility and efficacy of the sequential scan protocol is well validated and is currently considered as the standard scan mode in this patient population [17-18]. We found that a high pitch spiral scan protocol provided high image quality in patients with heart rates <55 bpm, which was in line with previously published smaller sized, non-randomized studies [13; 19]. However, we found a lower overall image quality using a high pitch spiral scan protocol compared to a narrow-window sequential scan protocol in patients with heart rates ≥55 bpm. This finding was in contradiction to previous studies which reported similar image quality in patients with a heart rate up to 70 bpm [10-11; 14].

Patients with a heart rate above 65 bpm were randomized between a sequential or retrospective spiral (with ECG pulsing) scan protocol. A retrospective spiral scan protocol with ECG pulsing is currently routinely used in this patient population [20-21] and the value of sequential scanning in this group is not yet established. Both protocols were scanned with a scan window which incorporates both the systolic and diastolic phase to obtain maximum image quality in order to make a reliable comparison possible. We observed a significant lower radiation exposure with sequential compared to retrospective spiral scanning and we did not find significant differences in overall image quality between both groups.

The use of our scan protocol recommendations to achieve optimal image quality at lowest dose, can substantially lower the dose of CTCA in clinical practice. However, in addition these results emphasize the dose reducing potential of heart rate lowering medica-

tion (e.g. β-blockers) prior to the CTCA scan in patients with heart rates >65 bpm, which may reduce the radiation exposure by 50%. Moreover, it may also improve overall image quality, especially in patients with heart rates >80 bpm (Fig 6b).

Aggressive pre-scan heart rate lowering medication may be considered in young patients to induce a heart rate <55 bpm, which permits the use of a high pitch spiral scan protocol which is associated with a low dose (0.81 mSv using 100 kV tube voltage).

LIMITATIONS

We only included patients in sinus rhythm, because application of high pitch spiral scan protocols is not possible in irregular heart rates. However, current prospective sequential protocols include an adaptive algorithm that registers arrhythmia and only scans when the heart rate is stable again, which seems promising for the feasibility of sequential scan protocols in patients with mild arrhythmia (e.g. a single premature beat during scanning). Until this has been properly established, the RS scan protocol should be used in patients with arrhythmia [22-23].

Finally, the results of this study only apply to a 128-slice Dual-Source CT scanner and cannot be extrapolated to other CT systems.

CONCLUSION

The correct selection of a low-dose CTCA scan protocol using a 128-slice dual-source CT scanner results in a significantly lower radiation dose and comparable image quality compared to previously established CTCA scan protocols.

Chapter 5

Image quality and radiation exposure using different low-dose scan protocols
in dual-source CT coronary angiography: a randomized study

REFERENCES

1   Johnson TR, Nikolaou K, Busch S, et al. (2007) Diagnostic accuracy of dual-source computed tomography in the diagnosis of coronary artery disease. Investigative radiology, 42(10):684-691.

2   Scheffel H, Alkadhi H, Plass A, et al. (2006) Accuracy of dual-source CT coronary angiography: First experience in a high pre-test probability population without heart rate control. European radiology, 16(12):2739-2747.

3   Vanhoenacker PK, Heijenbrok-Kal MH, Van Heste R, et al. (2007) Diagnostic performance of multidetector CT angiography for assessment of coronary artery disease: meta-analysis. Radiology, 244(2):419-428.

4   Weustink AC, Meijboom WB, Mollet NR, et al. (2007) Reliable high-speed coronary computed tomography in symptomatic patients. Journal of the American College of Cardiology, 50(8):786-794.

5   Brenner DJ, Hall EJ (2007) Computed tomography--an increasing source of radiation exposure. N Engl J Med, 357(22):2277-2284.

6   Fazel R, Krumholz HM, Wang Y, et al. (2009) Exposure to low-dose ionizing radiation from medical imaging procedures. N Engl J Med, 361(9):849-857.

7   Einstein AJ, Henzlova MJ, Rajagopalan S (2007) Estimating risk of cancer associated with radiation exposure from 64-slice computed tomography coronary angiography. JAMA, 298(3):317-323.

8   Gerber TC, Carr JJ, Arai AE, et al. (2009) Ionizing radiation in cardiac imaging: a science advisory from the American Heart Association Committee on Cardiac Imaging of the Council on Clinical Cardiology and Committee on Cardiovascular Imaging and Intervention of the Council on Cardiovascular Radiology and Intervention. Circulation, 119(7):1056-1065.

9   American College of Cardiology Foundation Task Force on Expert Consensus D, Mark DB, Berman DS, et al. (2010) ACCF/ACR/AHA/NASCI/SAIP/SCAI/SCCT 2010 expert consensus document on coronary computed tomographic angiography: a report of the American College of Cardiology Foundation Task Force on Expert Consensus Documents. Circulation, 121(22):2509-2543.

10   Sommer WH, Albrecht E, Bamberg F, et al. (2010) Feasibility and radiation dose of high-pitch acquisition protocols in patients undergoing dual-source cardiac CT. Ajr, 195(6):1306-1312.

11   Leschka S, Stolzmann P, Desbiolles L, et al. (2009) Diagnostic accuracy of high-pitch dual-source CT for the assessment of coronary stenoses: first experience. European radiology, 19(12):2896-2903.

12   Ertel D, Lell MM, Harig F, Flohr T, Schmidt B, Kalender WA (2009) Cardiac spiral dual-source CT with high pitch: a feasibility study. European radiology, 19(10):2357-2362.

13   Achenbach S, Marwan M, Ropers D, et al. (2010) Coronary computed tomography angiography with a consistent dose below 1 mSv using prospectively electrocardiogram-triggered high-pitch spiral acquisition. European heart journal, 31(3):340-346.

14   Alkadhi H, Stolzmann P, Desbiolles L, et al. (2010) Low-dose, 128-slice, dual-source CT coronary angiography: accuracy and radiation dose of the high-pitch and the step-and-shoot mode. Heart, 96(12):933-938.

15   Weustink AC, Mollet NR, Pugliese F, et al. (2008) Optimal electrocardiographic pulsing windows and heart rate: effect on image quality and radiation exposure at dual-source coronary CT angiography. Radiology, 248(3):792-798.

16   Shrimpton P (2004) Assessment of patient dose in CT: appendix C—European guidelines for multislice computed tomography. European Commission project MSCT: CT safety & efficacy–a broad perspective. (ed)^(eds) http://www.msct.eu/PDF_FILES/Appendix%20paediatric%20CT%20Dosimetry.pdf (accessed 20 November 2008).

17   Pflederer T, Jakstat J, Marwan M, et al. (2010) Radiation exposure and image quality in staged low-dose protocols for coronary dual-source CT angiography: a randomized comparison. European radiology, 20(5):1197-1206.

18   Arnoldi E, Johnson TR, Rist C, et al. (2009) Adequate image quality with reduced radiation dose in prospectively triggered coronary CTA compared with retrospective techniques. European radiology, 19(9):2147-2155.

19   Lell M, Marwan M, Schepis T, et al. (2009) Prospectively ECG-triggered high-pitch spiral acquisition for coronary CT angiography using dual source CT: technique and initial experience. European radiology, 19(11):2576-2583.

20   Brodoefel H, Burgstahler C, Tsiflikas I, et al. (2008) Dual-source CT: effect of heart rate, heart rate variability, and calcification on image quality and diagnostic accuracy. Radiology, 247(2):346-355.

21   Weustink AC, Neefjes LA, Kyrzopoulos S, et al. (2009) Impact of heart rate frequency and variability on radiation exposure, image quality, and diagnostic performance in dual-source spiral CT coronary angiography. Radiology, 253(3):672-680.

22   Marwan M, Pflederer T, Schepis T, et al. (2010) Accuracy of dual-source computed tomography to identify significant coronary artery disease in patients with atrial fibrillation: comparison with coronary angiography. European heart journal, 31(18):2230-2237.

23   Rist C, Johnson TR, Muller-Starck J, et al. (2009) Noninvasive coronary angiography using dual-source computed tomography in patients with atrial fibrillation. Investigative radiology, 44(3):159-167.

Chapter 6

Diagnostic accuracy of 128-slice dual source CT coronary angiography: a randomized comparison of different acquisition scan protocols

Lisan A. Neefjes
Alexia Rossi
Tessa S.S. Genders
Koen Nieman
Stella L. Papadopoulou
Anoeshka S. Dharampal
Carl J. Schultz
Annick C. Weustink
Marcel L. Dijkshoorn
Gert-Jan R. ten Kate
Admir Dedic
Marcel van Straten
Filippo Cademartiri
M.G. Myriam Hunink
Gabriël P. Krestin
Pim J. de Feyter
Nico R. Mollet

Chapter 6

Diagnostic accuracy of 128-slice dual source CT coronary angiography:
a randomized comparison of different acquisition scan protocols

ABSTRACT

Objective To compare diagnostic performance and radiation exposure of 128-slice Dual-Source CT coronary angiography (CTCA) protocols to detect coronary stenosis with >50% lumen obstruction.

Materials and Methods We prospectively included 459 symptomatic patients referred for CTCA. Patients were randomized between high-pitch spiral vs. narrow-window sequential CTCA protocols (heart rate <65bpm; group A), or between wide-window sequential vs. retrospective spiral protocols (heart rate >65bpm; group B). Diagnostic performance of CTCA was compared with quantitative coronary angiography in 267 patients.

Results Group A (231 patients, 146 men, heart rate 58±7bpm): high-pitch spiral CTCA yielded a lower per-segment sensitivity compared to sequential CTCA (89% vs. 97%, P=0.01). Specificity, PPV and NPV were comparable (95%,62%,99% vs. 96%, 73%,100%, P>0.05) but radiation dose was lower (1.16±0.60 vs. 3.82±1.65 mSv, P<0.001).

Group B (228 patients, 132 men, heart rate 75±11bpm): per-segment sensitivity, specificity, PPV and NPV were comparable (94%, 95%, 67%, 99% vs. 92%, 95%, 66%, 99%, P>0.05). Radiation dose of sequential CTCA was lower compared to retrospective CTCA (6.12±2.58 vs. 8.13±4.52 mSv, P<0.001). Per-vessel and per-patient diagnostic performance was comparable in both groups.

Conclusion Sequential CTCA should be used in patients with regular heart rates using 128-slice Dual-Source CT, providing optimal diagnostic accuracy with "as-low-as-reasonably-achievable" radiation dose.

INTRODUCTION

CT coronary angiography (CTCA) is currently considered a reliable technique to detect, and especially rule out significant stenoses in patients with stable angina with a low or intermediate pre-test probability of having coronary artery disease (CAD) [1-6]. However, its non-invasive nature has been challenged during past years in publications reporting increased life-time attributable risk estimates of developing cancer associated to high radiation exposure [7-8]. These studies prompted CT vendors to develop hardware and software improvements to reduce radiation exposure, e.g. tube current modulation (ECG-pulsing), automated tube current modulation adapted to the body-size, implementation of prospective sequential (step-and-shoot) protocols and lower tube voltages [9-13].

In addition to these radiation lowering techniques, 128-slice Dual Source CT systems offer a high temporal resolution of 75 ms, a pitch up to 3.4 and 2 wide detector arrays. Hence this DSCT system provides two low dose CTCA protocols: a) a newly introduced prospective high-pitch spiral protocol which allows CT data acquisition of the entire heart within 1 heart beat and b) a prospective sequential protocol for patients with low and high (>65 bpm) heart rates. However, the diagnostic performance and effect on radiation exposure of these low dose CTCA protocols in patients with various heart rates is currently widely debated [14-17].

The purpose of this study was to determine and compare the diagnostic performance and radiation exposure of different CTCA protocols using 128-slice Dual Source CT to detect or rule out obstructive CAD.

MATERIALS AND METHODS

Study population

The institutional review board approved the study and all patients gave informed consent. Between May 2009 and November 2010, 549 symptomatic patients with stable anginal complaints were referred to CTCA in our institution. Patients with known allergy to Iodinated contrast material (*n*=8), impaired renal function (serum creatinine >120 μmol/L) (*n*=18), history of bypass surgery (*n*=18), persistent arrhythmias (*n*=17) and patients who refused to give informed consent (*n*=25) were excluded.

CTCA was carried out as part of the clinical diagnostic work-up of these 463 symptomatic patients suspected of having obstructive CAD. In general, patients with negative CTCA in combination with a negative stress test and/or good response to medical treatment were not referred to conventional coronary angiography (CCA). Exceptions to this rule were made based at the discretion of the referring physician (e.g. discordance between

symptoms and the results of diagnostic tests). Finally, 267 patients (58%) underwent CCA within 5 weeks after CTCA and were used for primary data analysis. The remaining 196 patients with only CTCA were used to account for verification bias.

All patients received nitroglycerin (0.4 mg/dose) sublingually just before CT. Patients with a heart rate above 65 bpm received a single dose of 100 mg metoprolol orally 1 hour before CT. A heart rate above 65 bpm was accepted in patients with contra-indications to β-blockade or patients not sufficiently responding to the administered β-blocker.

Patients were categorized into 2 groups based on pre-CT heart rate (after administration of β-blocker). Group A comprised patients with a heart rate <65 bpm and group B patients with a heart rate ≥65 bpm. Patients in group A were randomized to undergo either prospective high-pitch spiral CTCA or prospective sequential CTCA with a narrow CT acquisition window. Patients in group B were randomized to undergo either prospective sequential CTCA with a wide CT acquisition window or retrospective spiral CTCA. Patients were randomized using a block randomization (block size 10).

CT data acquisition and post processing

All CT was performed using a 128-slice Dual Source CT system (Somatom Definition Flash, Siemens Healthcare, Forchheim, Germany). This CT system has 2 X-ray tubes and 2 detector arrays rotating in the same plane with an angular offset of 95^0. Gantry rotation time is 280 ms, which provides a temporal resolution of 75 ms using a heart rate independent single-segment reconstruction. Detector collimation is 2 x 64 x 0.6 mm. A z-axis flying focal spot is applied which results in an acquisition of 2 x 128 slices per rotation.

In the high-pitch spiral mode prospective ECG-triggering was used to obtain a single dataset in a single heart beat [18] starting at 55% of the R-R interval. In the sequential mode prospective ECG-triggering was used with a narrow (group A; 62-75% of the R-R interval) or wide (group B; 31-75%) CT acquisition window [19]. The entire heart was covered in 3 or 4 heart beats. In the retrospective spiral mode retrospective ECG-gating was used in combination with prospective ECG-pulsing with maximum tube current output during 31-75% of the R-R interval. Outside this window, 4% of the reference tube current was used.

Tube voltage and reference tube current were adapted to the body mass index (BMI) of the patient: ≤30 kg/m^2 BMI 100 kV and 370 mAs, >30 kg/m^2 BMI 120 kV and 320 mAs.

We used a volume of 75 mL iodinated contrast media (Ultravist 370 mg I/mL, Bayer-Schering AG, Berlin, Germany) with a flow rate of 6.0 mL/s (high-pitch spiral) or 80-100 mL (CT acquisition time dependent) with a flow rate of 5.5 mL/s (sequential and retrospective spiral) followed by a saline chaser of 45 mL with the same flow rate.

Datasets were reconstructed with a slice thickness of 0.75 mm, an increment of 0.4 mm, a field of view of 180 mm, a medium-soft convolution kernel (B26) and additionally a sharp convolution kernel (B46) in patients exhibiting coronary calcium. Datasets were reconstructed in the optimal diastolic and, if applicable, systolic phase to obtain maximum image quality.

CT analysis

All datasets were sent to a off-line workstation (MMWP, Siemens Healthcare, Forchheim, Germany). Two independent observers, L.A.N. and A.R. (with both 5 years experience in cardio-vascular imaging) evaluated all CTCA data sets to assess the presence or absence of CAD and categorize the lesions (≤50% or >50% lumen diameter reduction) per coronary segment (modified AHA 16 segment model[20]). More than 50% lumen diameter reduction was considered obstructive disease. Additionally the image quality per segment was assessed (1: poor image quality due to major artefacts; no diagnostic evaluation possible, 2: minor or no artefacts present; adequate image quality for reliable evaluation). Discrepancies were resolved in consensus. Small sized coronary segments (<1.5 mm diameter, manually measured at its origin) (n=1117/7803), segments distal to an occlusion (n=74/7803) or stented segments (n=97/7803) were excluded.. Segments with non-diagnostic image quality were considered significantly obstructed with a maximum of 1 assumed obstructive segment per vessel in order not to underestimate the disease severity in this symptomatic patient population.

Effective dose estimation

The dose length product (DLP) per CTCA was assessed and we calculated the mean estimated radiation dose by multiplying the DLP by the conversion coefficient of 0.014 mSv·mGy^{-1}·cm^{-1} for the chest [21].

Quantitative coronary angiography (QCA)

One cardiologist (K.N., 8 years of experience in conventional coronary angiography), unaware of the CTCA results, evaluated all coronary angiograms. Lumen diameter reduction of all available non-stented segments (≥1.5 mm diameter) was assessed and categorized (≤50% or >50% lumen diameter reduction) using a validated QCA algorithm (CAAS, version 5.7, Pie Medical Imaging, Maastricht, The Netherlands). Lumen reduction of >50% was considered significant obstructive disease.

Statistical analysis

Statistical analysis was performed using commercially available software (Stata, version 11 for Windows; StataCorp, College Station, Texas, USA and SPSS, version 15.0 for windows, SPSS, Chicago, USA). Continuous variables are shown as mean (SD) or median (IQR) and categorical variables as number (%). The t-test or Mann-Whitney U test was used to compare continuous variables and the Chi-square test or the Fisher exact test for the comparison of categorical variables.

Chapter 6

Diagnostic accuracy of 128-slice dual source CT coronary angiography:
a randomized comparison of different acquisition scan protocols

The diagnostic performance including sensitivity, specificity, positive predictive value (PPV), and negative predictive value (NPV) of CTCA for the detection or exclusion of significant coronary stenosis compared to QCA were calculated with corresponding 95% confidence intervals (CIs) in those patients that underwent CCA. These parameters were calculated per patient, per vessel and per segment.

To take into account the correlation between different segments in a patient, we analyzed measures of diagnostic accuracy on vessel-level and segment-level by using generalized estimating equations, with the assumption of a binomial distribution of the dependent variable, a logit-link function, the patient as cluster, an equal-correlation model within each cluster, and the robust sandwich estimator of the variance. The analyses were performed separately for randomization within group A and group B. An indicator variable was used to estimate the difference between the CTCA protocols in each randomization group.

To account for verification bias the data was re-analyzed using inverse probability weighting [22-23]. The probability of verification with CCA was calculated at the patient-level using all patients who underwent CTCA, and based on a logistic regression model with verification as the dependent variable with the following predictors: chest pain type, presence of previously diagnosed CAD and CTCA result per segment. Subsequently, the accuracy analyses were performed using only the patients who underwent angiography, each patient weighted by the inverse of their probability of undergoing CCA (verification).

Inter-observer variability and agreement between CTCA and CCA to detect obstructive CAD were described with kappa-statistics.

RESULTS

Our initial study population comprised 463 consecutive patients scheduled for CTCA of which 233 were classified into group A (<65 bpm pre-CT heart rate) and 230 patients into group B (>65 bpm) to be examined according to the assigned protocol after randomization (Fig. 1). Two patients randomized to undergo high-pitch spiral CTCA experienced a sudden increase in heart rate of >75 bpm immediately before the CT examination. Due to the increased probability of non-diagnostic results, both were excluded from the study and underwent retrospective spiral CTCA [14]. Two patients in group B, assigned to undergo retrospective spiral CTCA, were excluded because of lack of contrast material in the coronary arteries due to technical failure of the contrast material injector (n=1) or contrast extravasation subcutaneously (n=1).
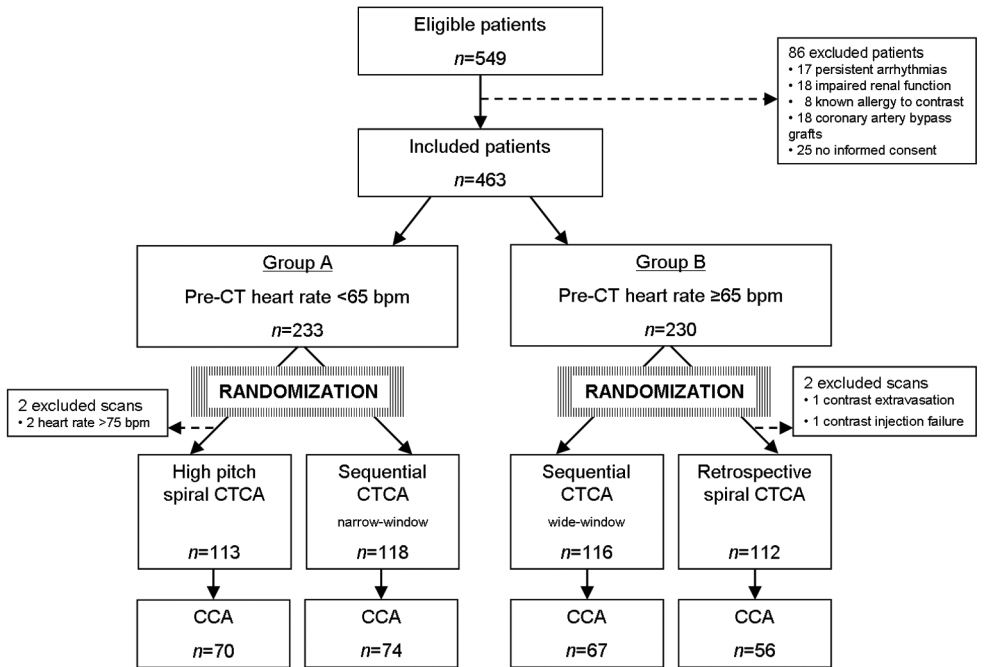
Fig. 1 Patient inclusion
Study design flowchart. CCA, conventional coronary angiography; CTCA, CT coronary angiography

In total 459 patients underwent CTCA of which finally 267 patients (58%) also underwent CCA (group A: high-pitch spiral, n=70; narrow-window sequential, n=74; group B: wide-window sequential, n=67 and retrospective spiral, n= 56).

Patient characteristics are shown in Table 1. In group A, the mean heart rate of patients examined with the high-pitch spiral CTCA protocol (57±6 bpm) was slightly lower than the heart rate in patients examined with the sequential CTCA protocol (60±7 bpm, p=0.01). In group B, the mean heart rate was similar between patients examined with the sequential CTCA protocol or the retrospective spiral CTCA protocol (75±10 vs. 75±12 bpm, respectively, P=0.93).

The patients that underwent both CTCA and CCA exhibited a prevalence of significant CAD based on CCA results of 79% (high-pitch spiral), 78% (narrow-window sequential), 76% (wide-window sequential) and 75% (retrospective spiral).

Diagnostic accuracy
The diagnostic performance, including the sensitivity, specificity, PPV and NPV of the 128-slice DSCT to detect or rule out significant coronary stenoses compared to CCA is shown in Table 2.

Chapter 6

Diagnostic accuracy of 128-slice dual source CT coronary angiography:
a randomized comparison of different acquisition scan protocols

Table 1 Patients characteristics

	All patients	Patients with CCA	Patients without CCA	P-value[f]
	n=459	n=267	n=192	
Age (years)	59 (11)	62 (11)	55 (11)	<0.001
Sex (male)	278 (61%)	181 (68%)	97 (50%)	<0.001
Heart rate (bpm)	67 (12)	65 (12)	69 (12)	<0.001
Risk factors				
Hypertension[a]	258 (56%)	166 (62%)	92 (48%)	<0.01
Diabetes Mellitus[b]	77 (17%)	46 (17%)	31 (16%)	0.76
Smoking[c]	152 (33%)	94 (35%)	58 (30%)	0.26
Hypercholesterolemia[d]	269 (59%)	177 (66%)	95 (48%)	<0.001
Family history of CAD	243 (53%)	140 (52%)	103 (54%)	0.80
Body Mass Index (kg/m^2)	27 (5)	27 (5)	27 (5)	0.40
Typical angina pectoris[e]	205 (45%)	161 (60%)	44 (23%)	
Atypical angina pectoris[e]	85 (19%)	34 (13%)	51 (27%)	
Non aginal chest pain[e]	169 (37%)	72 (27%)	97 (51%)	<0.001
Known CAD in history	71 (16%)	64 (24%)	7 (3%)	<0.001
Calcium score	45 (0-381)	242 (38-196)	1 (0-44)	<0.001
CCA				
No CAD	-	31 (12%)	-	-
Non-obstructive CAD	-	30 (11%)	-	-
Obstructive CAD	-	206 (77%)	-	-

Continuous data is expressed as mean (SD) and dichotomous data as n (%). The Calcium Score is expressed as median (IQR). CAD, Coronary Artery Disease; CCA, conventional coronary angiography; CTCA Computed Tomography Coronary Angiography; [a]Blood pressure >140/90 mm Hg or treatment for hypertension. [b]Treatment with oral anti-diabetic medicine or insulin. [c]Currently and/or in the past. [d]Total cholesterol >180ml/dl or treatment for hypercholesterolemia. [e]According to chest discomfort classification of Diamond et al.(J Am Coll of Cardiol 1983;1:574-5). [f]Patients with CCA vs. patient without CCA.

Segment-by-segment analysis
Group A:

In group A the number of non-assessable segments (quality score: 1) was significantly higher in the high-pitch spiral group (70 of 832 segments (8%)) compared to the narrow-window sequential group (23 of 906 segments (3%), *P*<0.001).

The sensitivity on a per-segment level was significantly lower for the high-pitch spiral CTCA protocol than for the narrow-window sequential protocol (89% vs. 97%, *P*=0.01).

Table 2 Diagnostic performance of 128-slice dual source CT coronary angiography for the detection of >50% coronary stenosis on CCA; analysis for 4 different CTCA protocols.

	n	TP	TN	FP	FN	kappa	Verification bias corrected analysis				Uncorrected analysis			
							Sensitivity %	Specificity %	PPV %	NPV %	Sensitivity %	Specificity %	PPV %	NPV %
SEGMENT-BASED ANALYSIS[a]														
High Pitch Spiral	832	118	626	73	15	0.67	89 (83-94)	95 (92-98)	62 (54-70)	99 (98-100)	89 (84-94)	89 (86-93)	63 (55-71)	98 (96-99)
Narrow-window sequential	906	129	719	54	4	0.78	97 (94-100)	96 (94-99)	73 (65-80)	100 (99-100)	97 (94-100)	93 (90-95)	73 (65-80)	99 (99-100)
Wide-window sequential	801	104	642	47	8	0.75	94 (89-98)	95 (93-97)	67 (59-76)	99 (99-100)	93 (88-98)	93 (91-95)	69 (61-78)	99 (98-100)
Retrospective Spiral	657	75	534	41	7	0.72	92 (85-98)	95 (93-98)	66 (56-75)	99 (99-100)	92 (86-98)	93 (90-96)	66 (57-75)	99 (98-100)
VESSEL-BASED ANALYSIS[a]														
High Pitch Spiral	270	92	137	36	5	0.69	95 (90-99)	90 (84-96)	71 (62-80)	99 (98-100)	95 (88-98)	79 (72-86)	73 (64-81)	97 (92-99)
Narrow-window sequential	293	94	169	30	0	0.78	100[b]	92 (87-97)	76 (68-85)	100[b]	100 (96-100)[c]	84 (78-90)	77 (69-85)	100 (98-100)[c]
Wide-window sequential	264	84	150	29	1	0.76	99 (96-100)	88 (82-94)	71 (61-80)	100 (99-100)	99 (96-100)	84 (78-89)	74 (66-83)	99 (98-100)
Retrospective Spiral	217	63	130	22	2	0.76	97 (92-100)	91 (86-96)	73 (62-83)	99 (98-100)	97 (92-100)	85 (80-91)	74 (65-83)	99 (96-100)
PATIENT-BASED ANALYSIS														
High Pitch Spiral	70	55	10	5	0	0.76	100[b]	91 (80-100)	89 (80-99)	100[b]	100 (94-100)[c]	67 (38-88)[d]	92 (85-99)	100 (69-100)[c]
Narrow-window sequential	74	58	11	5	0	0.78	100[b]	91 (79-100)	91 (82-99)	100[b]	100 (94-100)[c]	69 (41-89)[d]	92 (85-99)	100 (72-100)[c]
Wide-window sequential	67	51	10	6	0	0.72	100[b]	78 (55-100)	86 (75-97)	100[b]	100 (93-100)[c]	63 (35-85)[d]	90 (82-97)	100 (69-100)[c]
Retrospective Spiral	56	42	10	6	0	0.67	100[b]	78 (55-100)	85 (72-98)	100[b]	100 (92-100)[c]	57 (29-82)[d]	88 (78-97)	100 (63-100)[c]

FN, false negative; FP, false positive; NPV, negative predictive value; PPV, positive predictive value; TN, true negative; TP, true positive. [a]Analyses performed using generalized estimating equations unless indicated otherwise; [b]Corrected CI could not be calculated; [c]One-sided exact 97.5% CI; dexact 95% CI. Values in parentheses represent 95% CI unless indicated otherwise.

Chapter 6

Diagnostic accuracy of 128-slice dual source CT coronary angiography:
a randomized comparison of different acquisition scan protocols

High-pitch spiral CTCA incorrectly classified 15 segments of 133 diseased segments as having no significant stenoses vs. 4 incorrectly classified segments of 133 diseased segments using a narrow-window sequential protocol. No significant difference was found in specificity, PPV or NPV in group A (95% vs. 96%, *P*=0.50; 62% vs. 73%, *P*=0.07 and 99% vs. 100%, *P*=0.07, respectively).

Group B:
No significant difference in the number of non-assessable segments was found between the narrow-window sequential and the retrospective spiral CTCA protocol (22/801 (3%) vs. 18/657 (3%), *P*=0.99). Sensitivity (94% vs. 92%, *P*=0.62), specificity (95% vs. 95%, *P*=0.79), PPV (67% vs. 66%, *P*=0.81), and NPV (99% vs. 99%, *P*=0.94) on a per-segment level were comparable between both protocols.

Inter-observer variability for the detection of obstructive CAD on a per-segment level was good in all patients (k-value 0.77).

Vessel-by-vessel analysis
Group A:
Using the high-pitch spiral protocol 5 obstructed vessels were missed (1 right coronary artery (RCA), 2 left anterior descending arteries (LAD) and 2 left circumflex arteries (LCX)) while none were missed using the narrow-window sequential protocol. The lack of confidence intervals for the 100% sensitivity and NPV of the narrow-window sequential protocol hampers statistical comparison between the high-pitch spiral and the sequential protocol but no significant difference is assumed. Specificity and PPV on a per-vessel level are comparable (90% vs. 92%, *P*=0.65 and 71% vs. 76%, *P*=0.36).

Group B:
Wide-window sequential CTCA missed 1 obstructed vessel (LCX) and retrospective spiral CTCA missed 2 (LAD, LCX).

Sensitivity (99% vs. 97%, *P*=0.41), specificity (88% vs. 91%, *P*=0.45), PPV (71% vs. 73%, *P*=0.77), and NPV (100% vs. 99%, *P*=0.54) on a per-vessel level were comparable between the wide-window sequential protocol and the retrospective spiral protocol.

Patient-by-patient analysis
Group A:
None of the patients with significant CAD were missed by both the high-pitch spiral and the narrow-window sequential CTCA protocol. Consequently the sensitivity and NPV on a per-patient level of both CTCA protocols are 100% and no statistical difference is assumed. Specificity and PPV are comparable between both protocols (91% vs. 91%, *P*=NS and 89% vs. 91%, *P*=NS).

Group B:
All patients with obstructive disease on CCA were detected by CTCA using the wide-window sequential (Fig. 2) or the retrospective spiral CTCA protocol. Consequently the sensitivity and NPV on a per-patient level are 100% for both protocols and no statistical difference is assumed. Specificity and PPV were similar (78% vs. 78%, *P*=NS and 86% vs. 85%, *P*=NS).

Fig. 2 Prospective sequential CT coronary angiography protocol with a wide CT data acquisition window in a patient with a high heart rate

Male, 57 years old, presenting with atypical angina pectoris and a positive exercise test. Mean heart rate during CT was 74 beats per minute. Estimated radiation dose of the wide window sequential CTCA protocol was 3.9 mSv. Volume rendered CTCA images (VRT) reveal the anatomy of the left anterior descending coronary artery (LAD) (a) and the right coronary artery (RCA) (e). The curved multiplanar reconstruction image (cMPR) (b) and the VRT inlay (d) disclose a subtotal occlusion (arrow) of the proximal LAD, which was confirmed by CCA (c). The cMPR image (f) shows a non-diseased RCA which was confirmed by CCA (g).

Radiation dose
In group A the estimated radiation dose was significantly lower with the high-pitch spiral protocol than with the narrow-window sequential protocol (tube voltage 100 kV: 0.74±0.15 vs. 2.65±1.01 mSv, *P*<0.001 and 120 kV: 1.60±0.57 vs. 4.65±1.51 mSv, *P*<0.001) (Table 3). In group B the estimated radiation dose was significantly lower with the wide-window sequential protocol than with the retrospective spiral protocol (tube voltage 100 kV: 4.05±1.46 vs. 5.66±2.30 mSv, *P*<0.001 and 120 kV: 7.53±2.18 vs. 10.21±4.89 mSv, *P*<0.001) (Table 3).

Chapter 6

Diagnostic accuracy of 128-slice dual source CT coronary angiography:
a randomized comparison of different acquisition scan protocols

Table 3 Estimated radiation exposure

		DLP (mGy•cm)	Estimated dose[a] (mSv)
All patients (n=459)			
Group A	High Pitch Spiral	82.69 (42.80)	1.16 (0.60)
	Narrow-window sequential	273.13 (117.82)	3.82 (1.65)
Group B	Wide-window sequential	437.39 (183.87)	6.12 (2.58)
	Retrospective Spiral	581.24 (323.15)	8.13 (4.52)
Tube Voltage			
100 kV (n=204)			
Group A	High Pitch Spiral	52.83 (11.02)	0.74 (0.15)
	Narrow-window sequential	189.02 (72.37)	2.65 (1.01)
Group B	Wide-window sequential	288.87 (103.89)	4.05 (1.46)
	Retrospective Spiral	403.92 (163.81)	5.66 (2.30)
120 kV (n=255)			
Group A	High Pitch Spiral	114.18 (41.30)	1.60 (0.57)
	Narrow-window sequential	331.64 (107.66)	4.65 (1.51)
Group B	Wide-window sequential	537.94 (156.10)	7.53 (2.18)
	Retrospective Spiral	729.00 (348.99)	10.21 (4.89)

Data is expressed as mean (SD). DLP, dose length product. [a]Estimated dose was calculated by multiplying the DLP by the conversion coefficient of 0.014 mSv•mGy-1•cm-1 for the chest.

DISCUSSION

Our results show that sequential CT data acquisition provides good diagnostic performance at a low radiation dose in both groups undergoing CTCA Consequently, sequential CTCA should be used as a first-line scan protocol in concordance with the ALARA-principle.. Further dose reduction can be achieved with high-pitch spiral CTCA in patients with low heart rates, albeit at the expense of a lower diagnostic performance.

The strength of CTCA is its high negative predictive value and preliminary data suggest that CTCA is even the preferred first-line diagnostic investigation in patients with low-to-

intermediate risk of having significant CAD compared to exercise ECG-testing [24]. As a first-line test, CTCA should be as safe and non-invasive as possible since the vast majority of patients do not have significant CAD. The introduction of radiation lowering techniques has boosted the implementation of CTCA in a clinical routine setting. However, data on the impact of diagnostic accuracy using 128-slice dual source CTCA protocols is scarce. Some preliminary studies reported high diagnostic accuracy of high-pitch spiral CTCA in patients with low heart rates [15; 25]. Our results are in line with these previously published studies but we found 2 important limitations with respect to high-pitch spiral CTCA. Firstly, we detected significantly more non-assessable segments with high-pitch spiral CTCA vs. sequential CTCA. Secondly, we found a significantly lower sensitivity on a per-segment level. These observations indicate that sequential CTCA outperforms high-pitch spiral CTCA on a per-segment level. Although this difference is not found on a per-vessel nor per-patient level, we believe that a negative high-pitch spiral CTCA does not reliably exclude the presence of a significant stenosis because of a relatively high frequency of non-assessable segments (8%) mainly based on motion artefacts.

The results of our study indicate that the use of β-blockers in patients with high heart rates (>65 bpm) is an effective tool to reduce radiation exposure if the heart rate can be reduced to <65 bpm, which allows selection of a low dose CTCA protocol. If the use of β-blockers is not sufficient to reduce the heart rate <65 bpm or in the presence of contra-indications, a wide-window sequential CTCA protocol can be used as it provides similar diagnostic performance compared to retrospective spiral CTCA in patients with heart rates >65bpm.

Our results also demonstrate that radiation exposure can significantly be reduced using lower kV voltages (100 kV instead 120 kV) in patients with a BMI of <30 kg/m^2, which is in line with previous studies [11; 26]. The potential of this tool is currently not fully used as the selection of kV voltage based on BMI is rather arbitrary. Thus, selection of the appropriate protocol tailored to individual patient characteristics such as heart rate and geometry provides significant reduction of radiation dose while maintaining diagnostic accuracy.

In the near future further dose lowering by optimized use of lower tube voltages is to be expected due to 1) the recent introduction of automated tube voltage selection based on patient geometry which provides an optimal balance between tube current and tube voltage [27] and 2) the widespread application of iterative reconstruction, which limits the disadvantages of the use of lower tube voltages as it provides a significant higher contrast-to-noise ratio compared to conventional reconstruction algorithms [28].

Our study had a major limitation. Only a part of the included patients underwent CCA after the CTCA at the discretion of the referring physician who was aware of the CTCA results. As a result, most patients referred to CCA were at high risk having significant CAD.

Chapter 6

Diagnostic accuracy of 128-slice dual source CT coronary angiography:
a randomized comparison of different acquisition scan protocols

To account for this verification bias the accuracy analyses were weighted by the inverse of the probability of verification, based on all included patients who underwent CTCA. A limitation of our study is the exclusively inclusion of patients with stable heart rates and thus the results are not applicable to patients suffering any kind of arrhythmia including atrial fibrillation. Furthermore it is debatable whether a heart rate of 65 bpm is the correct cut-off heart rate for selection of CTCA protocol and acquisition window. We did extract these values from data of a retrospective acquisition protocol [19] and future studies are mandatory to determine the correct settings for sequential acquisition protocols.

In conclusion, we demonstrated that a sequential CTCA protocol should be the first choice in patients undergoing CT coronary angiography, combining high diagnostic performance with few non-assessable segments with relatively low radiation exposure.

REFERENCES

1   von Ballmoos MW, Haring B, Juillerat P, Alkadhi H (2011) Meta-analysis: diagnostic performance of low-radiation-dose coronary computed tomography angiography. Ann Intern Med, 154(6):413-420.

2   Mowatt G, Cummins E, Waugh N, et al. (2008) Systematic review of the clinical effectiveness and cost-effectiveness of 64-slice or higher computed tomography angiography as an alternative to invasive coronary angiography in the investigation of coronary artery disease. Health Technol Assess, 12(17):iii-iv, ix-143.

3   Vanhoenacker PK, Heijenbrok-Kal MH, Van Heste R, et al. (2007) Diagnostic performance of multidetector CT angiography for assessment of coronary artery disease: meta-analysis. Radiology, 244(2):419-428.

4   Weustink AC, Meijboom WB, Mollet NR, et al. (2007) Reliable high-speed coronary computed tomography in symptomatic patients. Journal of the American College of Cardiology, 50(8):786-794.

5   Pugliese F, Mollet NR, Hunink MG, et al. (2008) Diagnostic performance of coronary CT angiography by using different generations of multisection scanners: single-center experience. Radiology, 246(2):384-393.

6   Taylor AJ, Cerqueira M, Hodgson JM, et al. (2010) ACCF/SCCT/ACR/AHA/ASE/ASNC/NASCI/SCAI/SCMR 2010 appropriate use criteria for cardiac computed tomography. A report of the American College of Cardiology Foundation Appropriate Use Criteria Task Force, the Society of Cardiovascular Computed Tomography, the American College of Radiology, the American Heart Association, the American Society of Echocardiography, the American Society of Nuclear Cardiology, the North American Society for Cardiovascular Imaging, the Society for Cardiovascular Angiography and Interventions, and the Society for Cardiovascular Magnetic Resonance. J Am Coll Cardiol, 56(22):1864-1894. doi: S0735-1097(10)02529-5 [pii] 10.1016/j.jacc.2010.07.005

7   Einstein AJ, Henzlova MJ, Rajagopalan S (2007) Estimating risk of cancer associated with radiation exposure from 64-slice computed tomography coronary angiography. JAMA, 298(3):317-323.

8   Gerber TC, Carr JJ, Arai AE, et al. (2009) Ionizing radiation in cardiac imaging: a science advisory from the American Heart Association Committee on Cardiac Imaging of the Council on Clinical Cardiology and Committee on Cardiovascular Imaging and Intervention of the Council on Cardiovascular Radiology and Intervention. Circulation, 119(7):1056-1065.

9   Roobottom CA, Mitchell G, Morgan-Hughes G (2010) Radiation-reduction strategies in cardiac computed tomographic angiography. Clin Radiol, 65(11):859-867.

10 Bischoff B, Hein F, Meyer T, et al. (2010) Comparison of sequential and helical scanning for radiation dose and image quality: results of the Prospective Multicenter Study on Radiation Dose Estimates of Cardiac CT Angiography (PROTECTION) I Study. Ajr, 194(6):1495-1499.

11 Hausleiter J, Martinoff S, Hadamitzky M, et al. (2010) Image quality and radiation exposure with a low tube voltage protocol for coronary CT angiography results of the PROTECTION II Trial. JACC Cardiovasc Imaging, 3(11):1113-1123.

Chapter 6

Diagnostic accuracy of 128-slice dual source CT coronary angiography:
a randomized comparison of different acquisition scan protocols

12   Halliburton SS, Abbara S, Chen MY, et al. (2011) SCCT guidelines on radiation dose and dose-optimization strategies in cardiovascular CT. Journal of cardiovascular computed tomography, 5(4):198-224.

13   Sun ML, Lu B, Wu RZ, et al. (2011) Diagnostic accuracy of dual-source CT coronary angiography with prospective ECG-triggering on different heart rate patients. European radiology, 21(8):1635-1642.

14   Achenbach S, Marwan M, Ropers D, et al. (2010) Coronary computed tomography angiography with a consistent dose below 1 mSv using prospectively electrocardiogram-triggered high-pitch spiral acquisition. European heart journal, 31(3):340-346.

15   Alkadhi H, Stolzmann P, Desbiolles L, et al. (2010) Low-dose, 128-slice, dual-source CT coronary angiography: accuracy and radiation dose of the high-pitch and the step-and-shoot mode. Heart, 96(12):933-938.

16   Leschka S, Stolzmann P, Desbiolles L, et al. (2009) Diagnostic accuracy of high-pitch dual-source CT for the assessment of coronary stenoses: first experience. European radiology, 19(12):2896-2903.

17   Sommer WH, Albrecht E, Bamberg F, et al. (2010) Feasibility and radiation dose of high-pitch acquisition protocols in patients undergoing dual-source cardiac CT. Ajr, 195(6):1306-1312.

18   Ertel D, Lell MM, Harig F, Flohr T, Schmidt B, Kalender WA (2009) Cardiac spiral dual-source CT with high pitch: a feasibility study. European radiology, 19(10):2357-2362.

19   Weustink AC, Mollet NR, Pugliese F, et al. (2008) Optimal electrocardiographic pulsing windows and heart rate: effect on image quality and radiation exposure at dual-source coronary CT angiography. Radiology, 248(3):792-798.

20   Austen WG, Edwards JE, Frye RL, et al. (1975) A reporting system on patients evaluated for coronary artery disease. Report of the Ad Hoc Committee for Grading of Coronary Artery Disease, Council on Cardiovascular Surgery, American Heart Association. Circulation, 51(4 Suppl):5-40.

21   Shrimpton P (2004) Assessment of patient dose in CT: appendix C—European guidelines for multislice computed tomography. European Commission project MSCT: CT safety & efficacy–a broad perspective. (ed)^(eds) http://www.msct.eu/PDF_FILES/Appendix%20paediatric%20CT%20Dosimetry.pdf (accessed 20 November 2008).

22   Begg CB, Greenes RA (1983) Assessment of diagnostic tests when disease verification is subject to selection bias. Biometrics, 39(1):207-215.

23   Hunink MG, Polak JF, Barlan MM, O'Leary DH (1993) Detection and quantification of carotid artery stenosis: efficacy of various Doppler velocity parameters. Ajr, 160(3):619-625.

24   Weustink AC, Mollet NR, Neefjes LA, et al. (2010) Diagnostic accuracy and clinical utility of noninvasive testing for coronary artery disease. Ann Intern Med, 152(10):630-639.

25   Achenbach S, Goroll T, Seltmann M, et al. (2011) Detection of coronary artery stenoses by low-dose, prospectively ECG-triggered, high-pitch spiral coronary CT angiography. JACC Cardiovasc Imaging, 4(4):328-337.

26   Leschka S, Stolzmann P, Schmid FT, et al. (2008) Low kilovoltage cardiac dual-source CT: attenuation, noise, and radiation dose. European radiology, 18(9):1809-1817.

27   Yu L, Li H, Fletcher JG, McCollough CH (2010) Automatic selection of tube potential for radiation dose reduction in CT: a general strategy. Med Phys, 37(1):234-243.

28   Leipsic J, Labounty TM, Heilbron B, et al. (2010) Estimated radiation dose reduction using adaptive statistical iterative reconstruction in coronary CT angiography: the ERASIR study. Ajr, 195(3):655-660.

Chapter 7

Optimal acquisition windows for low dose DSCT coronary angiography in relation to heart rate

Lisan A. Neefjes
Gert-Jan R. ten Kate
Sandra Spronk
Marcel van Straten
Gabriel P. Krestin
Nico R. Mollet
Pim J. de Feyter
Annick C. Weustink

Part 3

*CT Coronary
plaque imaging*

Chapter 8

CT coronary plaque burden in asymptomatic patients with familial hypercholesterolemia

Lisan A. Neefjes
Gert-Jan R. ten Kate
Alexia Rossi
Annette J. Galema-Boers
Janneke G. Langendonk
Annick C. Weustink
Adriaan Moelker
Koen Nieman
Nico R. Mollet
Gabriel P. Krestin
Eric J. Sijbrands*
Pim J. de Feyter*
*Both authors contributed equally to this article

ABSTRACT

Objective To determine the calcium score and coronary plaque burden in asymptomatic statin treated patients with heterozygous familial hypercholesterolemia (FH) compared to a control group of patients with low probability of coronary artery disease, having non-anginal chest pain, using computed tomography (CT).

Materials and Methods One hundred and one asymptomatic FH patients (mean age 53±7 years; 62 men) and 126 patients with non-anginal chest pain (mean age 56±7 years; 80 men) underwent CT calcium scoring and CT coronary angiography. All FH patients were treated with statins during a period of 10±8 years prior to CT. The coronary calcium score and plaque burden were determined and compared between the two patient groups.

Results The median total calcium score was significantly higher in FH patients (Agatston score=87, IQR 5-367) compared to patients with non-anginal chest pain (Agatston score=7, IQR 0-125; p<0.001). The overall coronary plaque burden was significantly higher in FH patients (p<0.01). Male FH patients, whose low-density lipoprotein (LDL) cholesterol levels were reduced by statins below 3.0 mmol/l, had less coronary calcium (p<0.01) and plaque burden (p=0.02).

Conclusion The coronary plaque burden is high in asymptomatic middle-aged FH patients despite intense statin treatment.

INTRODUCTION

Familial hypercholesterolemia (FH) is an autosomal dominant disorder caused by mutations in the low-density lipoprotein (LDL) receptor gene and is characterized by elevated serum levels of LDL cholesterol, tendon xanthomas and high risk of coronary artery disease (CAD) [1-4].

Recently, we demonstrated that statin treatment greatly reduces the risk of CAD in FH patients who were detected in our nationwide screening program; the risk of myocardial infarction in these treated FH patients was not significantly higher than that of the general population, while the mean treated LDL cholesterol level was much higher than current target levels [5]. Although these data suggest that asymptomatic treated FH patients have only mild CAD, it provides no direct evidence of the presence and severity of residual CAD in treated FH patients. The use of cardiac CT enabled us to anatomically verify these findings.

Over the last few years cardiac CT has emerged as a safe, non-invasive modality for imaging coronary atherosclerosis. A non-enhanced scan shows the total amount of coronary calcium; while a contrast-enhanced CT coronary angiography (CTCA) permits evaluation of both calcified and non-calcified plaques as well as narrowing of the vessel lumen.

To date the presence of subclinical CAD in asymptomatic high-risk FH-population has only be studied by Miname et al. [6] in relatively young FH patients of whom only 66% were on previous statin treatment and all underwent a washout period of 6 weeks before evaluation.

The purpose of this single center study was to determine the presence and extent of coronary plaques in asymptomatic statin treated FH patients by CTCA and to compare these results directly with the CTCA findings in patients with non-anginal chest pain as a substitute for asymptomatic non FH patients. Additionally the relation between patient characteristics, risk factors and cholesterol levels and the extent of CAD was assessed.

MATERIALS AND METHODS

Study population
Between February 2008 and February 2009 we included 101 consecutive, asymptomatic patients with FH and 126 patients with non-anginal chest pain in our CTCA study, as the radiation exposure limits the choice of controls to patients with an indication for CTCA.

The FH patients were recruited from our outpatient lipid clinic. The following diagnostic criteria for FH were used: either 1) the presence of a documented LDL receptor mutation,

or 2) an LDL cholesterol level above the 95th percentile for sex and age in combination with at least one of the following: a) the presence of typical tendon xanthomas in the patient or in a first degree relative, or b) an LDL cholesterol level above the 95th percentile for age and sex in a first degree relative or c) proven CAD in the patient or in a first degree relative under the age of 60 [7]. From this group, patients who were symptomatic for CAD, defined as the presence of symptoms suggestive of ischemic heart disease or known CAD in their history, and patients with secondary causes of hypercholesterolemia such as renal, liver, or thyroid disease were excluded from the study.

The patients with non-anginal chest pain were recruited from a patient population without history of coronary artery disease referred by their general practitioner for evaluation of chest pain and underwent stress testing and cardiac CT. Non-anginal chest pain was defined as chest pain or discomfort that met one or none of the following typical angina characteristics: 1) substernal chest pain or discomfort that is 2) provoked by exertion or emotional stress and 3) relieved by rest and/or nitroglycerin [8].

Inclusion age was 40-70 years, except for women with FH it was 45-70 years. Exclusion criteria were renal insufficiency (serum creatinine >120 µmol/l), known contrast allergy and irregular heart rhythm (atrial fibrillation).

The institutional Ethical Review Board approved the study protocol. All patients gave written informed consent.

Scan protocol

Just prior to the scan all patients received nitroglycerin (0.4 mg/dose) sublingually.
All scans were performed with a Dual Source CT scanner (Somatom Definition, Siemens Medical Solutions, Forchheim, Germany). For the non-enhanced scan a prospective electrocardiogram (ECG)-triggered scan protocol was applied. The CTCA scan protocol, contrast protocol and reconstruction procedure have been described previously [9]. Briefly, the CTCA was obtained using a retrospective ECG-gated scan protocol with optimal heart rate-dependent ECG-pulsing [10] to lower the radiation dose. Maximum tube current was 380 mAs and tube voltage was 120 kV. The mean estimated radiation dose per CTCA, calculated by multiplying the dose length product (DLP) by the conversion coefficient of 0.014 mSv·mGy-1·cm-1 for the chest, was 7.9 mSv ± 2.4 mSv (range 3.9-16.4 mSv) [11]. Iodinated contrast agent (Ultravist 370 mgI/ml, Schering AG, Berlin, Germany), with a scan time dependent volume (94 ml (80-100 ml)), was administered for enhancement of the coronaries. The calcium score datasets were reconstructed with a slice thickness of 3 mm and an increment of 1.5 mm at 70% of the RR-interval. CTCA datasets were reconstructed using a slice thickness of 0.75 mm and an increment of 0.4 mm at an automatically or additionally manually determined optimal phase of the RR-interval. All datasets were sent to a dedicated workstation (Leonardo, Siemens).

CT analysis

The calcium score was calculated semi-automatically using dedicated software and expressed as the Agatston score per patient [12].

All CTCA scans were evaluated separately by two experienced readers and all discrepancies in evaluation were resolved during a consensus reading. Coronary plaque was defined as a separate structure within the vessel wall that could be clearly distinguished from the contrast enhanced lumen and the surrounding pericardial tissue. Per segment, using the AHA 16-segment model [13], the absence or presence of a coronary plaque was determined, as was the severity of the lumen narrowing (0, >0-50% and >50% diameter stenosis). Per patient the extent of CAD, defined as the number of segments with a non-obstructive (>0-50% diameter stenosis) or obstructive (>50% diameter stenosis) lesion, was determined. The plaque composition was also documented and classified as 1) calcified: plaque containing highly attenuating tissue that could be clearly separated from the contrast enhanced coronary lumen and 2) non-calcified: low attenuating lesions that could be clearly separated from the coronary lumen and the surrounding epicardial fat and myocardium. Vessel segments <1.5 mm in diameter were excluded from all analyses. The coronary plaque burden was expressed as the severity of coronary obstructions, the extent of CAD, the number of diseased coronary arteries, segments and plaque composition.

FH patient management

All included FH patients were regularly seen in the out patient clinic for monitoring their lipid levels and subsequent optimization of the medical treatment and early detection of complications of FH. They all received statins. Intense statin treatment was defined as the daily use of either: 80 mg of atorvastatin, 80 mg of simvastatin or 40 mg of rosuvastatin. We used a cut-off value of LDL cholesterol of <3.0 mmol/l to define patients with a substantial lowering of LDL cholesterol and to relate this to the extent of coronary artery disease.

Statistical analysis

Continuous variables are shown as mean [±SD] or median [IQR]. Categorical variables are expressed as number [frequency±SEM]. We used the t test or Mann-Whitney U test to compare continuous variables and the chi-square test or the Fisher exact test for the comparison of categorical variables. A p-value of <0.05 was considered significant. The relationship between the extent of CAD in FH patients, and the duration of statin treatment, the achievement of a LDL cholesterol level below 3 mmol/l, the high density lipoprotein (HDL), the maximum total cholesterol levels prior to treatment and the age at the start of statin treatment was assessed using a multivariate linear regression model.

Inter-observer and intra-observer variability are described with the k-statistics. Intra-observer variability was conducted in a sub-group of 30 randomly selected scans scored

twice by one observer, with a minimum of two months time interval between the two evaluations. All analyses were performed using SPSS for windows (version 15.0, SPSS, Chicago, USA).

RESULTS

Baseline

Figure 1 shows the inclusion flow chart. During the recruitment period 153 FH patients were eligible for the study of whom 101 gave informed consent. From the symptomatic population scheduled for cardiac CT, 146 patients were classified as having non-anginal chest pain of whom 126 were eligible for inclusion.

The patient characteristics are shown in table 1. All included HF patients received statins; 31 patients (32%) did not receive intense statin treatment because of severe side effects. Most FH patients (42%) used atorvastatin 80 mg (mean 68 mg), simvastatin (29%, mean 58 mg) and rosuvastatin (24%, mean 35 mg). Less commonly used lipid lowering drugs were pravastatin, colestyramine and ciprofibrate, ezetimibe was combined with statins in 59% of cases.

Of 126 controls, 72 patients had dyslipidemia. All these patients were treated with a cholesterol-lowering diet and 67% also used low dose statins: 31% used atorvastatin (mean 33 mg), 54% used simvastatin (mean 28 mg), 10% used rosuvastatin (mean 14 mg), pravastatin and ezetimibe were both used with a mean dose of 10 mg by 4 and 10 percent of controls respectively. Gender distribution was comparable between the FH patients and

the non-anginal patients (61±5% and 64±4% male, respectively, p=0.78). The mean age of the non-anginal controls was slightly higher (56 ± 7 versus 53 ± 7 years, p= 0.01). By selection dislipidemia and positive family history for cardiovascular disease were more frequently found in the FH patients, who exhibited significantly fewer other risk factors.

Table 1 Patient characteristics

| Variable	FH patients (n=101)	NACP patients (n=126)	p value
Male gender	62 (61%)	80 (64%)	0.78
Age (years)	53 (7)	56 (7)	0.01
Riskfactors			
Smoker†	22 (22%)	41 (33%)	0.03
Diabetes§	4 (4%)	19 (15%)	<0.01
Hypertension‡	25 (25%)	60 (48%)	<0.01
Dislipidemia	101 (100%)	72 (57%)	<0.001
Positive Family History	69 (68%)	58 (46%)	0.001
Body Mass Index (kg/m²)	26 (5)	25 (9)	0.22
Lipids			
Total Cholesterol (mmol/l)	5.4 (1.2)	5.0 (1.9)	0.09
LDL Cholesterol (mmol/l)	3.5 (1.1)	3.5 (1.1)	0.69
HDL Cholesterol (mmol/l)	1.4 (0.4)	1.3 (0.4)	0.09
Triglycerides (mmol/l)	1.4 (1.2)	1.6 (1.0)	0.10
Lipids related characteristics			
Maximum untreated total Cholesterol (mmol/l)	10.2 (2.3)	6,9 (2,0)‖	<0.001
Known LDL mutation	78 (77%)	.	.
Xanthomas	24 (24%)	.	.
Arcus Lipoides	27 (27%)	.	.
Duration of statin treatment (years)	10 (8)	3 (4)‖	<0.001
Age at start statin treatment (years)	42 (10)	53 (9)‖	<0.001
Intense statin treatment	69 (68%)	4 (8%)‖	<0.001
Dose-limiting side effects	31 (31%)	3 (6%)‖	<0.001
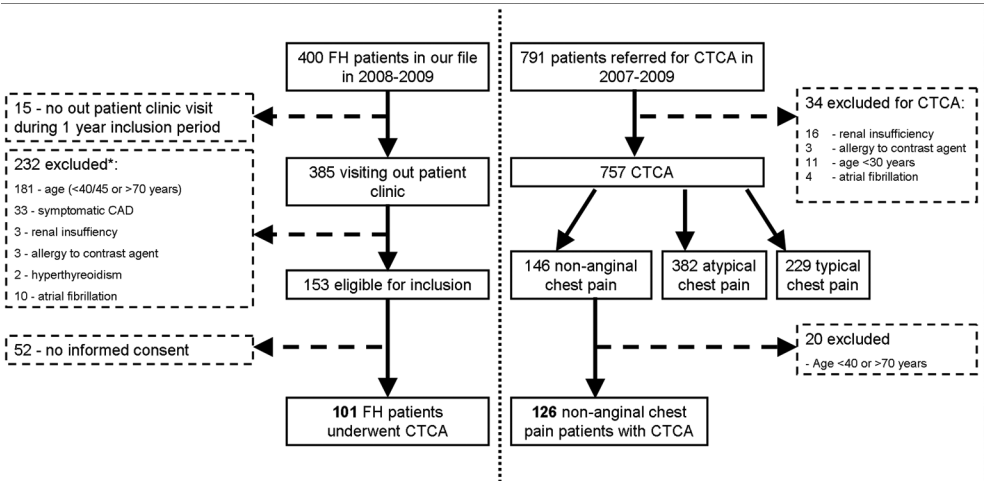
Figure 1 Patient inclusion flowchart. CAD, Coronary artery disease; CTCA, Computed Tomography Coronary Angiography; FH, Familial Hypercholesterolemia.

Concomitant ezetimibe treatment	60 (59%)	5 (10%)‖	<0.001
Calcium Score			
Total calcium score* (Agatston)	87 (5-367)	7.3 (0-125)	<0.001
0	20 (20%)	49 (39%)	
0-100	33 (33%)	42 (33%)	
>100-400	24 (24%)	20 (16%)	
>400	24 (24%)	15 (12%)	0.004

Continuous data are expressed as mean (SD) and dichotomous data as n (%). *The Calcium Score is expressed as median (Inter Quartile Range). CAD, Coronary Artery Disease; HDL, high-density lipoprotein; LDL, low-density lipoprotein; NACP, non-anginal chest pain. †Currently and/or in the past. ‡Blood pressure >140/90 mm Hg or treatment for hypertension. §Treatment with oral anti-diabetic medicine or insulin. ‖ n=48, NCAP patients treated with statins.

No complications occurred during or after scanning. All scans were included in the analysis. We excluded 43 segments because of insufficient image quality due to motion artifacts, leaving 3621 segments available for analysis. The κ statistics of the inter-observer and intra-observer variability for the evaluation of the stenosis severity per plaque was 0.80 and 0.82, respectively, and for the evaluation of plaque composition 0.83 and 0.83, respectively.

CT calcium score

The median total calcium score was significantly higher in FH patients (87, IQR 5-367) compared to patients with non-anginal chest pain (7, IQR 0-125; p<0.001), with less negative calcium scores in FH patients (20, 20±4%) than in non-anginal chest pain patients (49, 39±4%, p<0.001) (table 1). In FH patients men had a significantly higher total calcium score (149, IQR 24-430) than women (21, IQR 0-171; p=0,003) while in non-anginal chest pain patients this difference was not evident (13, IQR 0-153 and 1, IQR 0-99, respectively; p=0,221). The total calcium score was higher in FH patients in all age groups and increased with higher age (figure 2a).

CT coronary angiography

In table 2 the coronary plaque burden on a per patient and a per segment level is shown. The severity and extent of CAD on a per patient and a per segment level was significantly higher in FH patients than in non-anginal chest pain patients. In the FH group 15 (15±4%) patients did not have any signs of CAD and in the non-anginal chest pain group 41 (33±4%) patients presented with non-diseased coronary arteries (p=0.002). On a per segment level the severity of CAD and composition of plaque were significantly different between FH patients and controls for both men and women. The number of coronary segments with non-obstructive or obstructive CAD was higher in FH patients in all age groups and increased with higher age (figure 2b).

Table 2 CTCA plaque burden per patient and per segment

	All			Men			Women		
	FH patients	NACP patients	p-value*	FH patients	NACP patients	p-value*	FH patients	NACP patients	p-value*
Patient level level	n=101	n=126		n=62	n=80		n=39	n=46	
Severity of CAD									
No CAD	15 (15%)	41 (33%)		6 (10%)	26 (33%)		9 (23%)	15 (33%)	
Non-obstructive CAD	60 (59%)	53 (42%)		34 (55%)	33 (41%)		26 (67%)	20 (44%)	
Obstructive CAD	26 (26%)	32 (25%)	0.005*	22 (36%)	21 (26%)	0.005*	4 (10%)	11 (24%)	0.08*
All CAD; obstructive and non-obstructive CAD									
0 vessels	15 (15%)	41 (33%)		6 (10%)	26 (33%)		9 (23%)	15 (33%)	
1 vessel	15 (15%)	24 (19%)		5 (8%)	13 (16%)		10 (26%)	11 (26%)	
2 vessels	22 (22%)	26 (21%)		17 (27%)	16 (20%)		5 (13%)	10 (22%)	
3 vessels	48 (49%)	34 (27%)	0.002*	34 (55%)	25 (31%)	0.001*	15 (39%)	9 (20%)	0.20*
0 segments	15 (15%)	41 (33%)		6 (10%)	26 (33%)		9 (23%)	15 (33%)	
1-2 segments	20 (20%)	30 (24%)		10 (16%)	16 (20%)		10 (26%)	14 (30%)	
3-5 segments	22 (22%)	25 (20%)		14 (23%)	16 (20%)		8 (21%)	9 (20%)	
>5 segments	44 (44%)	30 (24%)	0.002*	32 (52%)	22 (28%)	0.003*	12 (31%)	8 (17%)	0.48*
Segment level	n=1609	n=2012		n=993	n=1281		n=616	n=731	
Severity of CAD									

			p			p			p
No CAD	1125 (70%)	1631 (81%)		648 (65%)	1018 (80%)		477 (77%)	613 (84%)	
Non obstructive CAD	428 (27%)	311 (16%)		296 (30%)	212 (17%)		132 (21%)	99 (14%)	
Obstructive CAD	56 (4%)	70 (4%)	<0.001*	49 (5%)	51 (4%)	<0.001*	7 (1%)	19 (3%)	<0.001*
Composition of plaque									
No CAD	1125 (70%)	1631 (81%)		648 (65%)	1018 (80%)		477 (77%)	613 (84%)	
Non-calcified plaque	49 (3%)	70 (4%)		26 (3%)	42 (3%)		23 (4%)	28 (4%)	
Calcified plaque	435 (27%)	311 (16%)	<0.001*	319 (32%)	221 (17%)	<0.001*	116 (19%)	90 (12%)	<0.01*

Data is expressed as n (%). CAD, Coronary Artery Disease; FH, familial hypercholesterolemia; NACP, non-anginal chest pain patients. * Values apply to the comparison between the 3 or 4 categories in the 2 columns left of the p-values.

Table 3 shows the relation between the calcium score and the presence of non-obstructive and obstructive plaque in FH patients.

In male FH patients, achieving LDL cholesterol below 3.0 mmol/l during statin treatment was significantly (p<0.01) associated with a lower plaque burden (table 4). In female FH patients we did not observe such a relationship between statin induced LDL cholesterol levels and coronary plaque burden.

Multivariate analysis revealed that age, gender, highest untreated total cholesterol levels and treated HDL cholesterol levels predicted the magnitude of the severity and extent of CAD in FH patients (data not shown).
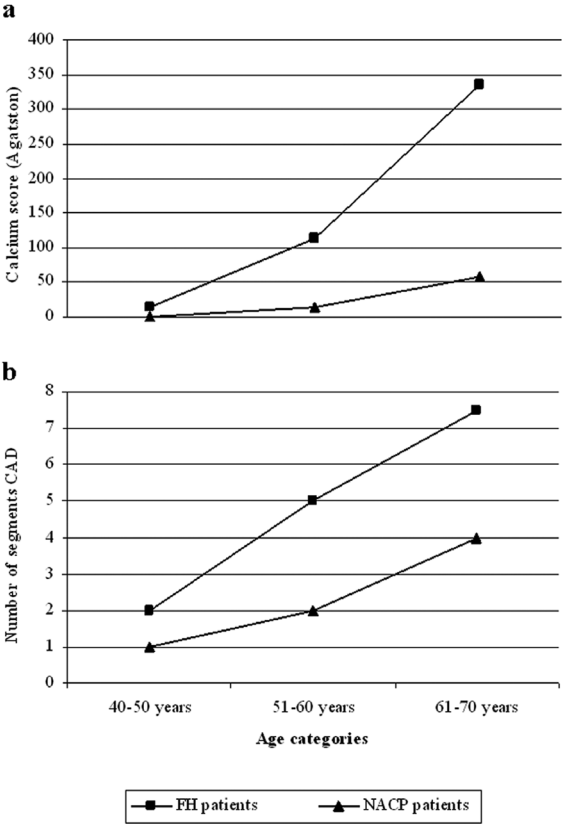
Figure 2 Calcium score and plaque burden according to different age categories. Calcium score and number of plaque containing segments are expressed as median per age group. FH, Familial Hypercholesterolemia; NACP, non-anginal chest pain.

Table 3 Calcium score in relation to CAD severity per patient

	Calciumscore (Agatston)			
	0 (n=20)	>0-100 (n=33)	>100-400 (n=24)	>400 (n=24)
No CAD	15 (75%)	0 (0%)	0 (0%)	0 (0%)
Non-obstructive CAD	5 (25%)	32 (97%)	15 (63%)	8 (33%)
Obstructive CAD	0 (0%)	1 (3%)	9 (37%)	16 (67%)

Data is expressed as n (% of calcium score group). CAD, Coronary Artery Disease.

Table 4 Coronary plaque burden according to achievement of the target value of 3.0 mmol/l LDL-Cholesterol in the blood in treated men with FH.

	≤ 3.0 mmol/l LDL (n=21)	> 3.0 mmol/l LDL (n=41)	p-value
Calciumscore			
0	5 (24%)	3 (7%)	
0-100	10 (48%)	8 (20%)	
>100-400	2 (10%)	14 (34%)	
>400	4 (19%)	16 (39%)	0.01
Plaque burden			
Severity of CAD			
No CAD	4 (19%)	2 (5%)	
Non-obstructive CAD	13 (62%)	21 (51%)	
Obstructive CAD	4 (19%)	18 (44%)	0.06
All CAD; obstructive and non-obstructive CAD			
0 segments	4 (19%)	2 (5%)	
1-2 segments	5 (24%)	5 (12%)	
3-5 segments	7 (33%)	7 (17%)	
>5 segments	5 (24%)	27 (66%)	0.02

Data is expressed as n (%). CAD, Coronary Artery Disease; LDL, low-density lipoprotein.

DISCUSSION

In the present study we demonstrated, using CT, that subclinical coronary atherosclerosis was present in the majority (85%) of asymptomatic patients with FH, despite 'normalization' of cholesterol levels with long term (10±8 years) statin treatment (figure 3).

Asymptomatic FH patients, at different age levels (40-50 years, 51-60 years and 61-70 years), had a higher calcium score and coronary plaque burden as compared to our

control group of patients with non-anginal chest pain having low probability of CAD, as well as compared to other coronary asymptomatic populations that underwent CT calcium-scoring [14-17] and CT coronary angiography [18]. Previous studies revealed that in 2-4% of symptomatic and asymptomatic patients with a calcium score of zero an obstructive coronary lesion is present [19-20]. In our study none of the 20 FH patients with a calcium score of 0 presented with an obstructive lesion or exhibited non-obstructive CAD in more than 2 segments. However, our study comprised only 20 FH-patients without coronary calcium, and larger studies are required to determine the prevalence of obstructive coronary artery disease in these patients.
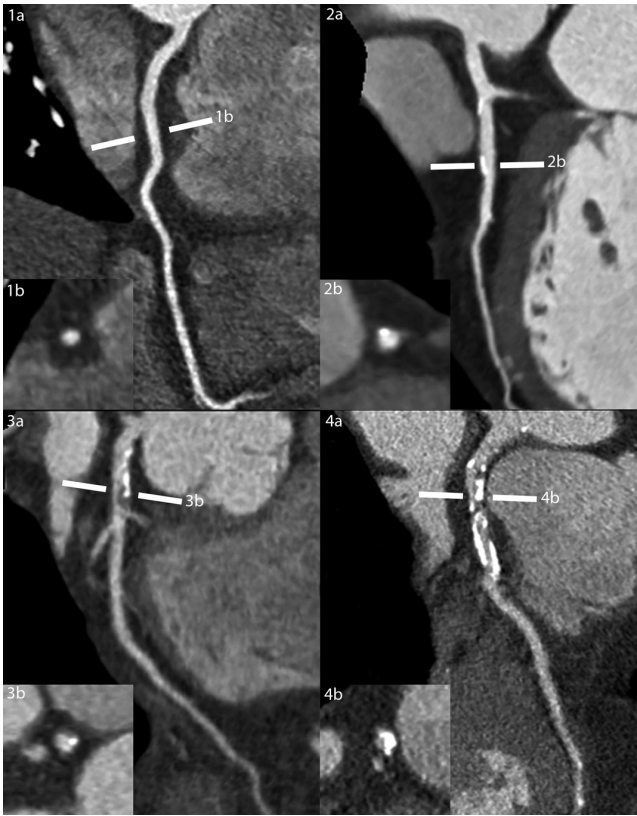

Figure 3 Curved Multi Planar Reconstructed (cMPR) CT images and cross sections of the left anterior descending coronary artery (LAD) of 4 asymptomatic patients with Familial Hypercholesterolemia showing a non-diseased vessel (1a, 1b), a non-obstructive calcified lesion (2a, 2b), an obstructive partly calcified lesion (3a, 3b) and an obstructive severely calcified lesion (4a, 4b).

Despite absence of symptoms, 26% of the FH patients exhibited obstructive CAD occurring at relatively young age averaging 53 ± 7 years. This was in a similar range as the 17% to 39% presence of obstructive CAD detected by CTCA in asymptomatic diabetic patients [21-23] and the 26% presence in our non-anginal chest pain group and also within the range of 16% to 62% in symptomatic coronary patients [24-25]. The 26% presence of obstructive CAD in our FH population however was a little higher than the 19% in a younger (45±13 years) FH population[6] and much higher than the approximately 5% in other high risk asymptomatic populations [18; 26].

The extent and severity of CAD, as established with CTCA, was higher in FH patients than in the non-anginal chest pain patients, but these differences were less striking in women where the differences were not statistically significant. This may be explained by the rela-

tively small numbers of women that may preclude reaching the level of significance. In addition we found an unexpectedly relatively high prevalence of obstructive lesions in women of the non-anginal chest pain population [18; 27]. This may be related to the fact that complaints of women often are misinterpreted as non-specific chest pain which may result in a delay in diagnostic testing and progression to a more advanced stage of CAD.

Clinical coronary artery disease in untreated patients with FH usually manifests in men between the ages of 30 and 50 years and in women between 50 and 70 years [28]. Statin treatment has shown to reduce the clinical manifestations in FH patients [5-6; 29]. In our study we studied middle aged FH patients who were free of coronary symptoms during approximately 10 years of statin treatment. Yet, CTCA revealed that the coronary plaque burden was substantial and that coronary artery disease was present in the majority (85%) of these patients. Apparently intense treatment with statins prevented progression to clinical expression of CAD but did not reduce the extent of coronary artery disease as was shown by the relatively high calcium scores, the presence of extensive non obstructive CAD (more than 2 coronary segments involved) in more than 60% of the patients and the presence of obstructive CAD in a quarter of these patients. This suggests that the coronary plaques in FH patients have been stabilized by statin treatment which has prevented the occurrence of coronary events. In our study we observed a higher prevalence of calcified plaques in the FH population than in the non-anginal chest pain population. Calcified plaques are known to be less vulnerable and less prone to rupture [30-31].

Notably, statin treatment was more effective in men in whom statins reduced LDL cholesterol levels to less than 3 mmol/l. These men had a lower calcium score and less CAD than men with higher LDL cholesterol levels.

Longer term follow up studies are necessary to demonstrate that statin treatment is associated with sustained reduction of symptomatic CAD and prolongation of life in these FH patients.

LIMITATIONS

We used non-anginal chest pain patients as controls instead of a group of healthy individuals, who may have had less coronary plaque burden, because CT associated radiation exposure makes it unethical to perform CTCA in asymptomatic volunteers. We selected this non-anginal chest pain patient group because we expected a prevalence of obstructive CAD of approximately 8% (women) to 22% (men)[27]. However, we found a higher prevalence of obstructive CAD in women (24%) but a comparable prevalence in men (26%). Nevertheless, we still observed a significantly higher coronary plaque burden in male and female treated FH patients.

It is known that CTCA is less able to detect small non-calcified plaques and therefore our reported prevalence of non-calcified lesions may be underestimated [32-33]. Furthermore it should be of note that CTCA, in particular in case of calcified lesions, may overestimate the severity of coronary stenosis [34], and hence the prevalence of obstructive lesions in our study population may have been overestimated.

Ideally we would have confirmed our CT findings with conventional invasive coronary angiography and intra vascular ultrasound which is the standard of reference for plaque detection, but our FH population was asymptomatic and thus additional CAG was considered unethical. However, it has been shown that moderate to large coronary plaques can be reliably detected by CTCA [35-36].

Our study was a cross-sectional observational study and does not allow evaluating progression of CAD in FH patients under statin treatment. And finally, our study was restricted to patients aged between 40-70 years, and findings may be different in elderly patients.

CONCLUSION

Despite long term intense statin treatment of middle aged patients with FH, the occurrence of CAD was higher than in a control group of patients with non-anginal chest pain as well as other asymptomatic populations. Non invasive low radiation exposure CT coronary imaging by demonstrating the extent and severity of underlying CAD may have a future role in the early detection of CAD, clinical management and prediction of risk in patients with FH.

REFERENCES

1   (1991) Risk of fatal coronary heart disease in familial hypercholesterolaemia. Scientific Steering Committee on behalf of the Simon Broome Register Group. BMJ (Clinical research ed, 303(6807):893-896.

2   Austin MA, Hutter CM, Zimmern RL, Humphries SE (2004) Familial hypercholesterolemia and coronary heart disease: a HuGE association review. American journal of epidemiology, 160(5):421-429.

3   de Sauvage Nolting PR, Defesche JC, Buirma RJ, Hutten BA, Lansberg PJ, Kastelein JJ (2003) Prevalence and significance of cardiovascular risk factors in a large cohort of patients with familial hypercholesterolaemia. Journal of internal medicine, 253(2):161-168.

4   Mabuchi H, Koizumi J, Shimizu M, Takeda R (1989) Development of coronary heart disease in familial hypercholesterolemia. Circulation, 79(2):225-232.

5   Versmissen J, Oosterveer DM, Yazdanpanah M, et al. (2008) Efficacy of statins in familial hypercholesterolaemia: a long term cohort study. BMJ (Clinical research ed, 337:a2423.

6   Miname MH, Ribeiro MS, 2nd, Parga Filho J, et al. (2010) Evaluation of subclinical atherosclerosis by computed tomography coronary angiography and its association with risk factors in familial hypercholesterolemia. Atherosclerosis, 213(2):486-491.

7   van Aalst-Cohen ES, Jansen AC, Tanck MW, et al. (2006) Diagnosing familial hypercholesterolaemia: the relevance of genetic testing. European heart journal, 27(18):2240-2246.

8   Diamond GA (1983) A clinically relevant classification of chest discomfort. Journal of the American College of Cardiology, 1(2 Pt 1):574-575.

9   Weustink AC, Mollet NR, Neefjes LA, et al. (2009) Preserved diagnostic performance of dual-source CT coronary angiography with reduced radiation exposure and cancer risk. Radiology, 252(1):53-60.

10 Weustink AC, Mollet NR, Pugliese F, et al. (2008) Optimal electrocardiographic pulsing windows and heart rate: effect on image quality and radiation exposure at dual-source coronary CT angiography. Radiology, 248(3):792-798.

11 Shrimpton P (2004) Assessment of patient dose in CT: appendix C—European guidelines for multislice computed tomography. European Commission project MSCT: CT safety & efficacy–a broad perspective. (ed)^(eds) http://www.msct.eu/PDF_FILES/EC%20CA%20Report%20 D5%20-%20Dosimetry.pdf (accessed 20 November 2008).

12 Agatston AS, Janowitz WR, Hildner FJ, Zusmer NR, Viamonte M, Jr., Detrano R (1990) Quantification of coronary artery calcium using ultrafast computed tomography. Journal of the American College of Cardiology, 15(4):827-832.

13 Austen WG, Edwards JE, Frye RL, et al. (1975) A reporting system on patients evaluated for coronary artery disease. Report of the Ad Hoc Committee for Grading of Coronary Artery Disease, Council on Cardiovascular Surgery, American Heart Association. Circulation, 51(4 Suppl):5-40.

14 Hoff JA, Chomka EV, Krainik AJ, Daviglus M, Rich S, Kondos GT (2001) Age and gender distributions of coronary artery calcium detected by electron beam tomography in 35,246 adults. The American journal of cardiology, 87(12):1335-1339.

15 McClelland RL, Chung H, Detrano R, Post W, Kronmal RA (2006) Distribution of coronary artery calcium by race, gender, and age: results from the Multi-Ethnic Study of Atherosclerosis (MESA). Circulation, 113(1):30-37.

16 Mitchell TL, Pippin JJ, Devers SM, et al. (2001) Age- and sex-based nomograms from coronary artery calcium scores as determined by electron beam computed tomography. The American journal of cardiology, 87(4):453-456, A456.

17 Nasir K, Raggi P, Rumberger JA, et al. (2004) Coronary artery calcium volume scores on electron beam tomography in 12,936 asymptomatic adults. The American journal of cardiology, 93(9):1146-1149.

18 Choi EK, Choi SI, Rivera JJ, et al. (2008) Coronary computed tomography angiography as a screening tool for the detection of occult coronary artery disease in asymptomatic individuals. Journal of the American College of Cardiology, 52(5):357-365.

19 Kelly JL, Thickman D, Abramson SD, et al. (2008) Coronary CT angiography findings in patients without coronary calcification. Ajr, 191(1):50-55.

20 Sosnowski M, Pysz P, Szymanski L, Gola A, Tendera M (2009) Negative calcium score and the presence of obstructive coronary lesions in patients with intermediate CAD probability. International journal of cardiology, Published Online First: 25 March 2009. doi:10.1016/j.ijcard.2009.01.077.

21 Scholte AJ, Schuijf JD, Kharagjitsingh AV, et al. (2008) Prevalence of coronary artery disease and plaque morphology assessed by multi-slice computed tomography coronary angiography and calcium scoring in asymptomatic patients with type 2 diabetes. Heart (British Cardiac Society), 94(3):290-295.

22 Rivera JJ, Nasir K, Choi EK, et al. (2009) Detection of occult coronary artery disease in asymptomatic individuals with diabetes mellitus using non-invasive cardiac angiography. Atherosclerosis, 203(2):442-448.

23 Iwasaki K, Matsumoto T, Aono H, Furukawa H, Samukawa M (2008) Prevalence of subclinical atherosclerosis in asymptomatic diabetic patients by 64-slice computed tomography. Coronary artery disease, 19(3):195-201.

24 Henneman MM, Schuijf JD, van Werkhoven JM, et al. (2008) Multi-slice computed tomography coronary angiography for ruling out suspected coronary artery disease: what is the prevalence of a normal study in a general clinical population? European heart journal, 29(16):2006-2013.

25 Ostrom MP, Gopal A, Ahmadi N, et al. (2008) Mortality incidence and the severity of coronary atherosclerosis assessed by computed tomography angiography. Journal of the American College of Cardiology, 52(16):1335-1343.

26 Bachar GN, Atar E, Fuchs S, Dror D, Kornowski R (2007) Prevalence and clinical predictors of atherosclerotic coronary artery disease in asymptomatic patients undergoing coronary multidetector computed tomography. Coronary artery disease, 18(5):353-360.

27 Diamond GA, Forrester JS (1979) Analysis of probability as an aid in the clinical diagnosis of coronary-artery disease. The New England journal of medicine, 300(24):1350-1358.

28 Civeira F, International Panel on Management of Familial H (2004) Guidelines for the diagnosis and management of heterozygous familial hypercholesterolemia. Atherosclerosis, 173(1):55-68.

29 Neil A, Cooper J, Betteridge J, et al. (2008) Reductions in all-cause, cancer, and coronary mortality in statin-treated patients with heterozygous familial hypercholesterolaemia: a prospective registry study. European heart journal, 29(21):2625-2633.

30 Hoffmann U, Moselewski F, Nieman K, et al. (2006) Noninvasive assessment of plaque morphology and composition in culprit and stable lesions in acute coronary syndrome and stable lesions in stable angina by multidetector computed tomography. Journal of the American College of Cardiology, 47(8):1655-1662.

31 Stary HC, Chandler AB, Dinsmore RE, et al. (1995) A definition of advanced types of atherosclerotic lesions and a histological classification of atherosclerosis. A report from the Committee on Vascular Lesions of the Council on Arteriosclerosis, American Heart Association. Arteriosclerosis, thrombosis, and vascular biology, 15(9):1512-1531.

32 Achenbach S, Moselewski F, Ropers D, et al. (2004) Detection of calcified and noncalcified coronary atherosclerotic plaque by contrast-enhanced, submillimeter multidetector spiral computed tomography: a segment-based comparison with intravascular ultrasound. Circulation, 109(1):14-17.

33 Leber AW, Knez A, Becker A, et al. (2004) Accuracy of multidetector spiral computed tomography in identifying and differentiating the composition of coronary atherosclerotic plaques: a comparative study with intracoronary ultrasound. Journal of the American College of Cardiology, 43(7):1241-1247.

34 Meijs MF, Meijboom WB, Prokop M, et al. (2009) Is there a role for CT coronary angiography in patients with symptomatic angina? Effect of coronary calcium score on identification of stenosis. Int J Cardiovasc Imaging, 25(8):847-854.

35 Achenbach S, Raggi P (2010) Imaging of coronary atherosclerosis by computed tomography. European heart journal, 31(12):1442-1448.

36 Perrone-Filardi P, Achenbach S, Mohlenkamp S, et al. (2010) Cardiac computed tomography and myocardial perfusion scintigraphy for risk stratification in asymptomatic individuals without known cardiovascular disease: a position statement of the Working Group on Nuclear Cardiology and Cardiac CT of the European Society of Cardiology. European heart journal, Published Online First: 14 July, 2010.

Chapter 9

Accelerated subclinical coronary atherosclerosis in patients with familial hypercholesterolemia

Lisan A. Neefjes
Gert-Jan ten Kate
Alexia Rossi
Koen Nieman
Annette J. Galema-Boers
Janneke G. Langendonk
Annick C. Weustink
Nico R. Mollet
Eric J. Sijbrands
Gabriel P. Krestin
Pim J. de Feyter

ABSTRACT

Objective We determined the extent, severity, distribution and type of coronary plaques in cardiac asymptomatic patients with familial hypercholesterolemia (FH) using computed tomography (CT).

Background FH patients have accelerated progression of coronary artery disease (CAD) with earlier major adverse cardiac events. Non-invasive CT coronary angiography (CTCA) allows assessing the coronary plaque burden in asymptomatic patients with FH.

Materials and Methods A total of 140 asymptomatic statin treated FH patients (90 men; mean age 52±8years) underwent CT calcium scoring (Agatston) and CTCA using a Dual Source CT scanner with a clinical follow-up of 29±8 months. The extent, severity (obstructive or non-obstructive plaque based on >50% or <50% lumen diameter reduction), distribution and type (calcified, non-calcified, or mixed) of coronary plaque were evaluated.

Results The calcium score was 0 in 28 (21%) of the patients. In 16% of the patients there was no CT-evidence of any CAD while 24% had obstructive disease. In total 775 plaques were detected with CT coronary angiography, of which 11% were obstructive. Fifty four percent of all plaques were calcified, 25% non-calcified and 21% mixed. The CAD extent was related to gender, treated HDL-cholesterol and treated LDL-cholesterol levels. There was a low incidence of cardiac events and no cardiac death occurred during follow-up.

Conclusion Development of CAD is accelerated in intensively treated male and female FH patients. The extent of CAD is related to gender and cholesterol levels and ranges from absence of plaque in one out of 6 patients to extensive CAD with plaque causing >50% lumen obstruction in almost a quarter of patients with FH.

INTRODUCTION

Familial hypercholesterolemia (FH) is an inherited autosomal dominant disorder of the lipoprotein metabolism with a prevalence of about 1 in 500 people. FH causes highly elevated serum levels of LDL cholesterol which might accumulate in large and medium sized arteries inducing development of early coronary atherosclerosis [1].

Cardiac CT has evolved as a safe, non-invasive imaging modality to assess coronary atherosclerosis in symptomatic [2-3] and in asymptomatic high-risk patients [4-7]. Detection of subclinical coronary atherosclerosis in patients with FH may provide insights into the accelerated development of coronary artery disease (CAD) in these asymptomatic subjects. Only few studies are available that report about the calcium score or coronary plaque burden in patients with FH [8-10]. Recently we reported the first results of CT coronary angiography (CTCA) in 101 asymptomatic patients with FH, describing the accelerated atherosclerosis in these patients compared to patients with non anginal chest pain [11]. In this present prospective cohort study of an extended patient population of 140 asymptomatic men and women with FH, who have been treated with high dosages of statins, we sought to evaluate in depth not only the CAD severity but also the extent, anatomical distribution and plaque composition of subclinical coronary atherosclerosis, using CT-coronary imaging. Additionally we assessed the relation of occult CAD with patient related variables and the occurrence of adverse cardiac events and all cause death during the follow-up period.

METHODS AND MATERIALS

Study population
Between February 2008 and July 2010 we prospectively invited 214 eligible cardiac asymptomatic statin treated patients with familial hypercholesterolemia to participate in this study as part of continuing recruitment of asymptomatic patients with FH. These patients visit the outpatient preventive clinic of the internal medicine department in our hospital at least once a year for optimization of the medical therapy and early detection of complications. All patients met the criteria for FH according to Aalst-Cohen et al [12], which can be summarized as either 1) the presence of a documented LDL-receptor mutation, or 2) an LDL-cholesterol level above the 95th percentile for gender and age in combination with the presence of typical tendon xanthomas in the patient or in a first degree relative, or 3) an LDL-cholesterol level above the 95th percentile for gender and age in a first degree relative or proven CAD in the patient or in a first degree relative under the age of 60. Patients with secondary causes of hypercholesterolemia such as renal, liver, or thyroid disease were excluded. In addition, all participants were asymptomatic for CAD, i.e. absence of symptoms suggestive of ischemic heart disease or history of CAD. Inclusion

age for women was between 45-70 years, for men between 40-70 years. Exclusion criteria for CTCA were renal insufficiency (serum creatinine >120 μmol/L) (n=4), known contrast allergy (n=3) and irregular heart rhythm (atrial fibrillation) (n=11).

Finally 140 patients with FH could be included after written informed consent, 90 men and 50 women, with a mean age 52±8 years (range 40-68 years).

The institutional Ethical Review Board approved the study protocol.

During their clinical work-up all patients were genetically screened for a LDL-receptor mutation. Lipid levels were obtained by standard methods in patients that were fasting for at least 12 hours. The total cholesterol-years score (mg-y/dL) was calculated as follows: (total cholesterol level at time of FH diagnosis x age at time of diagnosis) + (total cholesterol level after start statin treatment x years of statin treatment)[13]. Presence of tendon xanthomas was clinically evaluated by palpation by experienced clinicians during yearly clinical visits to our hospital.

Computed tomography coronary angiography

Patient preparation
Patients with a heart rate above 65 beats/minute received an oral dose of beta-blockers (100 mg metoprolol) 1 hour before the scan, in the absence of contraindications. Just prior to the scan all patients received nitroglycerin (0.4 mg/dose) sublingually.

Scan protocol
All scans were performed on a Dual Source CT scanner (First 101 scans: Somatom Definition, last 39 scans: Somatom Definition FLASH, Siemens Medical Solutions, Forchheim, Germany). For the non-enhanced scan we used a prospective ECG-triggered scan protocol with a tube current of 76 mAs at 70% of the RR-interval. Images were reconstructed with a slice thickness of 3 mm and an increment of 1.5 mm using a medium convolution kernel (B35f). The contrast enhanced CTCA was obtained using a retrospective ECG-gated scan protocol in the first 101 patients and a prospective ECG-triggered protocol in the last 39 patients. The maximum tube current was 380 mAs. We applied an optimized heart rate-dependent ECG-pulsing (retrospective) or ECG-padding (prospective) protocol with full dose during 62-75% of the RR-interval for heart rates <65 beats/minute and 31-75% for heart rates >65 beats/minute[14]. In addition, automated tube-current modulation was applied. Tube voltage was 120 kV. Pitch (mean 0.25, range 0.2-0.34) and scan time (mean 10.0 s, range 6.9-14.3 s) of the retrospective ECG-gated scans varied with the heart rate. Data of the prospective triggered scans were acquired during 3 or 4 heart beats dependent of the required scan length. Iodinated contrast agent (Ultravist 370 mgI/ml, Bayer Schering Pharma, Berlin, Germany), with a scan time dependent volume (94 ml (80-100 ml)), was administered at a flow rate of 5.5 ml/s through an antecubital vein, followed by a saline chaser of 40 ml at 5.5 ml/s. CTCA datasets were reconstructed at a slice

thickness of 0.75 mm, an increment of 0.4 mm, a medium-soft convolution kernel (B26) or a sharp convolution kernel (B46) when calcium was present. All datasets were sent to a dedicated workstation (MMWP, Siemens Medical Solutions, Forchheim, Germany).

The mean estimated radiation dose per CTCA, calculated by multiplying the dose length product (DLP) by the conversion coefficient of 0.014 mSv·mGy^{-1}·cm^{-1} for the chest, was 7.9 mSv ± 2.4 mSv (range 3.9-16.4 mSv)[15].

CT analysis
No complications occurred during or after scanning and all scans were included in the analysis. Using the non-enhanced CT scan the calcium score was calculated semi-automatically. The coronary calcium score is expressed as the Agatston score per patient.

Two experienced readers analyzed all CTCA scans separately and discrepancies in their evaluations were resolved by consensus. Per segment, using the modified AHA 17-segment model, the absence or presence of a coronary plaque was determined, as was the severity of the lumen narrowing (0, >0-20%, >20-50%, >50-70% and >70% diameter reduction). Obstructive CAD was defined as plaque causing >50% lumen diameter reduction.

We assessed a clinical CAD extent score per patient based on the severity of plaque per coronary segment. The score is the sum of the luminal stenosis of each individual segment (0 = 0%, 1 = >0-20%, 2 = >20-50%, 3 = >50-70% or 4 = >70% lumen diameter reduction). This results in a CAD extent score ranging from 0 to a theoretical maximum of 68.

Additionally the plaque composition was classified as 1) calcified: highly attenuating tissue for >70% of the plaque volume which could be clearly separated from the contrast enhanced coronary lumen, 2) non-calcified: low attenuating lesions that could be clearly separated from the coronary lumen and the surrounding epicardial fat or myocardium and c) mixed: containing both calcified and non-calcified tissue. The presence of positive remodeling (diameter at the lesion site at least 10% larger than at the reference site) was assessed in all non-calcified lesions. Vessel segments <1.5 mm in diameter were excluded from analysis

CTCA results were blinded for treating physicians and patients which precludes treatment decisions made based on these results.

Risk scores
The Framingham risk score (according to the NECP/ATPIII report 2002[16]) was calculated in all FH patients. In this NECP/ATPIII report diabetes mellitus is considered an equivalent of coronary heart disease and for this study patients with diabetes mellitus were considered to have a 10-years risk of 20%.

Follow-up

Patient files were examined for follow-up data and patients were approached by telephone when recent information was lacking in the files. Cardiac events (myocardial infarction, acute coronary syndrome (ACS), stable or unstable angina pectoris (AP), percutaneous coronary intervention and coronary artery bypass graft (CABG)) and (all cause) death were inventoried.

Statistical analysis

Continuous variables are shown as mean [±SD] or median [IQR]. Categorical variables are expressed as number [frequency]. We used the Mann-Whitney test to compare the CAD extent between male and female patients, between patients without and with diabetes ,mellitus type 2 and between patients without and with a cardiac event during follow-up time and to compare the Framingham risk score between patients without and with obstructive CAD.

The relationship between the calculated CAD extent and patient characteristics, cardiovascular risk factors and lipid levels was assessed using linear regression analysis. Variables with a univariate relationship (p<0.2) with the presence of obstructive coronary CAD were entered in the multivariate regression model using backward elimination (p<0.1). A p-value of <0.05 was considered statistically significant.

Inter-observer and intra-observer agreement is described with the k statistics. All analyses were performed using SPSS for windows (version 15.0, SPSS, Chicago, USA).

RESULTS

Baseline

The patient characteristics are shown in table 1. A positive family history for cardiovascular disease was reported in 71% (99/140) of the patients, hypertension in 26% (37/140), diabetes mellitus in 6% (9/140) and smoking in 29% (40/140). In 66% (93/140) of the patients a mutation in the LDL-receptor mutation has been identified. The 34% other patients were diagnosed with FH on clinical grounds.

CT analysis

Coronary artery disease per patient

A negative calcium score was present in 20% (28/140)) of our patients. The median coronary calcium score was 51 (IQR 2-350) (table 1). The total calcium score significantly increased with higher age (3 age categories, 40-49, 50-59, and 60-69 years) in both men (15.4 (0-287), 194 (38-488), and 521 (135-1001), respectively, (p<0.001) and women (0 (0-4), 32 (8-136), and 96 (51-662), respectively, p<0.001).

CTCA showed no plaques in 16% (23/140) of the patients. In 60% (84/140) of the patients only lesions causing <50% lumen obstruction were present and in 24% (33/140) one or more lesions of >50% lumen diameter stenosis were detected. Four patients had obstructive lesions in all three coronaries (3-vessel disease), 9 in 2 vessels and 20 in 1 vessel. Presence and severity of CAD per patient in both men and in women in 3 age categories are shown in figure 1A. Presence and severity of CAD per patient (no CAD, non-obstructive CAD and obstructive CAD) was significantly higher in patients at higher age in men (p=0.03) and in women (p=0.01).

Table 1

Variable	n=140
Gender (male)	90 (64%)
Age (years)	52 (8)
Riskfactors	
Smoker†	40 (29%)
Hypertension‡	37 (26%)
Diabetes§	9 (6%)
CAD positive in family history‖	99 (71%)
Body mass index (kg/m²)	26.6 (3.7)
Lipids (treated)	
Total cholesterol (mmol/l)	5.5 (1.4)
LDL-cholesterol (mmol/l)	3.5 (1.3)
HDL-cholesterol (mmol/l)	1.4 (0.4)
Triglycerides (mmol/l)	1.5 (1.5)
Total cholesterol-years score¶ (mg-years/dl)	18321 (5112)
FH related characteristics	
Known genetic disorder	93 (66%)
Age at start statin use (years)	43 (10)
Duration of statin use (years)	9 (7)
Maximum untreated total cholesterol (mmol/l)	9.7 (2.4)
Tendon xanthomas	33 (24%)
Arcus cornealis	31 (22%)

Calcium Score	
Total calcium score* (Agatston)	51 (2-350)
0	28 (20%)
0-100	51 (36%)
101-400	29 (21%)
>400	32 (23%)
CT coronary angiography	
presence of coronary plaque	23 (16%)
CAD extent#	7 (3-16)

Continuous data is expressed as mean (SD) and dichotomous data as n (%). *The calcium score and the CAD extent are expressed as median (Inter Quartile Range). CAD, Coronary Artery Disease; HDL, high-density lipoprotein; LDL, low-density lipoprotein. †*Currently and/or in the past*. ‡Blood pressure >140/90 mm Hg or treatment for hypertension. §Treatment with oral anti-diabetic medicine or insulin. ‖Premature CAD in 1st degree relative. ¶ Score according to Hoeg et al.(15) (pre treatment cholesterol * age at start treatment + post treatment cholesterol * years of treatment). # Score based on the sum of the severity of plaque per segment (0% lumen diameter stenosis=0; >0%-20%=1; >20%-50%=2; >50%-70%=3; >70%=4)

A calcium score of zero excluded obstructive CAD in this cohort of patients with FH. Patients with a calcium score of >400 exhibited obstructive CAD in 69% (22/32).

Coronary plaque analysis

After exclusion of 16 segments because of non-diagnostic image quality 1918 segments were available for analysis. Sixty percent (1144/1918) of the segments showed no signs of coronary artery disease. In 4% (70/1918) of the segments a lesion of more than 50% lumen diameter stenosis was detected. The CAD extent score increased at increasing age. In men the median CAD extent score (10 [4-17]) was significantly higher than in women (5 [2-11]; p=0.004) (figure 1). The CAD extent score was slightly higher in patients with a known LDL-mutation (10 (IQR 3-17) compared to patients without such mutation (6 (IQR 2-13)) although not significantly (p=0.06). A sub analysis in patients without (n=131) and with (n=9) diabetes mellitus type II showed no significant difference in calcium score (51 (2-346) vs. 89 (5-1580), respectively, p=0.57) and CAD extent (8 (3-16) vs. 5 (2-21), respectively, p= 0.86).

Plaque composition

Overall 54% (419/775) of the plaques were calcified, 25% (192/775) were non-calcified and 21% (163/775) were mixed. The percentage of calcified plaques increased with increasing age in both men and women. Most non-calcified plaques (146/192 (76%)) caused <20% lumen obstruction while the more severe plaques (>50% lumen diameter stenosis) were mainly caused by lesions containing calcium (calcified and mixed plaques) (60/70 (86%)). Of all non-calcified plaques 9 showed positive remodeling (9/192 (5%)).

Figure 1 Extent of coronary artery disease in relation to gender at different ages
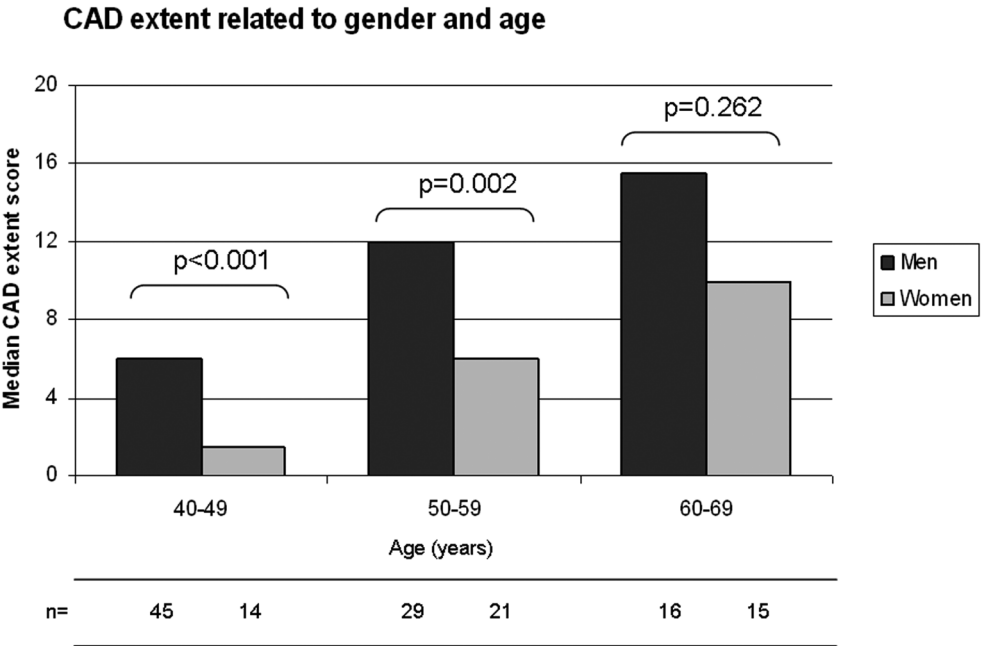
CAD, coronary artery disease.

Distribution and localization of coronary plaque

The majority of the plaques were located in the proximal and mid-parts of the coronary arteries of which the proximal (99/140 (71%)) part of the LAD showed plaque most frequently, while the mid-segment of the RCA showed the highest number of obstructive lesions (12/132 (9%)). The distal LCX showed the least atherosclerotic disease. The presence and the severity of CAD per coronary segment are shown in figure 2.

Risk scores

The median adjusted Framingham risk score in patients without obstructive CAD (4 (1-10)) is significantly lower than in patients with obstructive CAD (8 (5-12), p<0.001).

Follow up

Mean follow-up time was 29 ± 8 months (range 9-43 months). None of the patients died during the follow-up period, 2 patients experienced stable AP, 1 patient suffered an ACS and one patient had a positive exercise test without symptoms. All these 4 patients underwent CABG. The 4 patients requiring CABG had a significant higher CAD extent (median 24 (IQR 22-31)) than patients without a cardiac event (median CAD extent 7 (IQR 3-15), p<0.01) and they all 4 exhibited obstructive CAD.

Figure 2 Distribution of presence and severity of coronary plaque in the proximal, mid and distal segments of the coronary tree.
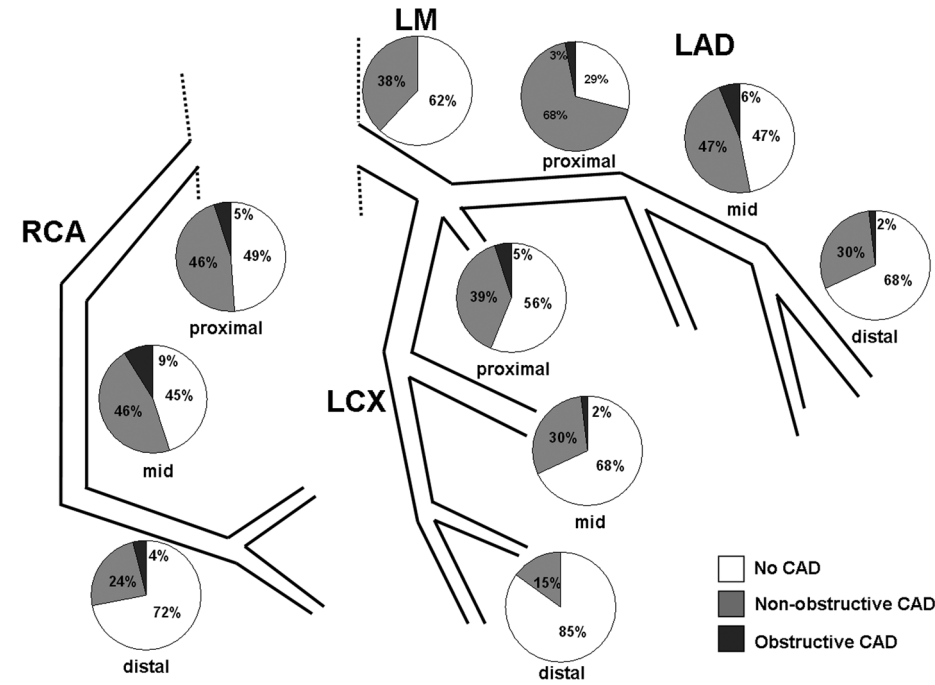
LAD, left anterior descending coronary artery; LCX, left circumflex coronary artery; LM, left main; RCA, right coronary artery. The distal RCA comprises segment 3, the posterior descending artery and the postero-lateral artery. The mid LAD includes segment 7 and the first diagonal, the distal LAD includes segment 8 and the second diagonal. The proximal LCX comprises segment 11 and the intermediate branch; the mid LCX segment 13 and the first marginal obtuse branch; the distal LCX includes segment 15 and the second obtuse marginal branch.

Relationship between patients characteristics and the CAD extent.

The results of the linear regression analysis are presented in table 2. The independent variables were gender (B -6.15, 95% CI -9.35- -2.89, p<0.01), treated HDL-values (B -4.77, 95% CI -8.97- -0.56, p=0.03), and treated LDL-values (B 1.48, 95% CI 0.25-2.61, p=0.02).

The κ statistics of the inter-observer agreement for the evaluation of the stenosis severity per plaque and the plaque composition were 0.78 and 0.83, respectively and of the intra-observer agreement 0.81 and 0.84, respectively.

Table 2

n=140	Univariate linear regression				Multivariate linear regression			
	B	SE of B	95% CI	p-value	B	SE of B	95% CI	p-value
Age (years)	**0.32**	**0.09**	**0.15 - 0.50**	**0.000**	0.24	0.13	-0.17 - 0.498	0.068
Gender (female)	**-4.30**	**1.44**	**-7.14 - -1.45**	**0.003**	**-6.15**	**1.63**	**-9.35 - -2.89**	**0.000**
Smoker†	0.99	1.57	-2.13 - 4.10	0.532	-	-	-	-
Diabetes†	0.65	2.90	-5.08 - 6.39	0.822	-	-	-	-
Hypertension†	**2.47**	**1.60**	**-0.69 - 5.64**	**0.125**	-	-	-	-
Positive Family History†	-1.53	1.56	-4.61 - 1.55	0.327	-	-	-	-
Body Mass Index (kg/m^2)	**0.40**	**0.19**	**0.02 - 0.78**	**0.038**	-	-	-	-
Known genetic disorder	-2.48	1.51	-5.47 - 0.51	0.103	-	-	-	-
Total cholesterol-years score	**0.02**	**0.01**	**0.01 - 0.03**	**0.001**	0.02	0.01	-0.00 - 0.03	0.064
LDL-cholesterol (mmol/l)	**1.23**	**0.56**	**0.13 - 2.32**	**0.029**	**1.48**	**0.56**	**0.25 - 2.61**	**0.018**
HDL-cholesterol (mmol/l)	**-5.47**	**1.85**	**-9.12 - -1.82**	**0.004**	**-4.77**	**2.12**	**-8.97 - -0.56**	**0.027**
Triglycerides (mmol/l)	0.35	0.48	-0.60 - 1.29	0.467	-	-	-	-
Tendon xanthomas	**3.02**	**1.70**	**-0.34 - 6.38**	**0.077**	-	-	-	**-**

* Score based on the sum of the severity of plaque per segment (0% lumen diameter stenosis=0; >0%-20%=1; >20%-50%=2; >50%-70%=3; >70%=4). † Definition as in table 1. Variables in bold (p<0.2) were entered in the multivariate regression model. Backward elimination was used in the multivariate model (p<0.10). B, regression coefficient; CI, confidence interval; HDL, high-density lipoprotein; LDL, low-density lipoprotein; SE, standard error.

DISCUSSION

FH is associated with an increased risk of adverse coronary artery disease although some FH patients with this condition reach a high age without significant complications. Non-invasive CT coronary plaque imaging is able to identify absence, presence and extent of CAD and could be used as a tool to differentiate asymptomatic patients with advanced CAD from those who are relatively unaffected, and thereby guide preventive or therapeutic measures. In our cross-sectional study of 140 asymptomatic statin treated patients with FH we found that 84% had detectable coronary plaque, and 24% had obstructive CAD (>50% diameter stenosis). Men exhibited more advanced coronary disease at a younger age than women.

Only 20% of this FH cohort had a zero calcium score, which is much lower than the 44-51% shown in 3 large scale population studies, i.e. MESA[17], HNR[18] and Budoff et al.[2] or the 35-80% of normal calcium scans in other asymptomatic populations [4; 19]. Notably a zero calcium score did not completely rule out presence of CAD, because non-calcified plaque was present in 4% of these calcium free patients. However, none of these plaques caused >50% luminal obstruction.

CTCA enables assessment of the total extent of coronary plaque per patient, which provides a more comprehensive evaluation of the coronary atherosclerosis than the assessment of the presence of obstructive lesions alone. In addition it has been reported that sudden adverse coronary outcomes are usually caused by vulnerable plaques and that the severity of stenosis is of less importance than the composition and the size of these plaques[20]. Min et al. showed that CTCA examination of the extent of CAD in symptomatic patients, including a stenosis severity score which is largely comparable to our CAD extent score, is of incremental value to assess all cause death [21].

CTCA did not reveal any CAD in 16% of this cohort of patients with FH, which is within the range of the absence of CAD in 7% to 36% asymptomatic diabetic patients [6-7], but much lower than the 32% to 79% of other high risk asymptomatic patients [4-5]. In addition we found obstructive CAD in 24% of our FH patients, although all were asymptomatic for CAD. In asymptomatic diabetic patients a comparable prevalence has been described [6-7], but in other high risk asymptomatic populations the prevalence of obstructive CAD of approximately 5% to 16% was much lower [4-5].

A previous study by Miname et al.[9] showed a lower prevalence of plaque (48%) in asymptomatic patients with FH than we found in our current study (84%). Calcium score (0 (IQR 0-748)) and prevalence of obstructive CAD (19%) were only slightly lower. However, the patient population of Miname et al. was younger (45±13 years) than ours (52±8 years) and comprised 64% women compared to 36% women in our population. Additionally none of the patients were on statin treatment during the study, whereas only 66% had been treated with statins previously.

The majority of coronary plaques were localized in the proximal and mid parts of the coronary arteries which is largely similar to the anatomical features of CAD in symptomatic patients. The proximal LAD exhibited plaque in 80% of the patients which might be of concern because lesions in the proximal LAD were associated with worse prognostic outcome [22].

With increasing age in men and in women the percentage of calcified plaque increased and consequently the percentage of non-calcified plaques decreased. This is in line with other CTCA studies in asymptomatic patients [4] and in symptomatic patients [23] and it corresponds with the suggestion that the advanced stages of coronary atherosclerosis are reflected by more intense calcifications [24]. There is still debate whether coronary plaque calcification is associated with stability or instability of a coronary plaque leading to coronary thrombosis. It has been shown that plaques that have a low CT density (non-calcified lipid plaques) and evidence of positive remodeling were associated with a higher likelihood of adverse coronary events [23; 25]. In our study we found positive remodeling in a small number of non-calcified plaques, but due to cross-talk of lumen attenuation and absolute plaque density [26], we could not accurately distinguish between fibrous and lipid tissue in those mainly small plaques.

We demonstrated that gender, treated HDL-cholesterol and treated LDL-cholesterol were significantly associated with the extent of CAD. Previously Junyent et al. also have shown the strong independent predictive value of HDL-cholesterol levels (negatively) for preclinical carotid atherosclerosis in patients with FH. Our results therefore confirm their suggested important role for HDL-raising therapies in future treatment strategies in patients with FH [27].

It has been shown that traditional risk factors do play an important role in patients with FH but the predictive value might be different than in the general population [28]. However, we could not confirm a significant relation between the traditional risk factors age, smoking, hypertension, diabetes or the specific FH related presence of tendon xanthomas or presence of a LDL-receptor mutation and the extent of CAD. This was probably the result of the limited number of patients with FH that were studied causing insufficient statistical power.

Nine patients with diabetes mellitus type 2 were included in our study and these patients may have a more extensive expression of CAD. However, a separate analysis of the patients with diabetes mellitus type 2 compared to patients without diabetes did not reveal a difference in extent of CAD.

Using an adjusted Framingham Risk Score we could demonstrate that there was a direct relation between the Framingham Risk Score and the presence of obstructive CAD. The FRS has been based on a general population and patients with FH were not enough represented in that study. Nevertheless, although the FRS in our population might under-

estimate the total 10-year CHD risk, it shows the positive relation between the risk factors and the CAD extent.

As has been recently reported by Hadamitzky et al. cardiac CT has incremental prognostic value in asymptomatic individuals [19]. In our study though, there was a low incidence of cardiac events during 29 months follow-up. We found a higher extent of CAD in the patients that developed stable angina or acute coronary syndrome followed by CABG during FU than in patients without development of clinical symptoms of CAD. Additional studies are warranted to establish whether it is reasonable to intensify medical preventive treatment in patients with evident CAD on CT to prevent progression of disease and development of adverse events and to continue or even lower current medical treatment in patients without subclinical coronary atherosclerosis on CT. Cardiac CT might lead to a more cost-effective allocation of preventive efforts.

Radiation exposure of CT coronary angiography remains a matter of concern. By using a dual source scanner with optimized scan protocols the mean estimated effective dose of a CTCA in our study was 7.9 mSv. To minimize the lifetime attributable risk of cancer and in women the risk of birth abnormalities in their offspring we included only women of at least 45 years and men of at least 40 years of age. However, due to recent technical improvements the effective radiation dose of a CTCA currently can be <3.0 mSv [29]. Decreasing the radiation dose is of positive influence on the harm-benefit ratio of CTCA, which might even induce extended use of CTCA for screening purposes or repetitive scanning for CAD progression follow up when CT-scanning below 1 mSv is definitively available.

Limitations
CTCA may not be able to detect very early coronary atherosclerosis which is beyond the spatial resolution of current CT-technology. CTCA tends to overestimate or underestimate the severity of obstructive CAD and in particular calcified plaques hinder precise severity assessment, due to blooming effects. In patients with a calcium score >10 (Agatston) and more explicit >400, the diagnostic accuracy of CTCA to exclude or detect obstructive CAD is hampered compared to patients with less calcium [30]. Our patients with FH were treated with intense lipid lowering drugs which will have modified the natural history of plaque progression. We included only patients aged 40 to 70 years old that may have affected the prevalence of CAD considering the strong relation of age and CAD in the elderly. However we sought to include patients in whom additional long lasting measures to prevent progression of CAD could be beneficial.

CONCLUSION

CT coronary imaging uniquely allows for non-invasive assessment of the extent, severity, anatomic distribution and plaque composition of coronary artery disease in asymptomatic patients with FH. The extent of CAD in this high risk population is related to lipid blood values and ranges from absence of detectable CAD in less than one out of six patients to obstructive CAD in nearly a quarter of patients despite the absence of symptoms. The anatomical distribution and composition of coronary plaques is similar to that of patients without FH.

Funding

REFERENCES

1   Austin MA, Hutter CM, Zimmern RL, Humphries SE (2004) Familial hypercholesterolemia and coronary heart disease: a HuGE association review. American journal of epidemiology, 160(5):421-429.

2   Budoff MJ, Shaw LJ, Liu ST, et al. (2007) Long-term prognosis associated with coronary calcification: observations from a registry of 25,253 patients. Journal of the American College of Cardiology, 49(18):1860-1870.

3   Meijboom WB, van Mieghem CA, Mollet NR, et al. (2007) 64-slice computed tomography coronary angiography in patients with high, intermediate, or low pretest probability of significant coronary artery disease. Journal of the American College of Cardiology, 50(15):1469-1475.

4   Choi EK, Choi SI, Rivera JJ, et al. (2008) Coronary computed tomography angiography as a screening tool for the detection of occult coronary artery disease in asymptomatic individuals. Journal of the American College of Cardiology, 52(5):357-365.

5   Iwasaki K, Matsumoto T, Aono H, Furukawa H, Samukawa M (2008) Prevalence of subclinical atherosclerosis in asymptomatic diabetic patients by 64-slice computed tomography. Coronary artery disease, 19(3):195-201.

6   Rivera JJ, Nasir K, Choi EK, et al. (2009) Detection of occult coronary artery disease in asymptomatic individuals with diabetes mellitus using non-invasive cardiac angiography. Atherosclerosis, 203(2):442-448.

7   Zeina AR, Odeh M, Rosenschein U, Zaid G, Barmeir E (2008) Coronary artery disease among asymptomatic diabetic and nondiabetic patients undergoing coronary computed tomography angiography. Coronary artery disease, 19(1):37-41.

8   Gidding SS, Bookstein LC, Chomka EV (1998) Usefulness of electron beam tomography in adolescents and young adults with heterozygous familial hypercholesterolemia. Circulation, 98(23):2580-2583.

9   Miname MH, Ribeiro MS, 2nd, Parga Filho J, et al. (2010) Evaluation of subclinical atherosclerosis by computed tomography coronary angiography and its association with risk factors in familial hypercholesterolemia. Atherosclerosis, 213(2):486-491.

10 Santos RD, Meneghelo RS, Chacra AP, Martinez TL, Ramires JA, Carvalho JA (2004) Detection of subclinical atherosclerosis by electron beam tomography in females with heterozygous familial hypercholesterolaemia. Heart (British Cardiac Society), 90(1):92-94.

11 Neefjes LA, Ten Kate GJ, Rossi A, et al. (2011) CT coronary plaque burden in asymptomatic patients with familial hypercholesterolaemia. Heart (British Cardiac Society), 97(14):1151-1157.

12 van Aalst-Cohen ES, Jansen AC, Tanck MW, et al. (2006) Diagnosing familial hypercholesterolaemia: the relevance of genetic testing. European heart journal, 27(18):2240-2246.

13 Hoeg JM, Feuerstein IM, Tucker EE (1994) Detection and quantitation of calcific atherosclerosis by ultrafast computed tomography in children and young adults with homozygous familial hypercholesterolemia. Arterioscler Thromb, 14(7):1066-1074.

14 Weustink AC, Mollet NR, Pugliese F, et al. (2008) Optimal electrocardiographic pulsing windows and heart rate: effect on image quality and radiation exposure at dual-source coronary CT angiography. Radiology, 248(3):792-798.

15 Shrimpton P (2004) Assessment of patient dose in CT: appendix C—European guidelines for multislice computed tomography. European Commission project MSCT: CT safety & efficacy–a broad perspective. (ed)^(eds) http://www.msct.eu/PDF_FILES/Appendix%20paediatric%20CT%20Dosimetry.pdf (accessed 20 November 2008).

16 National Cholesterol Education Program Expert Panel on Detection E, Treatment of High Blood Cholesterol in A (2002) Third Report of the National Cholesterol Education Program (NCEP) Expert Panel on Detection, Evaluation, and Treatment of High Blood Cholesterol in Adults (Adult Treatment Panel III) final report. Circulation, 106(25):3143-3421.

17 McClelland RL, Chung H, Detrano R, Post W, Kronmal RA (2006) Distribution of coronary artery calcium by race, gender, and age: results from the Multi-Ethnic Study of Atherosclerosis (MESA). Circulation, 113(1):30-37.

18 Schmermund A, Mohlenkamp S, Berenbein S, et al. (2006) Population-based assessment of subclinical coronary atherosclerosis using electron-beam computed tomography. Atherosclerosis, 185(1):177-182.

19 Hadamitzky M, Meyer T, Hein F, et al. (2010) Prognostic value of coronary computed tomographic angiography in asymptomatic patients. The American journal of cardiology, 105(12):1746-1751.

20 Falk E, Shah PK, Fuster V (1995) Coronary plaque disruption. Circulation, 92(3):657-671.

21 Min JK, Shaw LJ, Devereux RB, et al. (2007) Prognostic value of multidetector coronary computed tomographic angiography for prediction of all-cause mortality. Journal of the American College of Cardiology, 50(12):1161-1170.

22 Mark DB, Nelson CL, Califf RM, et al. (1994) Continuing evolution of therapy for coronary artery disease. Initial results from the era of coronary angioplasty. Circulation, 89(5):2015-2025.

23 Bamberg F, Dannemann N, Shapiro MD, et al. (2008) Association between cardiovascular risk profiles and the presence and extent of different types of coronary atherosclerotic plaque as detected by multidetector computed tomography. Arterioscler Thromb Vasc Biol, 28(3):568-574.

24 Stary HC, Chandler AB, Dinsmore RE, et al. (1995) A definition of advanced types of atherosclerotic lesions and a histological classification of atherosclerosis. A report from the Committee on Vascular Lesions of the Council on Arteriosclerosis, American Heart Association. Arteriosclerosis, thrombosis, and vascular biology, 15(9):1512-1531.

25 Motoyama S, Sarai M, Harigaya H, et al. (2009) Computed tomographic angiography characteristics of atherosclerotic plaques subsequently resulting in acute coronary syndrome. Journal of the American College of Cardiology, 54(1):49-57.

26 Cademartiri F, Runza G, Palumbo A, et al. (2010) Lumen enhancement influences absolute noncalcific plaque density on multislice computed tomography coronary angiography: ex-vivo validation and in-vivo demonstration. J Cardiovasc Med (Hagerstown), 11(5):337-344.

27 Junyent M, Cofan M, Nunez I, Gilabert R, Zambon D, Ros E (2006) Influence of HDL cholesterol on preclinical carotid atherosclerosis in familial hypercholesterolemia. Arteriosclerosis, thrombosis, and vascular biology, 26(5):1107-1113.

28   Civeira F, International Panel on Management of Familial H (2004) Guidelines for the diagnosis and management of heterozygous familial hypercholesterolemia. Atherosclerosis, 173(1):55-68.

29   von Ballmoos MW, Haring B, Juillerat P, Alkadhi H (2011) Meta-analysis: diagnostic performance of low-radiation-dose coronary computed tomography angiography. Ann Intern Med, 154(6):413-420.

30   Meijs MF, Meijboom WB, Prokop M, et al. (2009) Is there a role for CT coronary angiography in patients with symptomatic angina? Effect of coronary calcium score on identification of stenosis. Int J Cardiovasc Imaging, 25(8):847-854.

Chapter *10*

The effect of LDLR-negative genotype on CT coronary atherosclerosis in asymptomatic statin treated patients with heterozygous familial hypercholesterolemia

Gert-Jan ten Kate
Lisan A. Neefjes
Admir Dedic
Koen Nieman
Janneke G. Langendonk
Annette J. Galema-Boers
Jeanine E. Roeters van Lennep
Adriaan Moelker
Gabriel P. Krestin
Eric J. Sijbrands
Pim J. de Feyter

Chapter 10

The effect of LDLR-negative genotype on CT coronary atherosclerosis in asymptomatic
statin treated patients with heterozygous familial hypercholesterolemia.

ABSTRACT

Objective To evaluate the influence of LDL receptor (LDLR) -negative mutational status on CT coronary atherosclerosis in asymptomatic statin treated patients with heterozygous familial hypercholesterolemia (FH).

Materials and Methods Cardiac CT angiography (CCTA) was performed in 145 FH patients (93 men; mean age 52 ± 8) screened for LDLR and apolipoprotein B (APOB) mutations. The extent of coronary plaque was compared between two groups: 1) 59 patients (41%) heterozygous for LDLR-negative mutations (LDLR-negative) and 2) 86 patients (59%) with reduced or normal LDLR function (LDLR-positive) consisting of 32 LDLR-defective mutations, 8 APOB mutations and 46 patients in whom no mutation could be identified.

The diseased segments score (DSS) was the primary study endpoint defined as the number of coronary artery segments (0-17) with > 20% luminal diameter narrowing. We compared the DSS between LDLR-negative and LDLR-positive patients. Within the LDLR-positive group a secondary analysis was performed between identified (LDLR-defective, APOB) and unidentified mutational status.

Results The median DSS was higher in LDLR-negative than in LDLR-positive patients (4 (1-7) and 2 (0-5); P = 0.017). After adjustment for risk factors, LDLR-negative mutational status remained an independent predictor of the DSS (B = 1.09; P = 0.047). The DSS in the LDLR-positive group was similar for patients with identified and patients with unidentified mutational status.

Conclusion In asymptomatic statin treated patients with a clinical diagnosis of FH, LDLR-negative mutational status is associated with a higher extent of subclinical CT coronary atherosclerosis.

INTRODUCTION

Heterozygous familial hypercholesterolemia (FH; OMIM #143890) is an autosomal dominant disorder of the cholesterol metabolism caused by mutations in the low-density lipoprotein receptor gene (*LDLR*). FH is associated with in a lifelong elevation of LDL-cholesterol (C) levels, tendon xanthomas, the early onset of coronary artery disease (CAD) and excess mortality [1-6].

The clinical diagnosis of FH is based on personal and family history, physical examination and laboratory findings, but the presence of a functional mutation of the *LDLR* gene, the apolipoprotein B gene (*APOB*) or the proprotein convertase subtilisin / kexin type 9 gene (*PCSK9*) provides the unequivocal diagnosis of FH [7-9]. Such a molecular diagnosis is made in about 50-80% of clinically identified cases [10-11].

Five classes of LDLR gene mutations have been specified [12]. Class 1 and 2a LDLR mutations result in the absence of a functional LDLR protein (LDLR-negative mutations). Other classes result in LDLR proteins with residual function (LDLR-defective mutations). Despite its monogenic background, heterozygous FH shows a great variability in phenotypic expression [5; 13-14].

It has been suggested that LDLR-negative mutations correlate positively with detrimental lipid profiles, tendon xanthomas and risk of future coronary events [15-18]. Our goal was to verify the hypothesis that asymptomatic patients with a clinical diagnosis of FH and LDLR-negative mutations have a higher extent of subclinical CT coronary atherosclerosis as compared to patients with LDLR-positive mutational FH, despite statin treatment. Although statin treatment nowadays is routine clinical practice in FH patients, our findings might identify a subgroup at higher CAD risk.

Non-invasive coronary CT angiography (CCTA) allows for the accurate assessment of CAD [19-20]. No studies have been published comparing coronary atherosclerosis assessed by CCTA in FH patients with different LDLR mutational status.

METHODS

Study population
Between February 2008 and June 2011 we included 145 consecutive asymptomatic patients with a clinical diagnosis of FH. After diagnosis all patients were treated with statins. In three cases statin medication had to be stopped because of severe side effects. No patients had proven CAD or had any symptoms suggestive of ischemic heart disease. The absence of symptoms and negative cardiovascular history were verified before patient inclusion.

Chapter 10

The effect of LDLR-negative genotype on CT coronary atherosclerosis in asymptomatic
statin treated patients with heterozygous familial hypercholesterolemia.

Our study population was recruited from a total of 330 patients with a clinical diagnosis of FH that visited the outpatient lipid clinic at our institution during the inclusion period. The following diagnostic criteria for FH were used: either 1) the presence of a documented mutation of the LDLR, the APOB or the PCSK9 gene, or 2) an LDL-C level above the 95th percentile for gender and age in combination with a) the presence of typical tendon xanthomas in the patient or in a first degree relative, or b) an LDL-C level above the 95th percentile for gender and age in a first degree relative or, c) proven CAD in a first degree relative under the age of 60 [21]. Patients with secondary causes of hypercholesterolemia such as renal, liver, or thyroid disease were excluded from the study.

The inclusion age for the study varied from 40-70 years for men and for women from 45-70 years. Exclusion criteria were renal insufficiency (serum creatinine > 120 µmol/L), known contrast allergy or irregular heart rhythm (atrial fibrillation). The institutional Ethical Review Board approved the study protocol. All patients gave written informed consent.

DNA samples were taken of all FH patients and sent to a central laboratory for LDLR, APOB and PCSK9 mutational screening [22]. All patients were classified on the basis of their mutational status as: LDLR-negative, LDLR-defective, APOB mutation, PCSK9 mutation or unidentified mutation. Patients with unidentified mutations underwent testing but no mutation could be identified.

In a primary analysis we compared the diseased segments score (DSS) of LDLR-negative mutational FH with other clinical FH patients (LDLR-positive). Within the LDLR-positive group we did a secondary analysis comparing the DSS between patients with identified (LDLR-defective, APOB, PCSK9) and unidentified mutational status.

Scan protocol
All scans were performed on a dual source CT scanner (first 101 scans: Somatom Definition, last 44 scans: Somatom Definition FLASH, Siemens Medical Solutions, Forchheim, Germany). For the non-enhanced coronary calcium scan we used a prospective ECG-triggered scan protocol with a tube current of 76 mAs at 70% of the RR-interval. Images were reconstructed with a slice thickness of 3 mm and an increment of 1.5 mm using a medium convolution kernel (B35f).

CCTA was obtained using a retrospective ECG-gated spiral scan protocol in the first 101 patients and a prospective ECG-triggered axial protocol in the last 44 patients. The maximum tube current was 380 mAs. Both for spiral and axial scan modes (nominal) exposure was limited to the diastolic phase (62-75% of the R-R interval) for heart rates ≤ 65 beats per minute. Nominal exposure was extended beyond the mid-diastolic phase (31-75% of the R-R interval) in patients with a heart rate > 65 beats per minute [23]. In addition, automated tube-current modulation was applied. Tube voltage was 120 kV. Iodinated

contrast agent (Ultravist 370 mg/ml, Bayer Schering Pharma, Berlin, Germany), with a scan time dependent volume (94 ml (80-100 ml)), was administered at a flow rate of 5.5 ml/s through an antecubital vein followed by a saline chaser of 40 ml at 5.5 ml/s.

CCTA datasets were reconstructed at a slice thickness of 0.75 mm, an increment of 0.4 mm, a medium-soft convolution kernel (B26) or a sharp convolution kernel (B46) when calcium was present. All datasets were sent to a dedicated workstation (MMWP, Siemens Medical Solutions, Forchheim, Germany). The mean estimated radiation dose per CCTA, calculated by multiplying the dose length product (DLP) by the conversion coefficient of $0.014 \ mSv \cdot mGy^{-1} \cdot cm^{-1}$ for the chest, was 8.2 mSv ± 2.9 mSv (range 15) for the spiral scan protocol and 4.8 mSv ± 2.5 mSv (range 10) for the prospective protocol [24].

CT analysis
Two experienced readers, blinded with regard to the FH mutational status, evaluated all CCTA scans separately. Discrepancies in evaluation were resolved during a consensus reading.

Per segment, using a modified 17-segment model [25], the percentage of maximum luminal diameter narrowing was visually estimated and graded as either: 0%, 1-20%, 21-50%, 51-70% or > 70%. Vessel segments that were smaller than 1.5 mm in diameter were excluded from all analyses.

Per patient, coronary plaque burden was expressed in three ways: 1) the diseased segments score (DSS); 2) the CAD severity score and 3) the CAD extent score [2; 26]. The DSS was the primary endpoint of the study expressed as the total number of diseased coronary artery segments per patient (0-17) without grading stenosis severity: score = 1 for > 20% luminal diameter narrowing.

The CAD severity score includes stenosis grade in the quantification algorithm. The CAD severity score is the integrated sum of the stenosis severity (score 1-3) and the number of coronary artery lesions: score = 1 for 21-50%, score = 2 for 51-70% and score = 3 for > 70% luminal diameter narrowing.

Finally, coronary plaque burden was expressed as the CAD extent score that includes low-grade stenoses in the quantification algorithm. The CAD extent score is the integrated sum of the stenosis severity (score 1-4) and the number of coronary artery lesions: score = 1 for 1-20%, score = 2 for 21-50%, score = 3 for 51-70% and score = 4 for > 70% luminal diameter narrowing.

Stenosis severity per patient was graded as "no plaque or stenosis" (0-20% luminal diameter stenosis), "non-obstructive plaque" (21-50% luminal diameter stenosis) or "obstructive plaque" (> 50% luminal diameter stenosis) [26]. Patients with obstructive lesions were

Chapter 10

The effect of LDLR-negative genotype on CT coronary atherosclerosis in asymptomatic
statin treated patients with heterozygous familial hypercholesterolemia.

further specified according to plaque location (left main coronary artery, proximal right coronary artery, proximal left coronary artery or proximal circumflex coronary artery) and the presence of multiple obstructive plaques. Stenosis severity was also evaluated on a per segment basis.

Coronary calcium was expressed in Agatston units per patient and was calculated semi-automatically using dedicated software [27]. Finally, on a per segment basis, plaque composition was classified as either 1) calcified; plaque containing high attenuating tissue that could be clearly separated from the contrast enhanced coronary lumen, or 2) non-calcified; low attenuating lesions that could be clearly separated from the coronary lumen and the surrounding pericardial fat and myocardium, or 3) partially calcified; plaque containing both high and low attenuating tissue.

Statistical analysis
Categorical variables were expressed as numbers (percentages). The Pearson Chi-Square test was used for inter-group comparisons. Continuous variables with a normal distribution were shown as mean (± SD), skewed data as median (interquartile range). A T-test or Mann-Whitney U-test was used to compare continuous variables. A two-sided P-value of < 0.05 was considered statistically significant. Age categories (figures 1 and 4) were chosen on the basis of equal patient numbers in all groups (n = 48, n = 49 and n = 48).

We compared LDLR-negative and LDLR-positive mutational FH in terms of coronary atherosclerosis. The DSS was considered the primary endpoint of the study. In addition, the CAD severity score, the CAD extent score, stenosis severity, coronary calcium and plaque composition were defined as secondary endpoints.

The relationship between the DSS score and LDLR-negative mutational status, age, gender, smoking, hypertension, diabetes mellitus, HDL, LDL and maximum untreated cholesterol was assessed using linear regression analyses. Variables with a univariate relationship with the DSS (P < 0.2) were entered in a multivariate regression model. The predictive value for the inter-observer variability was calculated using the k statistic. Data were analyzed using SPSS for windows (version 17.0.2, SPSS, Chicago, USA).

RESULTS

Data analysis
All contrast enhanced CT scans were included in the study, 1970 coronary artery segments were available for analysis. The κ statistics of the inter-observer agreement for the evaluation of the stenosis severity per plaque and the plaque composition were 0.80 and 0.83 respectively.

Patient characteristics
General patient characteristics and risk factors were similar between groups except for mean age that was higher in LDLR-positive patients (table 1). As expected, LDLR-negative mutational FH was associated with higher total cholesterol, higher LDL-C and higher maximum untreated cholesterol. Patients with LDLR-negative mutations started using statins at a younger age, used statins for a longer period of time and more often had xanthomas or arcus lipoides.

Mutational types of LDLR gene
Fifty-nine patients (41%) had LDLR-negative mutations, 40 patients (28%) had LDLR-defective or APOB mutations and 46 patients (32%) had unidentified mutations. Within the LDLR-defective / APOB group, 8 patients (20%) had a functional mutation of the APOB gene. In none of the patients a PCSK9 mutation was found. Identified mutations and their functional classes are shown in table 2.

Coronary plaque burden
The DSS was higher in patients with LDLR-negative mutational FH (table 3). In addition, the CAD severity score and the CAD extent score were higher in patients with LDLR-negative mutations. Differences in plaque burden between LDLR-negative and LDLR-positive mutational FH increased with age (figure 1). Despite statin treatment, plaque burden was higher in carriers of LDLR-negative mutations.

Stenosis severity
As shown in table 3, the distribution of stenosis severity was significantly different between LDLR-negative and LDLR-positive mutational FH. The prevalence of obstructive plaque was higher in the LDLR-negative group. In addition, LDLR-negative patients had obstructive plaque in a proximal coronary artery segment more often. Although the majority of FH patients had some degree of CAD on CCTA, 19% of LDLR-negative and 33% of LDLR-positive patients had no detectable CAD. Within the LDLR-positive group the prevalence of obstructive plaque was higher in men as compared to women (figure 2).

On a segment level, the distribution of stenosis severity between LDLR-negative and LDLR-positive mutational FH was highly significant. In the LDLR-negative group more coronary artery segments were diseased.

Calcium score and plaque composition
Differences in calcium score between LDLR-negative and LDLR-positive mutational groups reached statistical significance (table 3). In the LDLR-negative group, the percentage of patients with calcium scores > 100 Agatston units was higher. Within the highest age category (58-70) LDLR-negative mutational FH was associated with higher levels of coronary calcium (figure 3). Notably, of all patients included in the study none had one or more obstructive lesions in combination with a calcium score ≤ 100 Agatston units. Low coronary calcium proved to be highly predictive for the absence of obstructive CAD.

Chapter 10

The effect of LDLR-negative genotype on CT coronary atherosclerosis in asymptomatic
statin treated patients with heterozygous familial hypercholesterolemia.

Table 1. Clinical characteristics of all FH patients

	LDLR-negative	LDLR-positive	P-value
	(N = 59)	(N = 86)	
General			
Age (years)	51 ± 7	53 ± 8	0.040
Gender (male)	38 (64)	55 (64)	0.955
Systolic blood pressure (mmHg)	130 ± 14	129 ± 12	0.683
Diastolic blood pressure (mmHg)	80 ± 8	80 ± 8	0.612
Body mass index (kg / m²)	27 ± 4	26 ± 3	0.534
Risk factors			
Smoking (current / former)	15 (25)	26 (30)	0.528
Hypertension *	13 (22)	25 (29)	0.344
Diabetes Mellitus	1 (2)	6 (7)	0.145
Positive family history †	45 (76)	57 (66)	0.196
On-treatment lipids			
Total cholesterol (mmol / L)	5.8 ± 1.6	5.3 ± 1.3	0.026
HDL (mmol / L)	1.4 ± 0.4	1.4 ± 0.4	0.818
LDL (mmol / L)	3.9 ± 1.4	3.2 ± 1.1	0.003
Triglyceride (mmol / L) ‡	0.94 (0.73 - 1.54)	1.12 (0.86 - 1.72)	0.060
FH related characteristics			
Maximum untreated cholesterol (mmol / L)	10.5 ± 2.7	9.1 ± 1.9	0.001
Statin treatment	58 (98)	84 (98)	0.793
Maximum statin treatment	41 (70)	47 (55)	0.072
Age at start of statin treatment	39 ± 9.6	46 ± 9.4	< 0.001
Duration of statin use (years)	11.1 ± 7.4	7.2 ± 7.0	0.004
Dose-limiting side effects	15 (25)	29 (34)	0.286
Concomitant Ezetimibe treatment	46 (78)	38 (44)	< 0.001
Xanthomas	26 (44)	10 (12)	< 0.001
Arcus Lipoides	18 (31)	14 (16)	0.042

Continuous data are expressed as mean ± SD or median (interquartile range), dichotomous data as N (%).

* Blood pressure >140 / 90 mmHg and / or anti-hypertensive treatment. † Proven coronary artery disease in 1st degree relative under the age of 60.

‡ Median (interquartile range), LDLR-negative = LDL receptor negative mutation, FH = familial hypercholesterolemia.

LDLR-positive = LDL receptor positive mutation (reduced or normal LDLR function).

HDL = high density lipoprotein, LDL = low density lipoprotein.

Table 2. Identified mutations of LDLR and APOB gene

Type of mutation	LDLR-negative		
	N	Class	Location
W23X	11	1	exon 2
313+1/ 2	11	1	intron 3
2.5 kb deletion of exon 7 / 8	7	1	exon 7 and exon 8
1359-1	7	1	intron 9
191-2	6	1	intron 2
16 kb deletion of exon 12 / 18	4	2A	exon 12 - exon 18
776delAT	2	1	exon 5
314-1	1	1	intron 3
314-3	1	1	intron 3
87delG	1	1	exon 6
1085delA	1	1	exon 8
2050del14bp	1	1	exon 14
1658delACT	1	1	exon 11
R329X	1	1	exon 7
2417insG	1	1	exon 17
D69N	1	2A	exon 3
4.4 kb duplication of exons 9 to 12	1	1	intron 12
C371X	1	1	exon 8
Total	**59**		

Chapter 10

The effect of LDLR-negative genotype on CT coronary atherosclerosis in asymptomatic
statin treated patients with heterozygous familial hypercholesterolemia.

	LDLR-defective / APOB		
N543H exon 11/ 2393del 9 exon 17	7	2B	exon 11 and exon 17
A684P	5	2B	exon 14
E207K	4	2B	exon 4
S285L	4	2B	exon 4
S426C	2	2B	exon 9
P664L	2	2B	exon 14
A410T	1	5	exon 9
Y468C	1	ND	exon 10
G314V	1	2B	exon 7
E187K	1	2B	exon 4
L401P	1	2B	exon 9
G571E	1	2B	exon 12
D481Y	1	2B	exon 10
C74R	1	3	exon 3
R3500Q	6	3	exon 26 of APOB
R3500L	2	3	exon 26 of APOB
Total	**40**		

LDLR = low density lipoprotein receptor, LDLR-negative = LDL receptor negative mutation,

LDLR-defective = LDL receptor defective mutation, APOB = mutation of the apolipoprotein B gene.

FH = familial hypercholesterolemia, ND = not defined.

Distribution of plaque composition between LDLR-negative and LDLR-positive groups was similar: non-calcified plaque; 10% versus 8%, partially calcified plaque; 32% versus 27%, and calcified plaque; 58% versus 65% (P = 0.287) (data not shown).
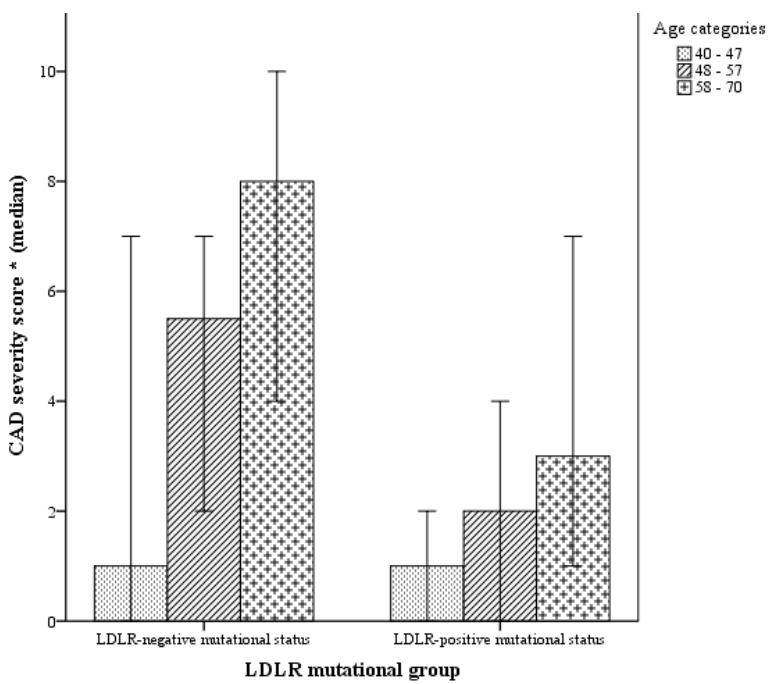

Figure 1 CAD severity score for LDLR mutational groups at different age.

CAD severity score (median) for both LDLR-negative and LDLR-positive mutational status at different age. * Integrated sum of stenosis severity and the number of coronary lesions: 21-50% = 1, 51-70% = 2, > 70% = 3. CAD = coronary artery disease, LDLR = low density lipoprotein receptor, neg = negative, pos = positive (reduced or normal LDLR function).

Age 40-47: median (IQR) (n) 1 (0-7) (n = 24) and 1 (0-3) (n = 24) (P = 0.279).

Age 48-57: median (IQR) (n) 6 (1-7) (n = 20) and 2 (0-4) (n = 29) (P = 0.023).

Age 58-70: median (IQR) (n) 8 (4-10) (n = 15) and 3 (1-8) (n = 33) (P = 0.021).

Relationship between patient characteristics and the diseased segments score

The results of the multivariate linear regression analysis are presented in table 4. There was no statistical significant interaction between LDLR-negative mutational status, LDL-C and maximum untreated cholesterol for predicting the DSS. LDLR-negative mutational status remained predictive of the DSS after correction for age, gender, smoking, hypertension, HDL cholesterol, LDL-C and maximum untreated cholesterol (B = 1.09, P = 0.047). Age (B = 0.21, P < 0.001), gender (B = 2.1, P = 0.001), HDL cholesterol (B = -1.8, P = 0.023) and maximum untreated cholesterol (B = 0.3, P = 0.009) also remained independent predictors of the DSS.

If we removed maximum untreated cholesterol from the multivariate linear regression model, the level of LDL-C became an independent predictor of the DSS (B = 0.5, P =
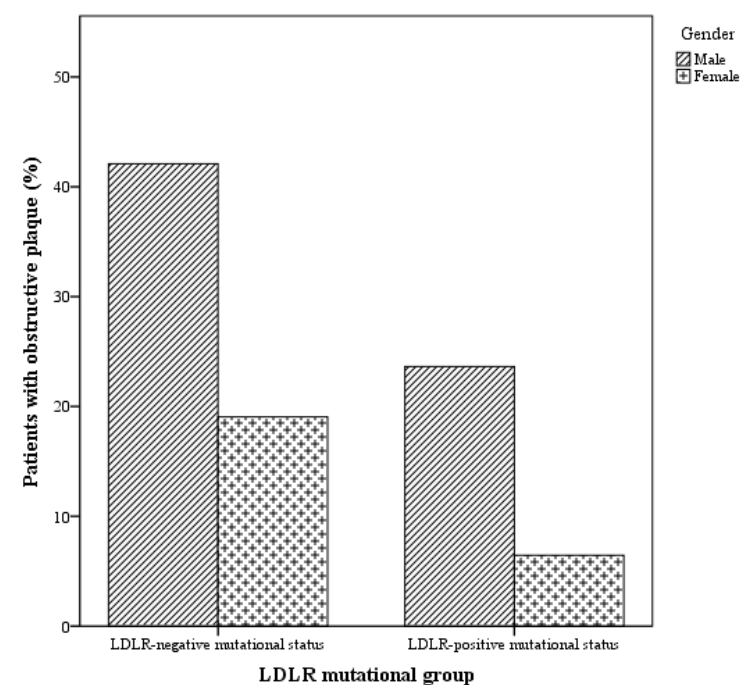
Chapter 10

The effect of LDLR-negative genotype on CT coronary atherosclerosis in asymptomatic
statin treated patients with heterozygous familial hypercholesterolemia.

Figure 2 Percentage of patients with obstructive plaque for both men and women per LDLR mutational group. Obstructive lesions defined as > 50% luminal diameter narrowing. LDLR = low density lipoprotein receptor, neg = negative, pos = positive (reduced or normal LDLR function).

LDLR-negative mutational status: number (percentage) 16 (42) and 4 (19) (P = 0.073).

LDLR-positive mutational status: number (percentage) 13 (24) and 2 (7) (P = 0.044).

0.015). LDLR-negative mutational status (B = 1.69, P = 0.001) and other independent predictors of the DSS remained statistically significant.

Secondary analysis; identified versus unidentified mutational status

In patients with LDLR-positive mutations, general patient characteristics, risk factors and cholesterol levels did not differ between identified and unidentified mutational status (table 5). Patients with identified mutations had lower triglyceride levels (P = 0.003), received higher dosages of statins (P < 0.001), started taking statins at a younger age (P < 0.001) and used statins for a longer period of time (P = 0.002).

The DSS, the CAD severity score and the CAD extent score did not differ between patients with identified and patients with unidentified mutational status (table 6). In addition, stenosis severity, calcium scores and plaque composition were similar. However, on a segment level, stenosis severity was higher in identified mutational FH (P = 0.018).

Table 3. Plaque characteristics of all FH patients

	LDLR-negative	LDLR-positive	P-value
Patient level	(N = 59)	(N = 86)	
Diseased segments score *	4 (1 - 7)	2 (0 - 5)	0.017
CAD severity score †	4 (1 - 8)	2 (0 - 5)	0.016
CAD extent score ‡	11 (4 - 18)	6 (2 - 12)	0.020
Stenosis severity §			0.039
No plaque or stenosis	11 (19)	28 (33)	-
Non-obstructive plaque	28 (47)	43 (50)	-
Obstructive plaque	20 (34)	15 (17)	-
Obstructive plaque (proximal segment)	10 (17)	5 (6)	0.031
Obstructive plaque (> 1 segment)	11 (19)	7 (8)	0.059
Calcium score			0.038
Agatston negative	11 (19)	17 (20)	-
Agatston > 0 - 100	15 (25)	38 (44)	-
Agatston > 100	33 (56)	31 (36)	-
Segment level	(N = 786)	(N = 1184)	
Stenosis severity			< 0.001
No plaque or stenosis	534 (68)	933 (79)	-
Non-obstructive plaque	211 (27)	218 (18)	-
Obstructive plaque	41 (5)	33 (3)	-

Continuous data are expressed as median (interquartile range), dichotomous data as n (%).

* Number of diseased segments (> 20% luminal diameter narrowing) (0 - 17).

† Integrated sum of the stenosis severity and the number of coronary artery lesions: 21 - 50% = 1, 51 - 70% = 2, > 70% = 3.

‡ Integrated sum of the stenosis severity and the number of coronary artery lesions: 1 - 20% = 1, 21 - 50% = 2, 51 - 70% = 3, > 70% = 4.

§ 0 - 20% defined as "no plaque or stenosis", > 50% as "obstructive plaque", FH = familial hypercholesterolemia.

LDLR-negative = LDL receptor negative mutation, LDLR-positive = LDL receptor positive mutation (reduced or normal LDLR function).
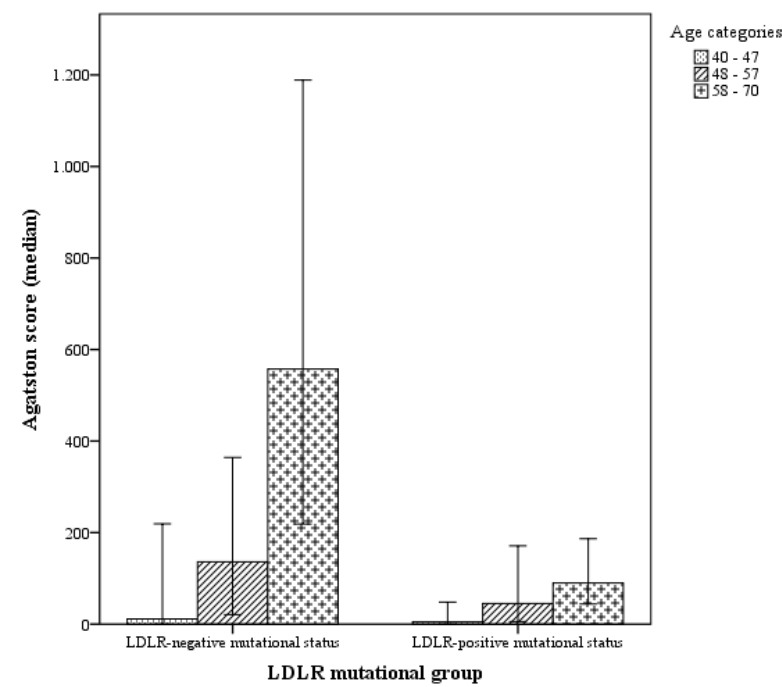
Chapter 10

The effect of LDLR-negative genotype on CT coronary atherosclerosis in asymptomatic
statin treated patients with heterozygous familial hypercholesterolemia.

Figure 3 Coronary calcium for LDLR mutational groups at different age.

The Agatston score (median) for both LDLR-negative and LDLR-positive mutational status at different age. LDLR
= low density lipoprotein receptor, neg = negative, pos = positive (reduced or normal LDLR function).

Age 40-47: median (IQR) (n) 11 (0-314) (n = 24) and 5 (0-77) (n = 24) (P = 0.323).

Age 48-57: median (IQR) (n) 136 (14-392) (n = 20) and 45 (2-212) (n = 29) (P = 0.172).

Age 58-70: median (IQR) (n) 557(219-1189) (n = 15) and 90 (27-488) (n = 33) (P = 0.027).

DISCUSSION

In asymptomatic statin treated patients with FH, we evaluated the effect of LDLR-negative
mutational status on the extent of coronary atherosclerosis using CCTA. The main finding
of this study can be summarized as: despite statin treatment, the extent of CT coronary
atherosclerosis is higher in carriers of LDLR-negative mutations.

After adjusting for LDL-C levels as achieved during statin treatment, LDLR-negative muta-
tional status remained an independent predictor of the DSS. This could have been caused
by the atherogenic effect of the higher levels of LDL-C associated with LDLR-negative
genotype before statin medication was initiated.

In addition, LDLR-negative mutational status remained an independent predictor of the
DSS after adjusting for the maximum total cholesterol level before statin treatment was

Table 4. Univariate and multivariate linear regression models for the predictive value of the diseased segments score [1] per patient

N = 145	Univariate linear regression				Multivariate linear regression *			
	B	SE of B	95% CI	P-Value	B	SE of B	95% CI	P-Value
LDLR-neg mutational FH	**1.35**	**0.57**	**(0.23 - 2.48)**	**0.019**	**1.09**	**0.54**	**(0.01 - 2.16)**	**0.047 ‡**
Age (years	**0.16**	**0.04**	**(0.09 - 0.23)**	**<0.001**	**0.21**	**0.04**	**(0.14 - 0.28)**	**< 0.001**
Gender (male)	**1.2**	**0.6**	**(0.1 - 2.4)**	**0.036**	**2.1**	**0.6**	**(0.9 - 3.3)**	**0.001**
Smoking	**1.3**	**0.6**	**(-1.1 - 1.4)**	**0.017**	0.6	0.6	(-0.5 - 1.7)	0.249
Hypertension †	1.2	0.6	(-0.1 - 2.5)	0.059	-0.4	0.6	(-1.6 - 0.8)	0.482
Diabetes Mellitus	0.1	1.3	(-2.5 - 2.7)	0.936	-	-	-	-
HDL	**-1.8**	**0.8**	**(-3.2 - -0.3)**	**0.022**	**-1.8**	**0.8**	**(-3.3 - -0.2)**	**0.023**
LDL (mmol/L)	**0.6**	**0.2**	**(0.1 - 1.0)**	**0.014**	0.4	0.2	(-0.1 - 0.8)	0.098
Max untreated cholesterol (mmol/L)	**0.5**	**0.1**	**(0.2 - 0.7)**	**<0.001**	**0.3**	**0.1**	**(0.1 - 0.6)**	**0.009**

Variables in bold (P < 0.2) were entered in the multivariate regression model. 1 Number of diseased coronary artery segments (> 20% luminal diameter narrowing) (0 - 17).

* No significant interaction between LDLR status and LDL-C / max untreated total cholesterol. † Blood pressure > 140 / 90 mmHg and / or anti-hypertensive treatment.

‡ Predictive value of LDLR-negative mutational status for diseased segments score after adjustment for age, gender, smoking, hypertension, HDL cholesterol, LDL-C and maximum untreated cholesterol.

B = unstandardized regression coefficient, SE = standard error, CI = confidence interval, HDL = high density lipoprotein, LDL = low density lipoprotein.

Chapter 10

The effect of LDLR-negative genotype on CT coronary atherosclerosis in asymptomatic
statin treated patients with heterozygous familial hypercholesterolemia.

Table 5. Clinical characteristics of LDLR-defective, APOB and unidentified mutational FH

	LDLR-defective APOB	Unidentified	
	(N = 40)	(N = 46)	
General			
Age (years)	52 ± 8	55 ± 8	0.103
Gender (male)	28 (70)	27 (59)	0.276
Systolic blood pressure (mmHg)	129 ± 13	129 ± 11	0.922
Diastolic blood pressure (mmHg)	79 ± 9	82 ± 7	0.151
Body mass index (kg / m²)	26 ± 4	27 ± 3	0.306
Risk factors			
Smoking (current / former)	10 (25)	16 (35)	0.324
Hypertension *	9 (23)	16 (35)	0.211
Diabetes Mellitus	2 (5)	4 (9)	0.502
Positive family history †	27 (68)	30 (65)	0.823
On-treatment lipids			
Total cholesterol (mmol / L)	5.3 ± 1.4	5.3 ± 1.3	0.874
HDL (mmol / L)	1.3 ± 0.4	1.4 ± 0.4	0.922
LDL (mmol / L)	3.4 ± 1.1	3.1 ± 1.1	0.166
Triglyceride (mmol / L) ‡	0.96 (0.77 - 1.43)	1.45 (0.99 - 1.92)	0.003
FH related characteristics			
Maximum untreated cholesterol (mmol/L)	9.5 ± 2.1	8.9 ± 1.6	0.172
Statin treatment	40 (100)	44 (96)	0.497
Maximum statin treatment	30 (75)	17 (37)	< 0.001
Age at start of statin treatment	42 ± 8	50 ± 9	< 0.001
Duration of statin use (years)	10 ± 7	5 ± 6	0.002
Dose-limiting side effects	9 (23)	20 (44)	0.040
Concomitant Ezetimibe treatment	23 (58)	15 (33)	0.020
Xanthomas	7 (18)	3 (7)	0.113
Arcus Lipoides	9 (23)	5 (11)	0.145

Continuous data are expressed as mean ± SD or median (interquartile range), dichotomous data as N (%).

* Blood pressure > 140 / 90 mm HG and / or anti-hypertensive treatment. † Premature coronary artery disease in 1st degree relative.

‡ Median (interquartile range). LDLR-negative = LDL receptor negative mutation, FH = familial hypercholesterolemia.

LDLR-positive = LDL receptor positive mutation (reduced or normal LDLR function).

HDL=high density lipoprotein, LDL=low density lipoprotein.

Table 6. Plaque characteristics of LDLR-defective, APOB and unidentified mutational FH

	LDLR-defective APOB	Unidentified	P-value
Patient level	(N = 40)	(N = 46)	
Diseased segments score *	3 (0 - 7)	2 (0 - 3)	0.285
CAD severity score †	3 (0 - 7)	2 (0 - 4)	0.281
CAD extent score ‡	7 (3 - 16)	6 (2 - 11)	0.257
Stenosis severity §			0.806
No plaque or stenosis	12 (30)	16 (35)	-
Non-obstructive plaque	20 (50)	23 (50)	-
Obstructive plaque	8 (20)	7 (15)	-
Obstructive plaque (proximal segment)	3 (8)	2 (4)	0.533
Obstructive plaque (> 1 segment)	4 (10)	3 (7)	0.556
Calcium score			0.285
Agatston negative	5 (12)	12 (26)	
Agatston > 0 - 100	19 (48)	19 (41)	
Agatston > 100	16 (40)	15 (33)	
Segment level	(N = 557)	(N = 627)	
Stenosis severity			0.018
No plaque or stenosis	419 (75)	514 (82)	-
Non-obstructive plaque	120 (22)	98 (16)	-
Obstructive plaque	18 (3)	15 (2)	-

Continuous data are expressed as median (interquartile range), dichotomous data as n (%).

* Number of diseased segments (> 20% luminal diameter narrowing) (0-17).

† Integrated sum of the stenosis severity and the number of coronary artery lesions: 21-50% = 1, 51-70% = 2, > 70% = 3.

‡ Integrated sum of the stenosis severity and number of coronary artery lesions (0-17): 1 - 20% = 1, 21 - 50% = 2, 51 - 70% = 3, > 70% = 4.

§ 0 - 20% defined as "no plaque or stenosis", > 50% as "obstructive plaque", FH = familial hypercholesterolemia.

LDLR-defective = LDL receptor defective mutation, APOB = mutation of the apolipoprotein B gene, unidentified = unidentified mutation.

initiated. It may be speculated that LDLR-negative genotype stimulates CAD via alternative pathways that are beyond elevated cholesterol levels.

The level of LDL-C as achieved during statin treatment was not an independent predictor of the DSS in the multivariate analysis. Patients with an LDLR-negative genotype received higher dosages of statins for a longer period of time and this may have influenced the latter analysis.

Chapter 10

The effect of LDLR-negative genotype on CT coronary atherosclerosis in asymptomatic statin treated patients with heterozygous familial hypercholesterolemia.

However, if we removed maximum untreated cholesterol from the multivariate linear regression model, LDL-C became a statistically significant predictor of the DSS. Apparently, the level of maximum untreated cholesterol overruled the predictive value of LDL-C and patients with relatively high levels of untreated cholesterol also have the highest levels of LDL-C during statin treatment.

There was no difference in the DSS between patients with identified and unidentified mutational status. Nonetheless, on a per segment basis, we found a higher prevalence of non-obstructive and obstructive CAD in patients with identified mutations. This could mean that we had insufficient power to demonstrate the rather small difference in plaque burden between identified and unidentified mutational status on a patient level.

In our study of patients with a clinical diagnosis of FH that was established on clinical characteristics, we found LDLR and APOB gene mutations in 68% of patients (99 out of 145) in line with the 50-80% observed in earlier studies [11; 28-29].

Carriers of LDLR-negative mutations had the most detrimental lipid profiles. However, triglyceride levels showed a strong trend of being higher in the LDLR-positive mutational group mainly caused by the relatively high levels in unidentified mutational FH. This possibly reflects the clinical characteristics of other forms of inherited dyslipidemia such as familial combined hyperlipidemia in this population [30].

Previous studies showed that the impact of LDLR-negative versus LDLR-defective mutations on the clinical expression of lipids, obstructive CAD on invasive angiography, xanthomas and adverse coronary events (angina, percutaneous coronary intervention or coronary artery bypass grafting) was more pronounced in carriers of LDLR-negative mutations [16-18] [15].

Our study differed from the above-described studies because we investigated FH patients who were asymptomatic and treated with statins for many years. Yet we still demonstrated with CT that the extent of coronary atherosclerosis was higher in patients with LDLR-negative mutations compared to LDLR-positive mutations.

We found a large variation in plaque burden in both LDLR-negative and LDLR-positive mutational FH. Although the majority of FH patients had plaque, 19% of LDLR-negative and 33% of LDLR-positive patients had no plaque or stenosis. This variation is in line with other studies demonstrating that some FH patients have no signs or symptoms of CAD while others are prematurely symptomatic or have obstructive CAD [18].

This observation potentially opens new avenues for cardiac CT that could be helpful for the early detection and evaluation of subclinical atherosclerosis and the differentiation of individual plaque-associated risk. Additionally cardiac CT could be used in FH popula-

tions if LDLR mutational screening is no clinical practice. Long term follow up studies are necessary to evaluate the relation between aspects of plaque and future risk of coronary artery events.

Limitations

Only patients between 40 and 70 years old were included because of concern with radiation exposure and extreme calcifications in younger and older patients respectively.

Subjects with LDLR-negative mutations were younger as compared to patients with LDLR-positive mutational FH. This could only have resulted in lower plaque burden scores in this population resulting in an underestimation of the atherogenic effect LDLR-negative mutations.

The selection of patients, those who are referred to our university lipid clinic, may have more severe atherosclerosis as compared to other FH patients. This could have influenced the total amount of observed plaque.

Atherosclerosis in patients with LDLR-negative mutations may have been underestimated due to survival bias. Patients, most susceptible for elevated LDL-C levels, may have developed symptoms or may even have died before study inclusion.

Finally, CCTA overestimates stenosis grade, especially in calcified lesions and therefore the reported prevalence of obstructive lesions may be overestimated.

CONCLUSION

In asymptomatic patients with a clinical diagnosis of FH, LDLR-negative mutations are associated with a higher extent of subclinical CT coronary atherosclerosis as compared to other patients with a clinical diagnosis of FH despite an earlier start of statin treatment at higher dosages.

Chapter 10

The effect of LDLR-negative genotype on CT coronary atherosclerosis in asymptomatic
statin treated patients with heterozygous familial hypercholesterolemia.

REFERENCES

1   Guardamagna O, Restagno G, Rolfo E, et al. (2009) The type of LDLR gene mutation predicts cardiovascular risk in children with familial hypercholesterolemia. J Pediatr, 155(2):199-204 e192.

2   Neefjes LA, Ten Kate GJ, Alexia R, et al. (2011) Accelerated subclinical coronary atherosclerosis in patients with familial hypercholesterolemia. Atherosclerosis, 219(2):721-727.

3   Neefjes LA, Ten Kate GJ, Rossi A, et al. (2011) CT coronary plaque burden in asymptomatic patients with familial hypercholesterolaemia. Heart, 97(14):1151-1157.

4   Gudnason V, Day IN, Humphries SE (1994) Effect on plasma lipid levels of different classes of mutations in the low-density lipoprotein receptor gene in patients with familial hypercholesterolemia. Arterioscler Thromb, 14(11):1717-1722.

5   Gaudet D, Vohl MC, Couture P, et al. (1999) Contribution of receptor negative versus receptor defective mutations in the LDL-receptor gene to angiographically assessed coronary artery disease among young (25-49 years) versus middle-aged (50-64 years) men. Atherosclerosis, 143(1):153-161.

6   Sijbrands EJ, Westendorp RG, Paola Lombardi M, et al. (2000) Additional risk factors influence excess mortality in heterozygous familial hypercholesterolaemia. Atherosclerosis, 149(2):421-425.

7   Civeira F, International Panel on Management of Familial H (2004) Guidelines for the diagnosis and management of heterozygous familial hypercholesterolemia. Atherosclerosis, 173(1):55-68.

8   Marks D, Thorogood M, Neil HA, Humphries SE (2003) A review on the diagnosis, natural history, and treatment of familial hypercholesterolaemia. Atherosclerosis, 168(1):1-14.

9   Brown MS, Goldstein JL (1976) Receptor-mediated control of cholesterol metabolism. Science, 191(4223):150-154.

10   Fouchier SW, Kastelein JJ, Defesche JC (2005) Update of the molecular basis of familial hypercholesterolemia in The Netherlands. Hum Mutat, 26(6):550-556.

11   de Sauvage Nolting PR, Defesche JC, Buirma RJ, Hutten BA, Lansberg PJ, Kastelein JJ (2003) Prevalence and significance of cardiovascular risk factors in a large cohort of patients with familial hypercholesterolaemia. J Intern Med, 253(2):161-168.

12   Hobbs HH, Russell DW, Brown MS, Goldstein JL (1990) The LDL receptor locus in familial hypercholesterolemia: mutational analysis of a membrane protein. Annu Rev Genet, 24:133-170.

13   Jansen AC, van Wissen S, Defesche JC, Kastelein JJ (2002) Phenotypic variability in familial hypercholesterolaemia: an update. Curr Opin Lipidol, 13(2):165-171.

14   Austin MA, Hutter CM, Zimmern RL, Humphries SE (2004) Familial hypercholesterolemia and coronary heart disease: a HuGE association review. Am J Epidemiol, 160(5):421-429.

15   Bertolini S, Cantafora A, Averna M, et al. (2000) Clinical expression of familial hypercholesterolemia in clusters of mutations of the LDL receptor gene that cause a receptor-defective or receptor-negative phenotype. Arterioscler Thromb Vasc Biol, 20(9):E41-52.

16   Vohl MC, Tchernof A, Dionne FT, et al. (1996) The apoB-100 gene EcoRI polymorphism influences the relationship between features of the insulin resistance syndrome and the hyper-apoB and dense LDL phenotype in men. Diabetes, 45(10):1405-1411.

17   Vohl MC, Gaudet D, Moorjani S, et al. (1997) Comparison of the effect of two low-density lipoprotein receptor class mutations on coronary heart disease among French-Canadian patients heterozygous for familial hypercholesterolaemia. Eur J Clin Invest, 27(5):366-373.

18   Sijbrands EJ, Westendorp RG, Defesche JC, de Meier PH, Smelt AH, Kastelein JJ (2001) Mortality over two centuries in large pedigree with familial hypercholesterolaemia: family tree mortality study. BMJ, 322(7293):1019-1023.

19   Meijboom WB, Meijs MF, Schuijf JD, et al. (2008) Diagnostic accuracy of 64-slice computed tomography coronary angiography: a prospective, multicenter, multivendor study. J Am Coll Cardiol, 52(25):2135-2144.

20   Weustink AC, Mollet NR, Neefjes LA, et al. (2010) Diagnostic accuracy and clinical utility of noninvasive testing for coronary artery disease. Ann Intern Med, 152(10):630-639.

21   van Aalst-Cohen ES, Jansen AC, Tanck MW, et al. (2006) Diagnosing familial hypercholesterolaemia: the relevance of genetic testing. Eur Heart J, 27(18):2240-2246.

22   Umans-Eckenhausen MA, Defesche JC, Sijbrands EJ, Scheerder RL, Kastelein JJ (2001) Review of first 5 years of screening for familial hypercholesterolaemia in the Netherlands. Lancet, 357(9251):165-168.

23   Weustink AC, Mollet NR, Pugliese F, et al. (2008) Optimal electrocardiographic pulsing windows and heart rate: effect on image quality and radiation exposure at dual-source coronary CT angiography. Radiology, 248(3):792-798.

24   Shrimpton PC, Wall BF, Yoshizumi TT, Hurwitz LM, Goodman PC (2009) Effective dose and dose-length product in CT. Radiology, 250(2):604-605.

25   Austen WG, Edwards JE, Frye RL, et al. (1975) A reporting system on patients evaluated for coronary artery disease. Report of the Ad Hoc Committee for Grading of Coronary Artery Disease, Council on Cardiovascular Surgery, American Heart Association. Circulation, 51(4 Suppl):5-40.

26   Min JK, Shaw LJ, Devereux RB, et al. (2007) Prognostic value of multidetector coronary computed tomographic angiography for prediction of all-cause mortality. J Am Coll Cardiol, 50(12):1161-1170.

27   Agatston AS, Janowitz WR, Hildner FJ, Zusmer NR, Viamonte M, Jr., Detrano R (1990) Quantification of coronary artery calcium using ultrafast computed tomography. J Am Coll Cardiol, 15(4):827-832.

28   Fouchier SW, Defesche JC, Umans-Eckenhausen MW, Kastelein JP (2001) The molecular basis of familial hypercholesterolemia in The Netherlands. Hum Genet, 109(6):602-615.

29   Heath KE, Gudnason V, Humphries SE, Seed M (1999) The type of mutation in the low density lipoprotein receptor gene influences the cholesterol-lowering response of the HMG-CoA reductase inhibitor simvastatin in patients with heterozygous familial hypercholesterolaemia. Atherosclerosis, 143(1):41-54.

30   Van Gaal LF, Peeters AV, De Block CE, de Leeuw IH, Thiart R, Kotze MJ (2001) Low-density lipoprotein receptor gene mutation analysis and clinical correlation in Belgian hypercholesterolaemics. Mol Cell Probes, 15(6):329-336.

Chapter *11*

Detection and quantification of coronary atherosclerotic plaque by 64-slice multidetector CT: a systematic head-to-head comparison with Intravascular Ultrasound

Stella-Lida Papadopoulou
Lisan A. Neefjes
Michiel Schaap
Hui-Ling Li
Ermanno Capuano
Alina G. van der Giessen
Johan C.H. Schuurbiers
Frank J. H. Gijsen
Anoeshka S. Dharampal
Koen Nieman
Robert Jan van Geuns
Nico R. Mollet
Pim J. de Feyter

Chapter 11

Detection and quantification of coronary atherosclerotic plaque by 64-slice multidetector CT:
a systematic head-to-head comparison with Intravascular Ultrasound

ABSTRACT

Objective We evaluated the ability of 64-slice multidetector computed tomography (MDCT) –derived plaque parameters to detect and quantify coronary atherosclerosis, using intravascular ultrasound (IVUS) as the reference standard.

Materials and Methods In 32 patients, IVUS and 64-MDCT was performed. The MDCT and IVUS datasets of 44 coronary arteries were co-registered using a newly developed fusion technique and quantitative parameters were derived from both imaging modalities. The threshold of >0.5mm of maximum wall thickness was used to establish plaque presence on MDCT and IVUS.

Results We analyzed 1364 coregistered 1-mm coronary cross-sections and 255 segments of 5-mm length. Compared with IVUS, 64-MDCT enabled correct detection in 957 of 1109 cross-sections containing plaque (sensitivity 86%). In 180 of 255 cross-sections atherosclerosis was correctly excluded (specificity 71%). On the segmental level, MDCT detected 213 of 220 segments with any atherosclerotic plaque (sensitivity 96%), whereas the presence of any plaque was correctly ruled out in 28 of 32 segments (specificity 88%). Interobserver agreement for the detection of atherosclerotic cross-sections was moderate, (Cohen's kappa coefficient K=0.51), but excellent for the atherosclerotic segments (K=1.0). Pearson's correlation coefficient for vessel plaque volumes measured by MDCT and IVUS was r=0.91 (P<0.001). Bland-Altman analysis showed a slight non-significant underestimation of any plaque volume by MDCT (p=0.5), with a trend to underestimate noncalcified and overestimate mixed/calcified plaque volumes (p =0.22 and p=0.87 respectively).

Conclusion MDCT is able to detect and quantify atherosclerotic plaque. Further improvement in CT resolution is necessary for more reliable assessment of very small and distal coronary plaques.

INTRODUCTION

The detection and accurate quantification of coronary plaque may potentially improve individualized risk stratification and allow the monitoring of patient's response to pharmacological treatment. Currently, intravascular ultrasound (IVUS) is considered the reference method to quantify coronary atherosclerosis [1]. However, the method is expensive, invasive and involves certain, albeit minimal risks, which makes it unsuitable for preventive plaque detection in asymptomatic individuals or routine serial assessment of atherosclerosis. Consequently, the ideal alternative to IVUS would be a non-invasive method of coronary imaging that enables accurate assessment of atherosclerotic plaque. Multidetector computed tomography (MDCT) has rapidly emerged as a noninvasive imaging modality for visualisation of the coronary arteries. Following the advances in MDCT technology and the improvement of spatial and temporal resolution with the introduction of 64-slice MDCT scanners, numerous studies have confirmed the ability of the technique to reliably detect and exclude significant coronary disease against invasive angiography [2-7]. The accuracy of detection and quantification of coronary plaque using MDCT compared to IVUS has been less extensively investigated and has been based mainly on qualitative visual plaque detection on MDCT. The aim of this study was to evaluate the ability of 64-slice CT to detect and quantify coronary atherosclerosis compared to IVUS, using similar quantitative parameters on MDCT and IVUS. For this systematic approach we applied a fusion technique recently developed in our institution [8], which allows us to co-register IVUS and MDCT images such that cross-sectional images can be compared head-to-head.

MATERIALS AND METHODS

Patients

Our study comprised patients who were treated in our institution for acute coronary syndromes between May 2005 and January 2006. Acute coronary syndrome (ACS) was defined as ST segment elevation myocardial infarction, non-ST-segment elevation myocardial infarction (troponin positive) or unstable angina (troponin negative). Immediately after initial management of the culprit lesions, these patients were asked to participate in the MDCT study. They were considered for inclusion only if an IVUS pullback was performed in one or more of their coronary arteries other than the treated vessel, if they had a heart rate lower than 70 bpm during the MDCT acquisition and had no prior coronary bypass surgery. Exclusion criteria included renal dysfunction (serum creatinine >120 mmol/L), contrast allergy and irregular heart rhythm. The institutional review board of our hospital approved the study, and all patients provided written informed consent before study participation.

Chapter 11

Detection and quantification of coronary atherosclerotic plaque by 64-slice multidetector CT:
a systematic head-to-head comparison with Intravascular Ultrasound

MDCT acquisition

All patients underwent CT coronary angiography with a 64-slice scanner (Sensation 64, Siemens, Forchheim, Germany), according to a previously published protocol [4]. Because patients having an ACS were already treated with intravenous nitrates and b-blockers, additional medication prior to CT scan was not necessary. Scan parameters were: gantry rotation time of 0.33 second; 32x 2 slices per rotation; 0.6 mm detector collimation; table feed of 3.8 mm per rotation; tube voltage of 120 kV; and tube current of 900 mAs. Prospective x-ray tube modulation was not applied. A bolus of 100 mL of contrast material (400 mgI/mL; Iomeron, Bracco, Milan, Italy) was injected intravenously at flow rate of 5 mL/s. The initiation of the scan was synchronized to the arrival of contrast in the coronary arteries by a bolus-tracking technique (threshold of 100 Hounsfield units). The estimated mean effective radiation dose was 17.0 ± 1.1 mSv, using the dose-length product and the conversion factor k (0.017 mSv/mGy/cm). Axial CT images were reconstructed with a slice thickness of 0.75 mm and 0.4 mm increments using a retrospectively ECG gating algorithm to obtain optimal, motion-free image quality, resulting in a temporal resolution of approximately 165 milliseconds and a spatial resolution of 0.4 mm. Optimal data sets with the best image quality were reconstructed mainly in the mid- to end-diastolic phase, using a medium-smooth convolution kernel, and were uploaded to an MDCT Picture Archiving and Communication System.

IVUS acquisition

The IVUS was performed using standard methodology. One or more of the coronary arteries of these patients were imaged by IVUS with commercially available catheter (40 MHz, Atlantis SR Pro, Boston Scientific, Boston, Massachusetts). After the intracoronary administration of 100 to 200 μg of nitroglycerin, IVUS images were acquired using automatic mechanical pullback devices operating at a continuous pullback speed of 0.5 mm/s [1]. Data were stored on DVD, transformed into the Digital Imaging and Communication in Medicine image standard, and archived for offline analysis with retrospective image-based gating [9] (axial spacing of gated IVUS images approximately 0.5 mm).

MDCT and IVUS co-registration

Datasets were transferred to an offline workstation for further analysis using an in-house developed tool, based on MeVisLab software (MeVisLab, Mevis, Bremen, Germany, http://www.mevislab.de). The registration procedure was performed by an independent investigator not involved in the later comparative analysis, and has been previously described in detail [8]. Briefly, the process was performed as follows: for each vessel of interest, the stack of ECG-gated IVUS images (axial distance of approximately 0.5 mm) was examined to identify bifurcations, which were used as landmarks. In order to register the MDCT to the IVUS images, a vessel centreline was manually drawn in the MDCT dataset starting from the ostium. Cross-sectional images, perpendicular to the centreline, were equidistantly generated at every 0.2 mm. The corresponding IVUS-derived landmarks were identified on this MDCT image set. After manual registration of the side branches, cross-

sectional MDCT images perpendicular to the centreline were generated again, but now such that the number of MDCT images between the landmarks was equal to the number of IVUS images between the landmarks. For each IVUS image the position and rotation of the corresponding MDCT image between the manually registered side branches was determined by linear interpolation. Therefore, only vessels with at least two bifurcations identifiable on both imaging modalities were co-registered. The goal of the registration process was to reconstruct cross-sectional MDCT images of the coronary artery at the same axial position where the IVUS images were obtained, enabling a head-to-head comparison between these images.

MDCT image analysis

For each vessel, the co-registered region of interest (ROI) was considered for plaque analysis. Both the inner lumen and the outer vessel boundaries were identified and manually annotated following a stepwise approach. Multiplanar reformatted images were generated and the lumen and vessel borders were traced longitudinally on at least 3 different vessel views; the intersections between these longitudinal contours and cross-sectional images at 1 mm intervals were calculated in order to create cross-sectional contours, which were examined and, if necessary, adjusted by an experienced observer. The settings for window level and width were previously optimized by an independent investigator and fixed at 740 HU and 220 HU respectively [10] (Rengo M. et al. *"Optimization of Window-Level Settings in CT Coronary Angiography for the Quantification of Coronary Lumen and Plaque"*, submitted). The annotation of lumen and the vessel wall boundaries was
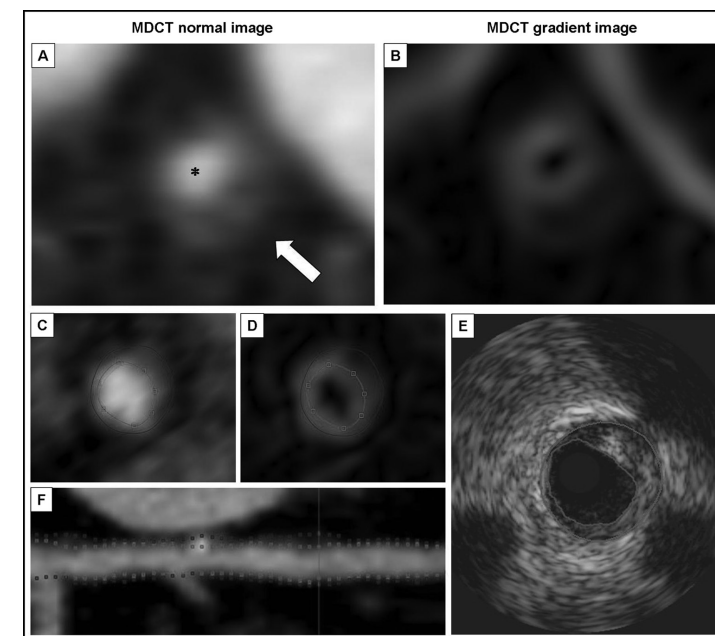

Figure 1. Example of generated cross-sectional MDCT images (1 mm interval). Panel A: in the normal MDCT image, the vessel lumen is brightly enhanced (asterisk), and a non-calcified, eccentric plaque is visible (arrow). Panel B: in the gradient MDCT image, the bigger change in image intensity is depicted brighter, which facilitates the discrimination of borders between tissues with different intensity. Panels C and D: analyzed normal and gradient image respectively; panel E: corresponding IVUS cross-section; panel F: longitudinal vessel view.

Chapter 11

Detection and quantification of coronary atherosclerotic plaque by 64-slice multidetector CT:
a systematic head-to-head comparison with Intravascular Ultrasound

also facilitated by gradient magnitude images, which are derived from the MDCT images (Figure 1A-B). They represent the magnitude of the image intensity gradient vector; the amount of local change in image intensity. The transition from high intensity lumen to the low intensity epicardial tissue is depicted in these images as a bright ridge. The plaque area was calculated by subtracting lumen area from vessel area. Plaques in which ≥50% of the plaque area was occupied by calcified tissue (in the respective cross-section) were classified as calcified, plaques with calcified tissue occupying <50% as mixed and plaques without any calcium as non-calcified. Typical example of non-calcified plaque visualised by MDCT and IVUS is shown in Figure 1 (C-F). The threshold of >0.5mm plaque thickness on MDCT was used to consider plaque present, similarly to IVUS. Plaque area and % plaque burden (plaque area/vessel area) measured by MDCT were also examined as potential quantitative parameters to detect plaque. A second investigator also blinded to the IVUS results, performed the same analysis independently on 22 randomly selected ROIs.

IVUS image analysis

IVUS analysis was performed off-line by an experienced cardiologist, blinded to the MDCT scans. Lumen and external elastic membrane (EEM) contours were manually traced to determine lumen area and vessel area using dedicated software (QCU-CMS, version 4.5, Leiden, the Netherlands). The measurements were performed according to the American College of Cardiology recommendations [1] and atherosclerotic plaques were defined as structures located between the media and the intima with a thickness of at least 0.5 mm.

Comparison between IVUS and 64-MDCT

The MDCT and IVUS annotated contours on the co-registered ROIs were compared at corresponding positions. The software determined the lumen area, vessel area and maximum wall thickness for the annotated MDCT contours at 1 mm increments and for the corresponding IVUS contours, which were obtained by interpolating the IVUS contours with cubic B-spline interpolation, at the position derived from the registration. Plaque volumes on MDCT and IVUS were calculated for the entire ROI by adding plaque volumes of all respective cross-sections, according to Simpson's rule. The co-registered ROIs were further divided into 5-mm segments for the purpose of evaluating diagnostic accuracy of MDCT to detect plaque on a segmental level, apart from the cross-sectional level.

Statistical analysis

Continuous variables were presented as means ± standard deviation, unless otherwise indicated, and categorical variables were reported as frequencies. Differences in baseline characteristics between patients included in the study and patients excluded were evaluated using chi-square test, Fisher's exact test, and unpaired Student's t-test, as appropriate. To take into account the potential correlation between the multiple cross-sections and segments derived from the same patient, generalized estimation equation (GEE) with binary logistic regression was applied to obtain patient-clustered values, adjusted

for distance from the ostium and type of vessel (RCA, LAD or LCX). Adjusted sensitivity, specificity, positive predictive value (PPV) and negative predictive value (NPV) of MDCT to detect plaque were calculated and the 95% confidence intervals were determined in addition to the crude (non-GEE based) analyses. Cohen's kappa was calculated to determine interobserver agreement. Receiver operating characteristics (ROC) curve analysis was performed in order to evaluate the ability of quantitative characteristics measured by MDCT to detect plaque, and the area under the curve (AUC) was calculated. Comparison between plaque volumes was performed using paired Student's t-test. Correlation and agreement between MDCT and IVUS measurements were evaluated by Pearson's correlation coefficient and Bland-Altman analysis respectively. The 95% limits of agreement were defined as the range of values between ± 2 standard deviations from the mean difference. A two-tailed p-value <0.05 was considered statistically significant. The statistical package SPSS 17.0 was used for the analysis.

RESULTS

Forty-seven vessels from 32 patients (mean age: 54 ± 10 years) with MDCT and IVUS of good image quality were successfully co-registered. From the total study population, 14 patients were not included in this analysis (4 did not have IVUS imaging, 2 had low quality IVUS imaging, 4 had low quality MDCT imaging and 4 could not be co-registered with the fusion technique due to technical problems, i.e. too few landmarks for matching). The mean time interval between IVUS and MDCT acquisitions was 4.8 ± 6.0 days. The baseline characteristics of all patients are presented in Table 1. Three vessels were excluded from further analysis because the ROI was occupied by long stents, thus 44 vessels were available for final head-to-head comparison [right coronary artery (RCA), n = 10; left anterior descending artery (LAD), n=22; left circumflex artery (LCX), n = 12]. The mean length of the investigated ROIs was 31 ± 14 mm and comprised a total of 1364 registered 1-mm cross-sections and 255 segments of 5-mm length.

Diagnostic performance on cross-sectional level

Presence of atherosclerotic plaque was confirmed by IVUS in 1109 out of the 1364 cross-sections (81.3%). Using the cut-off of >0.5 mm wall thickness, the 64-slice CT enabled a correct detection of any plaque in 957 of 1109 cross-sections, resulting in a sensitivity of 86%. Of these detected plaques, 755 were characterized as non-calcified (79%), 115 as mixed (12%) and 83 (1%) as calcified by MDCT. In 180 of 255 cross-sections, the presence of atherosclerotic lesions was correctly ruled out (specificity 71%). The 75 normal cross-sections misclassified by MDCT as diseased, were all incorrectly considered as containing non-calcified plaque. Both the crude and the adjusted analysis values for diagnostic performance are presented in Table 2. Coronary plaques that were missed on MDCT had smaller maximum plaque thickness (0.8 mm ±0.2 vs. 1.1 mm ±0.4, p <0.001) and plaque

Chapter 11

Detection and quantification of coronary atherosclerotic plaque by 64-slice multidetector CT:
a systematic head-to-head comparison with Intravascular Ultrasound

area (5.1 mm^2 ± 1.9 vs. 7.0 mm^2 ± 2.6, p <0.001) by IVUS, compared to the detected plaques (Table 3). The sensitivity of MDCT to detect plaque increased with plaque size (Figure 2-A), while it decreased with the distance from the coronary ostium (Figure 2-B), dropping below 80% for plaques located at 50 mm or more from the ostium. Logistic regression analysis confirmed that the distance from the ostium had a significant influence on sensitivity (odds ratio 1.38, 95% CI 1.09 – 1.76, for every 10 mm from the ostium). Moreover, the type of vessel had effect on the NPV (odds ratio 2.37, 95% CI 1.04 – 5.39). Cohen's kappa coefficient for the detection of atherosclerotic cross-sections using MDCT-derived wall thickness was 0.51, indicating moderate interobserver agreement.

Figure 2. Detection of plaque according to maximum intima thickness by IVUS (panel A) and according to distance from the coronary ostium (panel B).
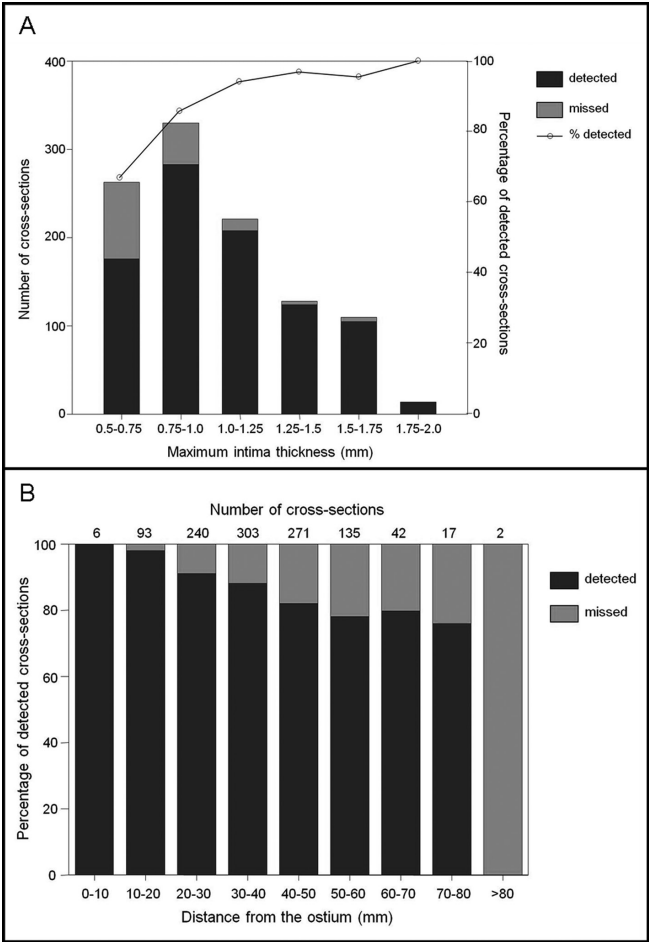
Cut-off values of MDCT-derived quantitative parameters for plaque detection

ROC curve analysis for MDCT maximal wall thickness, plaque area and plaque burden is shown in Figure 3. The MDCT maximal wall thickness presented non-significantly better discriminatory ability for plaque detection (AUC 0.876) than plaque area (AUC 0.847) and plaque burden (AUC 0.834). If MDCT plaque area and plaque burden were to be used as quantitative characteristics to detect plaque, the cut-off values of 3.8 mm^2 and 35% respectively would provide a sensitivity exceeding 80% with corresponding specificity values of 75% and 68%.

Figure 3. Receiver operating characteristics (ROC) curve analysis of quantitative characteristics measured by 64-slice MDCT.
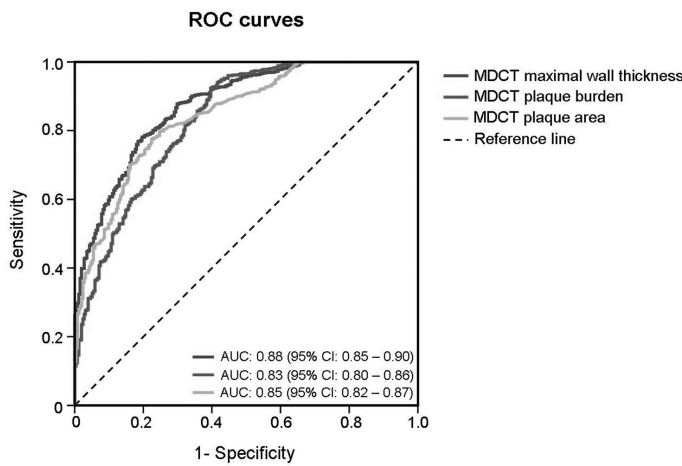
Diagnostic performance on segmental level

The analysis on a segmental basis revealed that MDCT correctly detected 213 of 220 segments with any atherosclerotic plaque (sensitivity 96%), whereas the presence of any plaque was correctly ruled out in 28 of 32 segments (specificity 88%). The majority of the segments with plaque detected by MDCT contained non-calcified plaque (154 out of 213, 72%). Mixed plaque was present in 44 segments (21%) and calcified plaque in 15 segments (7%). Four non-diseased segments were incorrectly characterized as containing non-calcified plaque. The crude and the adjusted analysis values for diagnostic performance are shown in Table 2. Mean plaque area measured by IVUS in the 10 segments with a false-negative MDCT result was 4.1 ± 1.5 mm^2 versus 6.7 ± 2.6 mm^2 (*P*=0.002) for the 213 segments with a true-positive MDCT result (Table 3). The interobserver agreement for the detection of atherosclerotic segments using MDCT-derived wall thickness was excellent (Cohen's kappa=1.0).

Plaque volume comparison between MDCT and IVUS

Pearson's correlation coefficient for regional plaque volumes measured by MDCT and IVUS was very good (*r*=0.91, *P*<0.001). Bland-Altman analysis showed a slight non-significant underestimation of plaque volume by MDCT (177 ± 101 mm^3 versus 181 ± 107 mm^3, *P*=0.5; see Figure 4), with a mean difference of -4.5 mm^3 and 95% limits of agreement between -92.7 and 83.7 mm^3. A sub-analysis per ROI plaque type revealed that non-calcified plaque volumes (n=19) were systematically but non-significantly underestimated (129.3 ± 88.2 mm^3 vs. 141.7 ± 93.2 mm^3, p=0.22). Plaque volume in the mixed/calcified ROIs (n=25) was slightly overestimated (213.2 ± 96.5 mm^3 vs. 211.7 ± 108.3 mm^3, p = 0.87).

Chapter 11

Detection and quantification of coronary atherosclerotic plaque by 64-slice multidetector CT:
a systematic head-to-head comparison with Intravascular Ultrasound
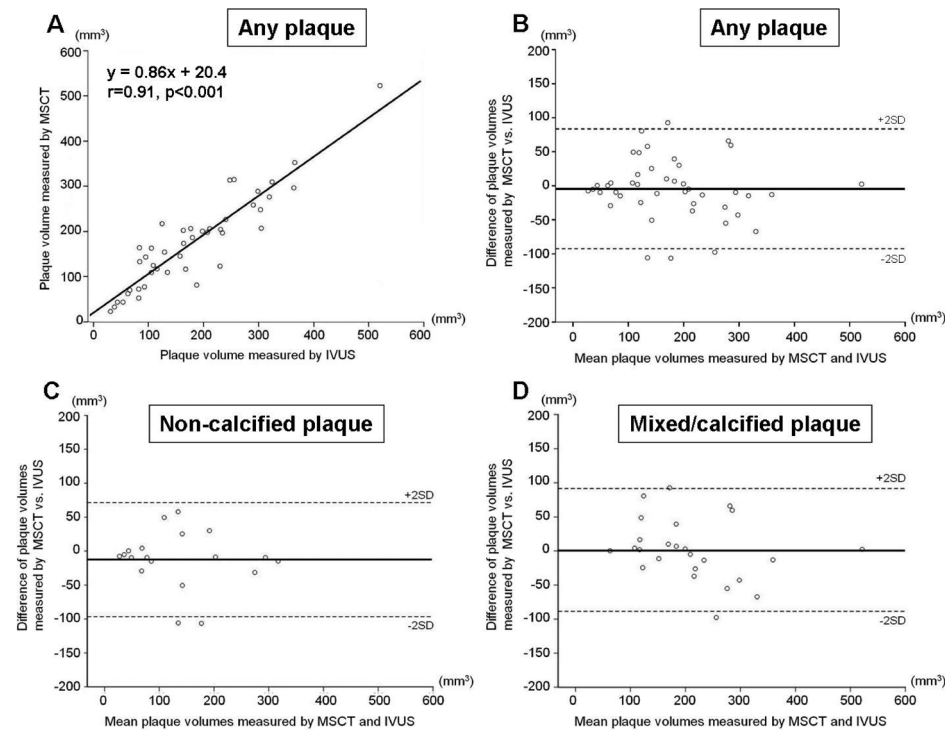

Figure 4. Correlation plot (A) and Bland-Altman analyses (B-D) for plaque volumes per vessel determined by IVUS versus 64-slice MDCT.

DISCUSSION

In the present study, we evaluated the ability of 64-slice MDCT to detect and quantify coronary atherosclerotic plaque, based on MDCT-derived parameters, using IVUS as a reference standard. The novel fusion technique we applied for the co-registration of IVUS and MDCT [8] provided cross-sectional images at identical positions for the whole length of the ROI and enabled a head-to-head comparison of the 2 imaging modalities.

The main findings of our study can be summarized as follows: plaque detection based on the threshold of >0.5mm for MDCT-derived maximum wall thickness resulted in a reasonably good diagnostic accuracy on the cross-sectional level (sensitivity 86%, specificity 71%), and very good on the segmental level (sensitivity 96%, specificity 88%). Moreover, the accurate detection of atherosclerotic plaque depended on plaque and vessel size. Smaller plaques could not be reliably detected, which was in accordance with previous reports [11-12]. Plaque location was also playing an important role for the diagnostic accuracy; the sensitivity significantly decreased for plaques located more distally. Finally, quantification of plaque volumes showed a significantly strong correlation between

MDCT and IVUS. The mean differences were small, with underestimation of non-calcified and overestimation for mixed/calcified plaque, however the limits of agreement were relatively wide.

MDCT angiography has the potential to become a non-invasive alternative to IVUS for plaque quantification and to be used for risk stratification of asymptomatic individuals or the assessment of atherosclerosis progression/regression. Previous studies [13-16] have focused on the comparison of MDCT- and IVUS-derived quantitative parameters, such as plaque area or plaque burden, showing moderate to good correlation, but the presence of atherosclerosis on MDCT was based on binary (yes/no) visual scoring. This is the first study, to our knowledge, that used a MDCT-derived quantitative parameter (wall thickness) to assess diagnostic accuracy on a slice-by-slice and segmental basis. Our data demonstrated that the detection of atherosclerotic plaque based on MDCT-derived quantitative parameters in a similar fashion to IVUS was feasible. Plaques located within the proximal 40 mm were detected with very high sensitivity (88-100%) and as invasive imaging studies have shown, the most clinically relevant lesions are highly clustered within the proximal sections of the coronaries [17-19]. Moreover, the very good diagnostic accuracy obtained at segmental level is promising for the potential development of prediction models based on plaque presence on a per-segment basis. Nevertheless, it is important to keep in mind that the clinical use of MDCT for detection of early atherosclerosis is still limited by the current spatial and temporal resolution of the technique. Further technical improvements of the acquisition and reconstruction techniques will enable more reliable visualization of the coronary arteries with better signal-to-noise ratio and decrease of partial voluming and motion artifacts.

Regarding the quantification of plaque volume by MDCT, our results add to the existing literature which only deals with stable angina patients. Several researchers compared plaque volumes derived from MDCT angiography with corresponding IVUS data and reported strong correlation and moderate agreement [20-25]. The differences between MDCT and IVUS volumetric measurements, which were also observed in our analysis, could be attributed to several technical and methodological factors. The spatial resolution of 64-slice CT may still be inadequate for accurate edge discrimination of MDCT images. The smaller coronary plaques, in particular non-calcified plaques, cannot be well defined and may occasionally not be detected, resulting in underestimation of plaque volume. Moreover, the real size of calcified plaque is overestimated by MDCT due to the blooming effects. Quantification of calcified plaque by IVUS can also be imprecise, because the acoustic shadowing in areas of calcification blocks the view of the outer vessel borders. In addition, on IVUS the outer boundaries were defined by the external elastic membrane (EEM), whereas on MDCT the outer vessel border was annotated at the adventitia-fat boundary, which may also have accounted for the discrepancies in the measurements. Furthermore, the IVUS images are not strictly perpendicular to the centerline, depending on the catheter position and vessel tortuosity. The slice thickness is

Chapter 11

Detection and quantification of coronary atherosclerotic plaque by 64-slice multidetector CT:
a systematic head-to-head comparison with Intravascular Ultrasound

slightly different between the two techniques, but this was largely overcome by the co-registration technique we used.

LIMITATIONS

This study was performed on a selected patient population with acute coronary syndromes and the examined vessels were only the major epicardial arteries, for which IVUS data were available. This population presented with high prevalence of disease and diagnostic accuracy might be lower in populations with lower prevalence, i.e. asymptomatic patients. In addition, some patients were excluded, however their characteristics were not different from the study group, thus we assumed that exclusion of these patients did not have any major influence on our study. Furthermore, the ROIs selected for our analysis were free of image artifacts (for instance caused by coronary motion or noise), whereas in everyday clinical routine those artifacts occasionally do occur. However, contrary to other studies, we have to point out that we included extensively calcified plaques. In addition, manual plaque segmentation largely depended on the individual operator and was rather time consuming; more automated validated software would be required for MDCT plaque analysis in a routine clinical setting. Finally, the high radiation exposure during MDCT coronary angiography remains a matter of concern. For this study, the estimated radiation exposure for the contrast-enhanced scan without prospective x-ray tube modulation was 17 ± 1 mSv; nevertheless, this radiation dose reflected the CT technology available at that time. Significant reduction of radiation dose can currently be achieved by implementation of several dose-saving techniques [26], which does result in effective dose comparable or lower than invasive coronary angiography. By applying image reconstruction algorithms, such as iterative reconstruction [27], supplementary to other radiation dose-saving techniques, dose reduction can be achieved with comparable image noise at lower tube currents.

CONCLUSIONS

The present study demonstrated that 64-MDCT is able to detect and quantify atherosclerotic plaque using MDCT-derived parameters. Further improvement in CT resolution is required for more reliable assessment of very small and distal coronary plaques.

Funding
This study was supported by a grant from the Fonds NutsOhra organization.

REFERENCES

1   Mintz GS, Nissen SE, Anderson WD, et al. (2001) American College of Cardiology Clinical Expert Consensus Document on Standards for Acquisition, Measurement and Reporting of Intravascular Ultrasound Studies (IVUS). A report of the American College of Cardiology Task Force on Clinical Expert Consensus Documents. J Am Coll Cardiol, 37(5):1478-1492.

2   Meijboom WB, Meijs MF, Schuijf JD, et al. (2008) Diagnostic accuracy of 64-slice computed tomography coronary angiography: a prospective, multicenter, multivendor study. J Am Coll Cardiol, 52(25):2135-2144.

3   Miller JM, Rochitte CE, Dewey M, et al. (2008) Diagnostic performance of coronary angiography by 64-row CT. N Engl J Med, 359(22):2324-2336.

4   Mollet NR, Cademartiri F, van Mieghem CA, et al. (2005) High-resolution spiral computed tomography coronary angiography in patients referred for diagnostic conventional coronary angiography. Circulation, 112(15):2318-2323.

5   Raff GL, Gallagher MJ, O'Neill WW, Goldstein JA (2005) Diagnostic accuracy of noninvasive coronary angiography using 64-slice spiral computed tomography. J Am Coll Cardiol, 46(3):552-557.

6   Schuijf JD, Pundziute G, Jukema JW, et al. (2006) Diagnostic accuracy of 64-slice multislice computed tomography in the noninvasive evaluation of significant coronary artery disease. Am J Cardiol, 98(2):145-148.

7   Pugliese F, Mollet NR, Hunink MG, et al. (2008) Diagnostic performance of coronary CT angiography by using different generations of multisection scanners: single-center experience. Radiology, 246(2):384-393.

8   van der Giessen AG, Schaap M, Gijsen FJ, et al. (2010) 3D fusion of intravascular ultrasound and coronary computed tomography for in-vivo wall shear stress analysis: a feasibility study. Int J Cardiovasc Imaging, 26(7):781-796.

9   De Winter SA, Hamers R, Degertekin M, et al. (2004) Retrospective image-based gating of intracoronary ultrasound images for improved quantitative analysis: the intelligate method. Catheter Cardiovasc Interv, 61(1):84-94.

10   Mollet NR, Rengo M, Neefjes LA, et al. (2008) Plaque Quantification by CT Coronary Angiography: Optimization of Window Level Settings.(ed)^(eds) Radiological Society of North America, 94th Scientific Assembly and Annual Meeting, Chicago, IL, USA,

11   Leber AW, Knez A, Becker A, et al. (2004) Accuracy of multidetector spiral computed tomography in identifying and differentiating the composition of coronary atherosclerotic plaques: a comparative study with intracoronary ultrasound. J Am Coll Cardiol,

12   van der Giessen AG, Toepker MH, Donelly PM, et al. (2010) Reproducibility, accuracy, and predictors of accuracy for the detection of coronary atherosclerotic plaque composition by computed tomography: an ex vivo comparison to intravascular ultrasound. Invest Radiol, 45(11):693-701.

13   Hur J, Kim YJ, Lee HJ, et al. (2009) Quantification and characterization of obstructive coronary plaques using 64-slice computed tomography: a comparison with intravascular ultrasound. J Comput Assist Tomogr, 33(2):186-192.

Chapter 11

*Detection and quantification of coronary atherosclerotic plaque by 64-slice multidetector CT:
a systematic head-to-head comparison with Intravascular Ultrasound*

14 Petranovic M, Soni A, Bezzera H, et al. (2009) Assessment of nonstenotic coronary lesions by 64-slice multidetector computed tomography in comparison to intravascular ultrasound: evaluation of nonculprit coronary lesions. J Cardiovasc Comput Tomogr, 3(1):24-31.

15 Sun J, Zhang Z, Lu B, et al. (2008) Identification and quantification of coronary atherosclerotic plaques: a comparison of 64-MDCT and intravascular ultrasound. AJR Am J Roentgenol, 190(3):748-754.

16 Voros S, Rinehart S, Qian Z, et al. (2011) Prospective Validation of Standardized, 3-Dimensional, Quantitative Coronary Computed Tomographic Plaque Measurements Using Radiofrequency Backscatter Intravascular Ultrasound as Reference Standard in Intermediate Coronary Arterial Lesions Results From the ATLANTA (Assessment of Tissue Characteristics, Lesion Morphology, and Hemodynamics by Angiography With Fractional Flow Reserve, Intravascular Ultrasound and Virtual Histology, and Noninvasive Computed Tomography in Atherosclerotic Plaques) I Study. JACC Cardiovasc Interv, 4(2):198-208.

17 Hong MK, Mintz GS, Lee CW, et al. (2008) A three-vessel virtual histology intravascular ultrasound analysis of frequency and distribution of thin-cap fibroatheromas in patients with acute coronary syndrome or stable angina pectoris. Am J Cardiol, 101(5):568-572.

18 Rodriguez-Granillo GA, Garcia-Garcia HM, Mc Fadden EP, et al. (2005) In vivo intravascular ultrasound-derived thin-cap fibroatheroma detection using ultrasound radiofrequency data analysis. J Am Coll Cardiol, 46(11):2038-2042.

19 Wang JC, Normand SL, Mauri L, Kuntz RE (2004) Coronary artery spatial distribution of acute myocardial infarction occlusions. Circulation, 110(3):278-284.

20 Achenbach S, Moselewski F, Ropers D, et al. (2004) Detection of calcified and noncalcified coronary atherosclerotic plaque by contrast-enhanced, submillimeter multidetector spiral computed tomography: a segment-based comparison with intravascular ultrasound. Circulation, 109(1):14-17.

21 Leber AW, Becker A, Knez A, et al. (2006) Accuracy of 64-slice computed tomography to classify and quantify plaque volumes in the proximal coronary system: a comparative study using intravascular ultrasound. J Am Coll Cardiol, 47(3):672-677.

22 Otsuka M, Bruining N, Van Pelt NC, et al. (2008) Quantification of coronary plaque by 64-slice computed tomography: a comparison with quantitative intracoronary ultrasound. Invest Radiol, 43(5):314-321.

23 Schepis T, Marwan M, Pflederer T, et al. (2010) Quantification of non-calcified coronary atherosclerotic plaques with dual-source computed tomography: comparison with intravascular ultrasound. Heart, 96(8):610-615.

24 Ugolini P, Pressacco J, Lesperance J, et al. (2009) Evaluation of coronary atheroma by 64-slice multidetector computed tomography: Comparison with intravascular ultrasound and angiography. Can J Cardiol, 25(11):641-647.

25 Dey D, Schepis T, Marwan M, Slomka PJ, Berman DS, Achenbach S Automated three-dimensional quantification of noncalcified coronary plaque from coronary CT angiography: comparison with intravascular US. Radiology, 257(2):516-522.

26 Raff GL, Chinnaiyan KM, Share DA, et al. (2009) Radiation dose from cardiac computed tomography before and after implementation of radiation dose-reduction techniques. JAMA, 301(22):2340-2348.

27 Leipsic J, Heilbron BG, Hague C (2011) Iterative reconstruction for coronary CT angiography: finding its way. Int J Cardiovasc Imaging.

Part 4

Summary and conclusions

Chapter **12**

Summary and conclusions

INTRODUCTION

CT coronary angiography has emerged as a widely used and reliable imaging modality to assess the absence or presence of coronary artery disease. In addition CT coronary angiography is able to determine the coronary plaque burden throughout the whole coronary tree. In chapter 2 and 3 an overview of the literature on CT coronary plaque imaging and the prognostic value of CT coronary angiography is presented.

CT CORONARY ANGIOGRAPHY: IMAGE QUALITY, DIAGNOSTIC ACCURACY AND RADIATION DOSE

 The image quality and diagnostic accuracy of CT coronary angiography seems to be related to certain patient characteristics and to the scanner and acquisition protocol used.

In a large study of 927 symptomatic patients undergoing CT coronary angiography using adaptive ECG-pulsing, the influence of heart rate frequency and heart rate variability on radiation dose, image quality and diagnostic performance was determined (chapter 4). Heart rate frequency and heart rate variability showed no significant relation with image quality nor with diagnostic accuracy. Radiation dose was significantly lower in patients with a high heart rate frequency compared to those with a low frequency. A high heart rate variability was significantly related to an increase in radiation dose because of the adaptive ECG-pulsing algorithm that automatically adjusted the radiation window during the scan, when the heart rate significantly varies, to maintain high image quality.

The second generation 128-slice dual source CT scanner offers several different CT coronary angiography acquisition protocols. Patients referred for CT coronary angiography were divided into two groups based on pre-scan heart rate (group 1: < 65 beats per minute; group 2: ≥ 65 beats per minute). They were randomized to undergo 1) prospective high pitch spiral or narrow-window prospective sequential scanning in the first group and 2) wide-window prospective sequential or retrospective spiral scanning in group 2. In chapter 5 we compared the image quality and radiation dose and their relationship with heart rate of the different scan protocols. A high pitch spiral CTCA scan protocol offered a significant reduction in radiation dose compared to a narrow-window sequential scan protocol. However, image quality was only maintained in a selected patient population with a very low (<55 beats per minute) heart rate. A wide-window sequential scan protocol offered a significant reduction in radiation dose compared to a retrospective spiral scan protocol and provides similar image quality.

Then we compared the ability of the different CT coronary angiography protocols to detect coronary lesion with more than 50% lumen diameter narrowing with quantitative

invasive coronary angiography in 267 patients (chapter 6). The results of this study confirmed the findings of chapter 5. Sequential scanning provided good diagnostic performance at a relatively low radiation dose (2.65 – 7.53 mSv; dependent on scan window and tube voltage). Further dose reduction can be achieved with high-pitch spiral scanning in patients with low heart rates, albeit at the expense of a lower diagnostic performance. Retrospective spiral acquisition provided comparable diagnostic performance at a significantly higher radiation dose compared to the wide-window sequential protocol and thus should be abandoned in patients with a stable heart rate. Taking into account the image quality, diagnostic performance and radiation exposure the prospective sequential protocol is preferred for CT coronary angiography in patients with a stable heart rate.

Finally we studied 100 patients that underwent CT coronary angiography using a sequential protocol for further optimization of this acquisition protocol in relation to heart rate to provide diagnostic quality at the lowest radiation exposure (chapter 7). For each CT coronary angiography the image quality of 10 datasets, representing 10 different time-points in the cardiac cycle (RR-interval), was determined. The optimal reconstruction window for sequential CT coronary angiography using a second generation Dual Source CT scanner, was 40-45% of the RR-interval in patients with a heart rate of ≥70 beats per minute and 70-75% in patients with a heart rate <70 beats per minute. Using these small reconstruction windows as acquisition windows radiation dose would be reduced substantially (1.5±0.6 mSv to 2.8±0.7 mSv, dependent on the tube potential used).

CT CORONARY PLAQUE IMAGING

The autosomal dominant disorder Familial Hypercholesterolemia is associated with an increased risk of coronary artery disease, irrespective of the presence of symptoms of coronary ischemia. However, some patients with FH will never suffer an adverse cardiac event. We evaluated the visualization of the coronary vessels by CT coronary angiography for assessing direct evidence of having coronary atherosclerosis.

We studied 101 statin treated asymptomatic patients with familial hypercholesterolemia and 126 patients with non-anginal chest pain, who all underwent CT calcium scoring and CT coronary angiography (chapter 8). The coronary calcium score and the total atherosclerotic plaque burden were compared between these two groups of patients. Despite intense statin treatment to lower the serum cholesterol the occurrence of CAD was significantly higher in patients with FH.

In a extended population of 140 treated patients with FH the extent, severity and distribution of CAD and type of plaque were evaluated using CT coronary angiography (chapter 9). Despite their genetic predisposition for development of CAD, 1 out of 6 patients did

not have show any signs of coronary atherosclerosis. Nevertheless we found obstructive coronary lesions in a quarter of patients, in spite of the absence of symptoms. The extent of coronary atherosclerosis is related to gender and serum cholesterol levels. Presence and severity of subclinical CAD in patients with FH is comparable to that of asymptomatic patients with diabetes mellitus. The composition of plaques and the anatomical distribution of CAD throughout the coronary tree is similar to that of patients without FH.

In 50 to 80% of identified cases of patients with FH the genetic disorder is known. We evaluated the relation between CT coronary angiography plaque burden and the presence of the several currently known genetic disorders causing FH in 145 patients with FH (chapter 10). Our results showed that LDL receptor negative mutational status in is related to a higher extent of CAD compared to other genetic mutations even though all patients were intensively treated with statins.

Early detection of subclinical CAD (screening) using non-invasive CT coronary angiography in high risk patients might influence risk prediction and clinical management in the future. However, accurate assessment of atherosclerotic coronary plaque using CT coronary angiography is mandatory for detection of early plaques in asymptomatic individuals and serial evaluation of progression of coronary atherosclerosis. In addition a modality for screening or serial examinations should preferably be low risk, non-invasive, cheap and fast, which makes CT coronary angiography suitable. In 32 patients the detection of coronary plaque and quantification of plaque volume were evaluated by CT coronary angiography (chapter 11). Compared to Intravascular Ultrasound, the gold standard for coronary plaque assessment, CT coronary angiography was able to detect the majority of plaques and only slightly underestimated the plaque volumes.

FUTURE PERSPECTIVE

To explore the current and future position of CT coronary angiography in the diagnosis of patients with suspected coronary artery disease or individuals at high risk for coronary artery disease, a six level hierarchical model of efficacy can be used [1]. At the first level of technical efficacy the temporal resolution as well as the spatial resolution of CT coronary angiography have improved with latest generation scanners but are still limited compared to invasive coronary angiography. Radiation exposure of CT coronary angiography has been reduced to 1.0-3.0 mSv and new technical developments as iterative reconstruction might lower the dose to less than 1 mSv. The high diagnostic accuracy (level 2) of CT coronary angiography has been studied extensively and especially the high negative predictive value supports the use of CT coronary angiography as a first line test. Nevertheless, CT coronary angiography is currently not able to reliable identify flow limiting coronary lesions that are subject for revascularization therapies. New CT applications

for functional testing (CT-FFR, CT myocardial perfusion, CT intracoronary attenuation gradient assessment) are being developed and tested but not yet clinically implemented.

CT coronary angiography shows the highest diagnostic thinking efficacy (level 3) in patients with an intermediate pre-test probability according to the Bayesian theory. However, the influence of CT coronary angiography on therapeutic decision making (level 4) is still rather limited despite high diagnostic accuracy and prognostic value of CT coronary angiography. Only few exploratory studies are reported on the use of CT coronary angiography in asymptomatic individuals. At this moment comparative effectiveness research [2] on patient outcome and societal efficacy (level 5 and 6) is sparse. In conclusion: the precise clinical role of CT coronary angiography in symptomatic patients, in comparison to other widely used non-invasive CAD detection modalities, has not been established. Currently there is no clinical role for CT coronary angiography in asymptomatic (high-risk) individuals. Results of comparative effectiveness research on using CT coronary angiography for different clinical indications are needed to define the position of CT coronary angiography in the future.

REFERENCES

1   Fryback DG, Thornbury JR (1991) The efficacy of diagnostic imaging. Med Decis Making, 11(2):88-94.
2   Hlatky MA, Douglas PS, Cook NL, et al. (2012) Future directions for cardiovascular disease comparative effectiveness research: report of a workshop sponsored by the National Heart, Lung, and Blood Institute. J Am Coll Cardiol, 60(7):569-580.

Samenvatting en conclusies

INTRODUCTIE

CT coronair angiografie heeft zich ontwikkeld tot een veel gebruikte en betrouwbare beeldtechniek om de aan- of afwezigheid van aderverkalking in de kransslagaderen aan te tonen. Tevens kan met CT coronair angiografie de uitgebreidheid van aderverkalking in de kransslagaderen bepaald worden. In hoofdstuk 2 en 3 wordt een overzicht gegeven van de literatuur over het afbeelden van plaque in de kransslagaderen met CT en de prognostische waarde van CT coronair angiografie.

CT CORONAIR ANGIOGRAFIE: BEELDKWALITEIT, DIAGNOSTISCHE ACCURAATHEID EN STRALINGSDOSIS

De beeldkwaliteit en diagnostische accuraatheid van CT coronair angiografie lijkt gerelateerd aan bepaalde patiënten karakteristieken, de gebruikte CT scanner en het acquisitie protocol.

In een grote studie met 927 symptomatische patiënten die CT coronair angiografie ondergingen, gebruikmakend van een adaptief ECG-pulsing algoritme, werd de invloed van de hartslagfrequentie en hartslagvariabiliteit op stralingsdosis, beeldkwaliteit en diagnostische accuraatheid onderzocht (hoofdstuk 4). Hartslagfrequentie en hartslagvariabiliteit vertoonden geen significante relatie met beeldkwaliteit en diagnostische accuraatheid. De stralingsdosis was significant lager in patiënten met een hoge hartslagfrequentie vergeleken met patiënten met een lage frequentie. Een grote hartslagvariabiliteit was gerelateerd aan een significante toename in stralingsdosis door het adaptieve ECG-pulsing algoritme. Dit algoritme paste automatisch het stralingswindow aan op het moment dat de hartslag duidelijk varieerde, om hoge beeldkwaliteit te behouden.

De tweede generatie 128-slice dual source CT scanners bieden mogelijkheid tot het gebruiken van verschillende CT coronair angiografie acquisitie protocollen. Patiënten verwezen voor CT coronair angiografie, werden verdeeld in twee groepen aan de hand van hun hartslagfrequentie (groep1: <65 slagen per minuut; groep 2: ≥65 slagen per minuut). Vervolgens werd per groep gerandomiseerd om 1) een prospectief high pitch spiral protocol of een prospectief sequentieel protocol met een smal stralingswindow en 2) een prospectief sequentieel protocol met een breed stralingswindow of een retrospectief spiraal protocol te ondergaan. In hoofdstuk 5 hebben we de beeldkwaliteit en de stralingsdosis in relatie met de hartslagfrequentie bepaald van deze verschillende protocollen. Het high pitch spiral protocol gaf een significante verlaging van de stralingsdosis vergeleken met het sequentiële protocol met een smal stralingswindow. De beeldkwaliteit bleef

echter achter en was slechts hetzelfde in een specifieke patiënten groep met een zeer lage hartslagfrequentie (<55 slagen per minuut). Het sequentiële protocol met een breed stralingswindow gaf een significant lagere stralingsdosis dan het retrospectieve spiraal protocol terwijl de beeldkwaliteit vergelijkbaar was.

Vervolgens hebben we het vermogen van de verschillende CT coronair angiografie protocollen om een >50% vernauwing van de kransslagaderen aan te tonen, vergeleken met invasieve coronair angiografie in 267 patiënten (hoofdstuk 6). De resultaten van deze studie onderschreven de bevindingen van hoofdstuk 5. Sequentieel scannen leverde een goede diagnostisch accuraatheid op terwijl de stralingsdosis relatief laag was (2.65 – 7.53 mSv; afhankelijk van gebruikte stralingswindow en buis potentiaal). Verdere vermindering van de stralingsdosis in patiënten met een lage hartslag kan bereikt worden door gebruik te maken van het high pitch spiral protocol maar dat gaat dan wel ten koste van de diagnostische accuraatheid. Het retrospectieve spiraal protocol leidde tot een zelfde diagnostische accuraatheid maar met een significant hogere stralingsdosis vergeleken met het sequentiële protocol met breed stralingswindow en zou dus niet gebruikt moeten worden in patiënten met een stabiele hartslagfrequentie. Rekening houdend met beeldkwaliteit, diagnostische accuraatheid en stralingsdosis is het sequentiële acquisitieprotocol het scanprotocol van voorkeur in patiënten met een stabiele hartslag die CT coronair angiografie moeten ondergaan.

Vervolgens hebben we in 100 patiënten die sequentiële CT coronair angiografie ondergingen onderzocht hoe dit acquisitie protocol verder geoptimaliseerd kon worden om hoge beeldkwaliteit te verkrijgen met een zo laag mogelijke stralingsdosis (hoofdstuk 7).

Van elk CT coronair angiogram is de beeldkwaliteit van 10 datasets, die op 10 verschillende tijdspunten in het RR-interval vervaardigd zijn, bepaald. Het optimale reconstructiewindow voor sequentiële CT coronair angiografie gebruikmakend van een tweede generatie dual source scanner was 40-45% van het RR-interval voor patiënten met een hartslag [3]70 slagen per minuut en 70-70% voor patiënten met een hartslag <70 slagen per minuut. Wanneer we deze geoptimaliseerde acquisitie windows gebruikt zouden hebben zou de stralingsdosis substantieel lager geweest zijn (1.5±0.6 mSv tot 2.8±0.7 mSv, afhankelijk van het gebruikte buis potentiaal).

AFBEELDING VAN ADERVERKALKING IN DE KRANSSLAGADEREN MET CT

De autosomaal dominante afwijking Familiaire Hypercholesterolemie (FH) is geassocieerd met een verhoogd risico op ziekte van de kransslagaderen, ongeacht de aanwezigheid van symptomen. Echter sommige patiënten met FH zullen nooit een probleem met hun

hart krijgen. Om de aan- of afwezigheid van aderverkalking in de kransslagaderen aan te tonen hebben we middels CT coronair angiografie de kransslagaderen afgebeeld. In dit onderzoek zijn 101 klachtenvrije patiënten met FH en 146 patiënten met niet-angineuze klachten bestudeerd. Allen ondergingen een blanco CT ter verkrijging van de calcium-score en een CT coronair angiografie (hoofdstuk 8). De calcium score en de totale athe-rosclerotische plaque belasting in de kransslagaderen is vergeleken tussen deze twee patiënten groepen. Ondanks de intensieve behandeling met statines om de cholesterol waardes in het bloed te verlagen kwam aderverkalking in de kransslagaderen significant vaker voor in patiënten met FH dan in patiënten met niet-angineuze klachten. In een uit-gebreidere populatie van 140 patiënten met FH hebben we de uitgebreidheid, de ernst, de compositie en de anatomische verdeling van de aderverkalking bestudeert door mid-del van CT coronair angiografie (hoofdstuk 9). Hoewel allen genetische aanleg voor het ontwikkelen van aderverkalking in de kransslagaderen hebben, waren er in 1 op de 6 pa-tiënten geen tekenen van aderverkalking waarneembaar. Tegelijkertijd werd in bijna een kwart van de patiënten significante vernauwingen in de kransslagaderen gezien. De uit-gebreidheid van aderverkalking is gerelateerd aan geslacht en cholesterol waardes in het bloed. Aanwezigheid en ernst van subklinische aderverkalking in patiënten met FH zijn vergelijkbaar met die in klachtenvrije patiënten met diabetes mellitus. De compositie en de anatomische verdeling van de aderverkalking was hetzelfde als in patiënten zonder FH.

Van 50 tot 80% van de patiënten die gediagnosticeerd zijn met FH is de genetische afwij-king bekend. We hebben de relatie tussen aderverkalking zichtbaar op CT coronair an-giografie en de verschillende genetische afwijkingen die FH veroorzaken onderzocht in 145 klachtenvrije patiënten met FH (hoofdstuk 10). Uit onze resultaten blijkt dat patiënten met een mutatie waardoor een van de cholesterol receptoren (LDL-receptor) afwezig is, meer en ernstiger aderverkalking lieten zien vergeleken met patiënten met een andere genetische afwijking zelfs al werden alle patiënten intensief behandeld met statines.

Vroege detectie van kransslagaderverkalking (screening) gebruikmakend van CT coro-nair angiografie in klachtenvrije hoogrisico patiënten kan mogelijk de risico inschatting en het klinische handelen in de toekomst beïnvloeden. Een techniek die ingezet wordt voor screening moet bij voorkeur een laag risico op complicaties hebben en niet-invasief, goedkoop en snel zijn. Rekening houdend met deze eigenschappen komt CT coronair angiografie mogelijk in aanmerking om ingezet te worden voor screening. Hoogrisico klachtenvrije patiënten kunnen dan met CT coronair angiografie onderzocht worden om atherosclerose in een vroeg stadium te detecteren en het verdere ziektebeloop te evalu-eren. Om de accuraatheid om plaque te beoordelen te onderzoeken werd in 32 patiënten met een acuut coronair syndroom de aanwezigheid van plaque en het plaquevolume bepaald met CT coronair angiografie (hoofdstuk 11). In vergelijking met intravasculaire echografie, de gouden standaard voor plaque beoordeling, was CT coronair angiografie in staat de meerderheid van de lesies te detecteren terwijl het volume van de plaques slechts gering werd onderschat.

TOEKOMST PERSPECTIEF

Om de huidige en de toekomstige rol van CT coronair angiografie in patiënten met de verdenking op hartziekte te evalueren kan een hiërarchisch model met 6 niveaus gebruikt worden [1]. Op het niveau van technische werkzaamheid (niveau 1) kan gesteld worden dat zowel de temporele als de spatiële resolutie verbeterd zijn in de laatste generatie scanners maar dat ze nog wel beperkt zijn in vergelijking met invasieve coronair angio-grafie. De stralingsdosis van CT coronair angiografie is teruggebracht tot 1,0-3,0 mSv en nieuwe technische ontwikkelingen zoals iteratieve reconstructie maken het mogelijk dit nog verder verlagen tot minder dan 1,0 mSv. De hoge diagnostische accuraatheid (niveau 2) van CT coronair angiografie is uitgebreid onderzocht en met name de hoge negatief voorspellende waarde onderschrijft de rol van CT coronair angiografie als een test om ziekte uit te sluiten. CT coronair angiografie is momenteel nog niet in staat om op be-trouwbare wijze de mate van bloedstroombelemmering veroorzaakt door aderverkalking in de kransslagaderen te identificeren. Nieuwe CT toepassingen voor het testen van de aanwezigheid van ischemie (CT-functional flow reserve (FFR), CT myocard perfusie en het aantonen van een CT intracoronaire aankleuringsgradient) worden ontwikkeld maar zijn nog niet klinisch geïmplementeerd.

CT coronair angiografie laat de hoogste werkzaamheid op het diagnostische denken zien (niveau 3) in patiënten met een intermediaire kans op hartziekte voorafgaand aan de test in navolging van de theorie van Bayes. Toch is de invloed van CT coronair angiografie op het maken van therapeutische beslissingen (niveau 4) nog niet zo hoog ondanks de bewezen hoge diagnostische accuraatheid en prognostische waarde. Slechts een paar onderzoeken over het gebruik van CT coronair angiografie in klachtenvrije individuen zijn beschreven. Op dit moment zijn vergelijkende effectiviteitonderzoeken [2] schaars wat betreft resultaten op patiënt en op maatschappelijk niveau (niveau 5 en 6).

Concluderend kunnen we stellen dat de precieze rol van CT coronair angiografie in symptomatische patiënten, in vergelijking met andere gevestigde niet-invasieve technie-ken om hartziekte aan te tonen, nog niet geheel duidelijk. Momenteel is er geen klinische rol weggelegd voor CT coronair angiografie in klachtenvrije individuen.

Uitkomsten van vergelijkende effectiviteitonderzoeken met betrekking tot de klinische indicaties zijn nodig om de positie van CT coronair angiografie te bepalen, nu en in de toekomst.

REFERENTIES

1   Fryback DG, Thornbury JR (1991) The efficacy of diagnostic imaging. Med Decis Making, 11(2):88-94.

2   Hlatky MA, Douglas PS, Cook NL, et al. (2012) Future directions for cardiovascular disease comparative effectiveness research: report of a workshop sponsored by the National Heart, Lung, and Blood Institute. J Am Coll Cardiol, 60(7):569-580. doi: S0735-1097(12)01587-2 [pii] 10.1016/j.jacc.2011.12.057

Chapter 13

Dankwoord

Promotieonderzoek kun je onmogelijk alleen uitvoeren. Er zijn dan ook vele mensen die mij gedurende mijn promotietraject geholpen, ondersteund en geïnspireerd hebben. Enkelen hiervan wil ik in het bijzonder noemen:

Allereerst dank voor mijn promotoren zonder wie dit proefschrift er niet zou zijn geweest.

Beste professor de Feyter, ondanks alle beren die ik steeds op de weg zag, is er dan uiteindelijk toch dit proefschrift. Hartelijk dank voor uw begeleiding en uw zeer waardevolle en steeds weer inspirerende wetenschappelijke input.

Beste professor Krestin, zeer bedankt voor alle geboden kansen en mogelijkheden op de afdeling Radiologie in het EMC. Hoewel ik eind 2011, wat betreft het verloop van mijn loopbaan, een andere keuze heb gemaakt dan in de lijn der verwachting lag, ben ik u zeer erkentelijk dat ik meerdere jaren deel uit heb mogen maken van uw afdeling.

Graag wil ik professor de Roos, professor de Jaegere en professor Niessen hartelijk danken voor het plaatsnemen in de leescommissie en voor de deskundige beoordeling van mijn proefschrift.

Professor Hunink, professor Sijbrands, en Koen Nieman, erg fijn dat u in de grote promotiecommissie wilde plaatsnemen en hartelijke dank voor eerdere kritische en waardevolle evaluaties van mijn manuscripten.

Lieve Tirza, ik bewonder je toewijding, je tomeloze energie en je inzet voor je patiënten. Je bent niet alleen een collega maar bovenal ook een vriendin en ik ben blij dat jij naast mij wil staan als paranimf.

Gert-Jan, ik had me geen betere "mede-CAMPER-onderzoeker" kunnen wensen. Niet alleen vanwege je precieze manier van onderzoek doen maar ook door je nuchtere kijk op 'problemen' of tegenslagen, waardoor we er achteraf vaak hard om hebben kunnen lachen. Dank dat je mijn paranimf wil zijn.

Nico, jouw enthousiasme over cardiale CT heeft mij aangezet tot het aanvangen met het in dit proefschrift beschreven onderzoek. Je heldere kijk op onderzoeksresultaten, je Bourgondische instelling en je soms wel erg lange Brabantse kwartiertjes maakten dat onderzoek doen nooit saai werd; hartelijke dank.

Annick, met jou als mijn 'voorganger' in de onderzoeksgroep had ik een goed en inspirerend voorbeeld om te volgen. Dank voor je bijdrages aan en kritische beoordelingen van manuscripten.

Collega's van de cardiac imaging groep, Alexia, Anoeshka, Admir en Elina, wat hebben we een hoop dingen samen beleefd. Niet alleen interessante onderzoeken met mooie resultaten en bijbehorende publicaties en presentaties maar ook de Excalibur, etentjes, stappen, feesten, lunchen, Sinterklaasavond en nog veel meer. Dank voor jullie bijdrage aan dit proefschrift maar vooral ook voor de leuke en bijzondere tijd! Grazie!

Maar er zijn natuurlijk nog veel meer mensen die in meer of mindere mate een bijdrage hebben geleverd aan de totstandkoming van dit proefschrift. Dat zijn in willekeurige volgorde: Adriaan, Mohamed, Kei, Ermanno, Stamos, Rick, Marisa, Matthijs, Marco, Francesca, Filippo, Bob, Sharon, Michiel, Coert, Joost, Alina, Tessa, Frank, Jolanda, Jurgen, Linda, Jolanda, Fania, Erik-Jan, Rick, Jeroen, Mart, Marcel, Marcel, Berend, Ronald, Annemarie, Esther, Marja, Carl, Tjebbe, Paul, Robert-Jan, Titia, Erna, Jan-Willem, Lydia, Wim, Marieke, Wendy, Annelies, Janneke, Annette, Behiye, Sandra, Ton, Martijn, Mike, Trijne, Marjolein, Erik, alle onderzoekspatiënten en alle overige betrokken medewerkers van de afdelingen Radiologie, Cardiologie, Interne geneeskunde, de COEUR en het ICIN: BEDANKT!

En tot slot:

Lieve papa en mama, lieve Janne, jullie oprechte interesse en medeleven zijn een constante aanmoediging geweest om dit proefschrift tot stand te brengen.

Lieve Floor, het is niet echt een voorleesboek geworden maar er staan wel heel veel leuke letters in. Lieve Willem, misschien kun je dit boekje ook proberen te verslinden; letterlijk dan. Lieve Polle, kus.

Jullie maken mijn leven mooi.

Publications

PUBLICATIONS

1. ten Kate GJ, **Neefjes LA**, Dedic A, Nieman K, Langendonk JG, Galema-Boers AJ,
    Roeters van Lennep J, Moelker A, Krestin GP, Sijbrands EJ, de Feyter PJ.
    The effect of LDLR-negative genotype on CT coronary atherosclerosis
    in asymptomatic statin treated patients with heterozygous familial
    hypercholesterolemia.
    Atherosclerosis. 2013 Apr;227(2):334-41.

2. **Neefjes LA**, Rossi A, Genders TS, Nieman K, Papadopoulou SL, Dharampal AS,
    Schultz CJ, Weustink AC, Dijkshoorn ML, Ten Kate GJ, Dedic A, van Straten M,
    Cademartiri F, Hunink MG, Krestin GP, de Feyter PJ, Mollet NR.
    Diagnostic accuracy of 128-slice dual-source CT coronary angiography: a
    randomized comparison of different acquisition protocols.
    Eur Radiol. 2013 Mar;23(3):614-22.

3. Dedic A, Rossi A, Ten Kate GJ, **Neefjes LA**, Galema TW, Moelker A, van Domburg RT,
    Schultz CJ, Mollet NR, de Feyter PJ, Nieman K.
    First-line evaluation of coronary artery disease with coronary calcium scanning or
    exercise electrocardiography.
    Int J Cardiol. 2013 Feb 20;163(2):190-5.

4. Metz C, Schaap M, Klein S, Baka N, **Neefjes LA**, Schultz C, Niessen W, van Walsum T.
    Registration of 3D+t Coronary CTA and Monoplane 2D+t X-Ray Angiography.
    IEEE Trans Med Imaging. 2013 Feb 6.

5. Dharampal AS, Papadopoulou SL, Rossi A, Weustink AC, Mollet NR, Meijboom WB,
    Neefjes LA, Nieman K, Boersma E, de Feijter PJ, Krestin GP.
    Computed tomography coronary angiography accuracy in women and men at low
    to intermediate risk of coronary artery disease.
    Eur Radiol. 2012 Nov;22(11):2415-23.

6. Papadopoulou SL, Brugaletta S, Garcia-Garcia HM, Rossi A, Girasis C, Dharampal AS,
    Neefjes LA, Ligthart J, Nieman K, Krestin GP, Serruys PW, de Feyter PJ.
    Assessment of atherosclerotic plaques at coronary bifurcations with multidetector
    computed tomography angiography and intravascular ultrasound-virtual histology.
    Eur Heart J Cardiovasc Imaging. 2012 Aug;13(8):635-42.

7. Metz CT, Baka N, Kirisli H, Schaap M, Klein S, **Neefjes LA**, Mollet NR, Lelieveldt B, de
    Bruijne M, Niessen WJ, van Walsum T.
    Regression-based cardiac motion prediction from single-phase CTA.
    IEEE Trans Med Imaging. 2012 Jun;31(6):1311-25.

8. Dedic A, Ten Kate GJ, **Neefjes LA**, Rossi A, Dharampal A, Rood PP, Galema TW,
    Schultz C, Ouhlous M, Moelker A, de Feyter PJ, Nieman K.
    Coronary CT angiography outperforms calcium imaging in the triage of acute
    coronary syndrome.
    Int J Cardiol. 2012 May 7. [Epub ahead of print]

9. Weustink AC, **Neefjes LA**, Rossi A, Meijboom WB, Nieman K, Capuano E, Boersma E,
    Mollet NR, Krestin GP, de Feyter PJ.
    Diagnostic performance of exercise bicycle testing and single-photon emission
    computed tomography: comparison with 64-slice computed tomography coronary
    angiography.
    Int J Cardiovasc Imaging. 2012 Mar;28(3):675-84.

10. Papadopoulou SL, **Neefjes LA**, Garcia-Garcia HM, Flu WJ, Rossi A, Dharampal AS,
    Kitslaar PH, Mollet NR, Veldhof S, Nieman K, Stone GW, Serruys PW, Krestin GP, de
    Feyter PJ.
    Natural history of coronary atherosclerosis by multislice computed tomography.
    JACC Cardiovasc Imaging. 2012 Mar;5(3 Suppl):S28-37.

11. **Neefjes LA**, Ten Kate GJ, Alexia R, Nieman K, Galema-Boers AJ, Langendonk JG,
    Weustink AC, Mollet NR, Sijbrands EJ, Krestin GP, de Feyter PJ.
    Accelerated subclinical coronary atherosclerosis in patients with familial
    hypercholesterolemia.
    Atherosclerosis. 2011 Dec;219(2):721-7.

12. **Neefjes LA**, Dharampal AS, Rossi A, Nieman K, Weustink AC, Dijkshoorn ML, Ten
    Kate GJ, Dedic A, Papadopoulou SL, van Straten M, Cademartiri F, Krestin GP, de
    Feyter PJ, Mollet NR.
    Image quality and radiation exposure using different low-dose scan protocols in
    dual-source CT coronary angiography: randomized study.
    Radiology. 2011 Dec;261(3):779-86.

13. Papadopoulou SL, **Neefjes LA**, Schaap M, Li HL, Capuano E, van der Giessen AG,
    Schuurbiers JC, Gijsen FJ, Dharampal AS, Nieman K, van Geuns RJ, Mollet NR, de
    Feyter PJ.
    Detection and quantification of coronary atherosclerotic plaque by 64-slice
    multidetector CT: a systematic head-to-head comparison with intravascular
    ultrasound.
    Atherosclerosis. 2011 Nov;219(1):163-70.

14. Schaap M, van Walsum T, **Neefjes L**, Metz C, Capuano E, de Bruijne M, Niessen W.
    Robust shape regression for supervised vessel segmentation and its application to coronary segmentation in CTA.
    IEEE Trans Med Imaging. 2011 Nov;30(11):1974-86.

15. **Neefjes LA**, de Feyter PJ.
    CT coronary angiography: a new unique prognosticator?
    Heart. 2011 Sep;97(17):1363-4.

16. **Neefjes LA**, Ten Kate GJ, Rossi A, Galema-Boers AJ, Langendonk JG, Weustink AC, Moelker A, Nieman K, Mollet NR, Krestin GP, Sijbrands EJ, de Feyter PJ.
    CT coronary plaque burden in asymptomatic patients with familial hypercholesterolaemia.
    Heart. 2011 Jul;97(14):1151-7..

17. van der Giessen AG, Gijsen FJ, Wentzel JJ, Jairam PM, van Walsum T, **Neefjes LA**, Mollet NR, Niessen WJ, van de Vosse FN, de Feyter PJ, van der Steen AF.
    Small coronary calcifications are not detectable by 64-slice contrast enhanced computed tomography.
    Int J Cardiovasc Imaging. 2011 Jan;27(1):143-52.

18. Weustink AC, Mollet NR, **Neefjes LA**, Meijboom WB, Galema TW, van Mieghem CA, Kyrzopoulous S, Eu RN, Nieman K, Cademartiri F, van Geuns RJ, Boersma E, Krestin GP, de Feyter PJ.
    Diagnostic accuracy and clinical utility of noninvasive testing for coronary artery disease.
    Ann Intern Med. 2010 May 18;152(10):630-9.

19. Schultz CJ, Moelker A, Piazza N, Tzikas A, Otten A, Nuis RJ, **Neefjes LA**, van Geuns RJ, de Feyter P, Krestin G, Serruys PW, de Jaegere PP.
    Three dimensional evaluation of the aortic annulus using multislice computer tomography: are manufacturer's guidelines for sizing for percutaneous aortic valve replacement helpful?
    Eur Heart J. 2010 Apr;31(7):849-56.

20. Metz C, Baka N, Kirisli H, Schaap M, van Walsum T, Klein S, **Neefjes L**, Mollet N, Lelieveldt B, de Bruijne M, Niessen W.
    Conditional shape models for cardiac motion estimation.
    Med Image Comput Comput Assist Interv. 2010;13(Pt 1):452-9.

21. Nieman K, Galema TW, **Neefjes LA**, Weustink AC, Musters P, Moelker AD, Mollet NR, de Visser R, Boersma E, de Feijter PJ.
    Comparison of the value of coronary calcium detection to computed tomographic angiography and exercise testing in patients with chest pain.
    Am J Cardiol. 2009 Dec 1;104(11):1499-504.

22. Weustink AC, **Neefjes LA**, Kyrzopoulos S, van Straten M, Neoh Eu R, Meijboom WB, van Mieghem CA, Capuano E, Dijkshoorn ML, Cademartiri F, Boersma E, de Feyter PJ, Krestin GP, Mollet NR.
    Impact of heart rate frequency and variability on radiation exposure, image quality, and diagnostic performance in dual-source spiral CT coronary angiography.
    Radiology. 2009 Dec;253(3):672-80.

23. Kyrzopoulos S, **Neefjes LA**, De Feyter P.
    Cardiac multidetector computed tomography: where do we stand?
    Hellenic J Cardiol. 2009 Nov-Dec;50(6):523-35. Review.

24. Nieman K, Galema T, Weustink A, **Neefjes L**, Moelker A, Musters P, de Visser R, Mollet N, Boersma H, de Feijter PJ.
    Computed tomography versus exercise electrocardiography in patients with stable chest complaints: real-world experiences from a fast-track chest pain clinic.
    Heart. 2009 Oct;95(20):1669-75.

25. Weustink AC, Mollet NR, **Neefjes LA**, van Straten M, Neoh E, Kyrzopoulos S, Meijboom BW, van Mieghem C, Cademartiri F, de Feyter PJ, Krestin GP.
    Preserved diagnostic performance of dual-source CT coronary angiography with reduced radiation exposure and cancer risk.
    Radiology. 2009 Jul;252(1):53-60.

26. Schaap M, **Neefjes L**, Metz C, van der Giessen A, Weustink A, Mollet N, Wentzel J, van Walsum TW, Niessen W.
    Coronary lumen segmentation using graph cuts and robust kernel regression.
    Inf Process Med Imaging. 2009;21:528-39.

27. Metz CT, Schaap M, Klein S, **Neefjes LA**, Capuano E, Schultz C, van Geuns RJ, Serruys PW, van Walsum T, Niessen WJ.
    Patient specific 4D coronary models from ECG-gated CTA data for intra-operative dynamic alignment of CTA with X-ray images.
    Med Image Comput Comput Assist Interv. 2009;12(Pt 1):369-76.

28. Weustink AC, Mollet NR, Pugliese F, Meijboom WB, Nieman K, Heijenbrok-Kal MH, Flohr TG, **Neefjes LA**, Cademartiri F, de Feyter PJ, Krestin GP.
     Optimal electrocardiographic pulsing windows and heart rate: effect on image quality and radiation exposure at dual-source coronary CT angiography.
     Radiology. 2008 Sep;248(3):792-8.

BOOK CHAPTERS

In: Cademartiri F, Mollet NR, Hoffmann U. An atlas of Investigation and Diagnosis: CT Coronary Angiography. Oxford, UK: Atlas Medical Publishing Ltd; 2011.

1. **Neefjes LA**, Weustink AC, Capuano E, Rengo M, Cademartiri F, Mollet NR
    Spectrum of Diseases: Coronary Calcium and Atherosclerotic Plaques: Prognostic Value.

2. Meijboom WB, **Neefjes LA**, Weustink AC, Capuano E, Cademartiri F, Mollet NR
    Spectrum of Diseases: Coronary Stenosis.

3. Pugliese F, Capuano E, **Neefjes LA**, Rengo M, Cademartiri F, Mollet NR
    Spectrum of Diseases: Coronary Stent Imaging.

4. Weustink AC, Capuano E, **Neefjes LA**, Palumbo A, Maffei E, Cademartiri F, Mollet NR
    Spectrum of Diseases: Coronary Artery Bypass Grafts.

5. Capuano E, **Neefjes LA**, Weustink AC, Rengo M, Cademartiri F, Mollet NR
    Case Studies: Stable Angina Pectoris.

Presentations

NHS wetenschapsdag 2008, Amsterdam, The Netherlands.

1. Neefjes LA, Boogers MM, Cramer MJM, Bax JJ, de Feyter PJ.
   Modification of risk with MSCT-coronary angiography in high-risk cardiac asymptomatic patients. (poster presentation)

ESCR 2008, Porto, Portugal.

2. Neefjes LA, Neoh RE, Rengo M, Kyrzopoulos S, Weustink AC, Mollet NR, Krestin GP, de Feyter PJ.
   Reliable detection of ostial lesions using CTCA: even better than CA? (poster and oral presentation)

RSNA 2008, Chicago, USA.

3. Neefjes LA, Dijkshoorn ML, Weustink AC, Rengo M, Pugliese F, de Feyter PJ, Krestin GP, Mollet NR.
   Lowering radiation exposure in CT Coronary Angiography: a decision tree. (poster presentation)

4. Neefjes LA, Weustink AC, Rengo M, Moelker A, de Feyter PJ, Krestin GP, Mollet NR.
   Usefulness of CT Coronary Angiography in Patients with Coronary Chronic Total Occlusion. (poster presentation)

5. Neefjes LA, Neoh RE, Weustink AC, Rengo M, Kyrzopoulos S, de Feyter PJ, Krestin GP, Mollet NR.
   Detection of coronary ostial lesions. Is CT Coronary Angiography better than Conventional Coronary Angiography? (poster presentation)

ECR 2009, Vienna, Austria.

6. Neefjes LA, Neoh RE, Rengo M, Kyrzopoulos S, Weustink AC, Mollet NR, Krestin GP, de Feyter PJ.
   Dual source computed tomography angiography for detecting coronary ostial lesions: superior to conventional coronary angiography? (poster presentation)

9th SOMATOM World Summit 2009, Valencia, Spain.

7. Neefjes LA, Mollet NR, Rossi A, Weustink AC, de Feyter PJ, Krestin GP.
   Advantages of low dose CT-coronary angiography in the evaluation of low risk patients. (oral presentation)

8. Neefjes LA, Rossi A, Dijkshoorn ML.
   CT Coronary Angiography: Somatom Definition Flash -first experience in the Erasmus Medical Center Rotterdam-. (poster presentation)

Radiologendagen 2009, Amsterdam, the Netherlands.

9. Neefjes LA, Rossi A, Mollet NR, Langendonk JG, Sijbrands EJG, Weustink AC, Moelker A, Schultz C, Dharampal AS, Capuano E, Krestin GP, de Feyter PJ.
   Dual Source CT Coronary Plaque Assessment in Cardiac Asymptomatic Patients with Familial Hypercholesterolaemia. (oral presentation)

RSNA 2009, Chicago, USA.

10. Neefjes LA, Dijkshoorn ML, Rossi A, Weustink AC, Capuano E, Dharampal AS, de Feyter PJ, Mollet NR, Krestin GP.
    The next generation Dual Source CT Coronary Angiography; protocol selection and optimization. (poster presentation)

ECR 2010 Vienna, Austria.

11. Neefjes LA, Capuano E, Rengo M, van der Giessen AG, Schaap M, Flu WJ, Krestin GP, de Feyter PJ, Mollet NR.
    Detection of coronary atherosclerotic plaque progression by CT coronary angiography: a 3 year follow-up study. (oral presentation)
12. Neefjes LA, Rossi A, Sijbrands EJG, Langendonk JG, Galema-Boers AM, Weustink AC, Mollet NR, Krestin GP, de Feyter PJ.
    Dual Source CT coronary plaque assessment in cardiac asymptomatic patients with familial hypercholesterolemia. (poster presentation)
13. Neefjes LA, Dharampal AS, Rossi A, Dijkshoorn ML, Moelker A, Weustink AC, de Feyter PJ, Krestin GP, Mollet NR.
    Image quality and radiation dose of CT coronary angiography using a novel prospective high pitch spiral scan protocol in comparison with an adaptive step and shoot protocol. (poster presentation)

Cardiac MRI&CT, Clinical update 2011, Cannes, France.

14. Neefjes LA, ten Kate GR, Rossi A, Moelker A, Galema-Boers JMH, Nieman K, Mollet
     NR, Sijbrands EJG, Krestin GP, de Feyter PJ.
     CT coronary imaging in statin treated asymptomatic patients with familial
     hypercholesterolemia. (poster presentation)

ESC 2011, Paris, France.

15. Neefjes LA, ten Kate GR, Rossi A, Galema-Boers JMH, Nieman K, Sijbrands EJG,
     Krestin GP, Mollet NR, de Feyter PJ.
     CT coronary angiography in asymptomatic high risk patients with familial
     hypercholesterolemia. (poster presentation)

Radiologendagen 2011, Maastricht, the Netherlands.

16. Neefjes LA, Rossi A, Dharampal AS, Weustink AC, Nieman K, Krestin GP, de Feyter PJ,
     Mollet NR.
     Diagnostic performance of 128-slice dual source CT coronary angiography
     -a randomized study-. (oral presentation)

ESCR 2011, Amsterdam, the Netherlands.

17. Neefjes LA, ten Kate GJ, Rossi A, Galema-Boers JMH, Sijbrands EJG, Krestin GP, Mollet
     NR, de Feyter PJ.
     Subclinical Coronary Atherosclerosis in High Risk Patients with Familial
     Hypercholesterolemia. (oral presentation)

PhD portfolio

Name:　　　　　　　　　　Lisan A. Neefjes
Erasmus MC Department:　Radiology and Cardiology
Research School:　　　　　COEUR
Promotors:　　　　　　　Prof. dr. G.P. Krestin
　　　　　　　　　　　　　　Prof. dr. P.J. de Feyter

Courses (21.2 ECTS)

General academic skills

Integrity in Research	2008
Biomedical English Writing and Communication	2009

Research skills

Introduction in clinical epidemiology	2008
Classical Methods for Data-analysis	2008
Diagnostic research	2009

In-depth courses

Pathophysiology of ischemic heart disease	2007
IVUS course	2007
Vascular clinical epidemiology	2008
Cardiovascular imaging and diagnostics	2008
SWC Cardiac Imaging	2008

Conferences/seminars (including presentations) (20.5 ECTS)

Coeur Research Seminars	2008-2010
NHS wetenschapsdag	2008
ESCR 2008	2008
RSNA 2008	2008
Congress Cardiology and Vascular Medicine Update and Perspective	2009
ECR 2009	2009
9th SOMATOM World Summit	2009

Radiologendagen	2009
ESOR Galen Cardiac Course	2009
3de Sectiedag cardiovasculaire Radiologie	2009
RSNA 2009	2009
ECR 2010	2010
COEUR PhD day	2010
Cardiac MRI&CT update 2011	2011
ECS 2011	2011
Radiologendagen 2011	2011
ESCR 2011	2011

Teaching activities (2.7 ECTS)

Lecture Medical Students:	2009
-Introduction cardiac MRI and CT-	
Workshop Cardiac CT (ECR 2009)	2009
Lecture Medical Students:	2010
-Introduction cardiac MRI and CT-	
Workshop Cardiac CT (ECR 2010)	2010

Curriculum Vitae

Lisan Anna Elisabeth Neefjes was born on January 20th, 1981 in Roosendaal, the Netherlands. After finishing high school in 1999 (Gymnasium, Gertrudis College, Roosendaal), she started studying medicine at the Erasmus University Rotterdam. In 2006 she obtained her medical degree and started her radiology training in the department of radiology at the Erasmus Medical Center in Rotterdam under the supervision of Professor G.P. Krestin. After 17 months she took a break from her training to work as a research fellow at the Cardiology and Radiology departments of the Erasmus Medical Center in Rotterdam and at the ICIN Netherlands Heart Institute in Utrecht under the supervision of Professor P.J. de Feyter and Professor G.P. Krestin. Her achievements in the field of CT coronary angiography resulted in this PhD thesis. After long and careful reflection, she has decided not to continue her radiology training. She is currently working as a youth health care physician at the GGD in Goes, the Netherlands.